

THESIS FOR THE DEGREE OF LICENTIATE OF ENGINEERING

**Assessment of safety characteristics for Li-ion battery cells by
abuse testing**

FREDRIK LARSSON



CHALMERS

Department of Applied Physics

Chalmers University of Technology

Göteborg, Sweden 2014

Assessment of safety characteristics for Li-ion battery cells by abuse testing

FREDRIK LARSSON

Thesis for the degree of Licentiate of Engineering

© Fredrik Larsson, 2014

Department of Applied Physics

CHALMERS UNIVERSITY OF TECHNOLOGY

SE-412 96 Göteborg

Sweden

www.chalmers.se

Telephone: +46 (0)31-772 00 00

Author's e-mail: vegan@chalmers.se

Printed by Chalmers Reproservice

Göteborg, Sweden 2014

Assessment of safety characteristics for Li-ion battery cells by abuse testing

FREDRIK LARSSON

Department of Applied Physics, Chalmers University of Technology

ABSTRACT

Despite the many advantages with lithium-ion batteries there can be disadvantages in form of safety issues. In an abuse situation a Li-ion cell can undergo a thermal runaway releasing excessive heat, flammable and toxic gas emissions and eventually accompanied by disassembling/explosion and fire. Abuse tests are a method for assessment of the safety characteristics of Li-ion batteries. Results on cells and electrolytes from abuse testing by overcharge, short circuiting, external heating and fire test are presented and discussed.

The thermal runaway was studied by external heating of various commercial Li-ion cells with cylindrical and pouch packaging. Cells with lithium cobalt based oxides showed a thermal runaway at around 200 °C with a maximum rate of temperature increase of about 5000 °C/min. Cells with lithium iron phosphate (LFP) showed significantly lower reactivity but a thermal runaway did still occur for some cells.

Short circuit and overcharge tests of LFP pouch cells showed in most cases temperature increases below about 100 °C. Fires did not occur in these tests except one unexpected fire during an overcharge test. The fire tests show that the reactivity of Li-ion cells in a fire are dependent on the state of charge (SOC), however, the total heat release shows a low SOC dependence. Toxic emissions of hydrogen fluoride (HF), phosphorous oxyfluoride (POF₃) and phosphorus pentafluoride (PF₅) were studied by FTIR in fire experiments conducted on electrolytes and cells. The results are extrapolated to obtain an estimate of the possible emissions from a fire in an electric vehicle.

Keywords: Lithium-ion, battery, safety, abuse test, overcharge, short circuit, thermal runaway, fire, toxic gases

LIST OF PUBLICATIONS

- I. F. Larsson, P. Andersson, B.-E. Mellander, “Are electric vehicles safer than combustion engine vehicles?”, in: B. Sandén, P. Wallgren (Eds.), *Systems perspectives on Electromobility*, Chalmers University of Technology, Göteborg, ISBN 978-91-980973-9-9, p 33-44, 2014.
- II. F. Larsson, B.-E. Mellander, “Energy storage system safety in electrified vehicles”, *Fires in vehicles (FIVE) 2012*, Conference proceedings, p 303-306, Chicago, USA.
- III. F. Larsson, B.-E. Mellander, “Abuse by external heating, overcharge and short circuiting of commercial lithium-ion battery cells”, *Journal of the Electrochemical Society*, 161 (10) A1611-A1617 (2014), DOI: 10.1149/2.0311410jes.
- IV. P. Andersson, P. Blomqvist, A. Lorén, F. Larsson, ”Using FTIR to determine toxic gases in fires with Li-ion batteries”, Submitted to *Fire and Materials*.
- V. F. Larsson, P. Andersson, P. Blomqvist, A. Lorén, B.-E. Mellander, ”Characteristics of Lithium-ion batteries during fire tests”, *Journal of Power Sources*, in press, DOI: 10.1016/j.jpowsour.2014.08.027.

ACKNOWLEDGEMENTS

I am very grateful to Professor Bengt-Erik Mellander for all this knowledge and positive spirit supporting me. Many thanks also to my other supervisors, Petra Andersson and Ingvar Albinsson. Thanks to all fantastic colleagues at SP and Chalmers. Special thanks to Ingvar Karlson and Maurizio Furlani.

I gratefully acknowledge the Swedish Energy Agency and the FFI-program, the Swedish Fire Research Board and the Swedish Fire Protection Association for financial support. Special thanks to FKG and Stephen Wallman for the support. I would also like to thank the former company Effpower for supporting the initiation of my PhD-project and Peter Leisner, head of department of SP Electronics, for arranging the continuity of the project from Effpower. The project partners of the FFI-project “*FFI Safer battery systems in electrified vehicles – develop knowledge, design and requirements to secure a broad introduction of electrified vehicles*” are also gratefully acknowledged.

To my family and especially to beautiful Malin and Holger.

Fredrik Larsson
Göteborg, August 2014

CONTENTS

ABSTRACT	I
LIST OF PUBLICATIONS.....	III
ACKNOWLEDGEMENTS.....	V
1 INTRODUCTION.....	3
2 PAPER I: ARE ELECTRIC VEHICLES SAFER THAN COMBUSTION ENGINE VEHICLES? ...	6
3 PAPER II: ENERGY STORAGE SYSTEM SAFETY IN ELECTRIFIED VEHICLES	7
4 PAPER III: ABUSE BY EXTERNAL HEATING, OVERCHARGE AND SHORT CIRCUITING OF COMMERCIAL LITHIUM-ION BATTERY CELLS	8
5 PAPER IV: USING FTIR TO DETERMINE TOXIC GASES IN FIRES WITH LI-ION BATTERIES.....	11
6 PAPER V: CHARACTERISTICS OF LITHIUM-ION BATTERIES DURING FIRE TESTS.....	13
7 CONCLUSIONS	15
8 REFERENCES.....	16

1 INTRODUCTION

The world is facing environmental changes and a diminishing oil supply. The greenhouse effect poses a threat to our civilization, and CO₂ emissions are believed to be the main contributor to an increased temperature. The transportation sector has a large share of the CO₂ emissions. The fossil driven traffic also results in severe air pollution in many cities which results in health problems. Sweden has a goal to reach a fossil independent vehicle fleet in the year 2030 and to have a carbon neutral society in the year 2050 [1]. One way to reach those goals is to use batteries and electrify the combustion engine propelled vehicles of today; passenger cars, heavy-duty vehicles, etc.

Electrified vehicles (xEV) use either pure electric propulsion or combined electric and combustion engine propulsion. The pure electric vehicle (EV) has zero tail pipe emissions and has an energy storage system typically consisting of lithium-ion (Li-ion) batteries. The hybrid electric vehicle (HEV) and plug-in hybrid electric vehicle (PHEV) typically uses a smaller sized battery. The HEV battery technology most often used today for e.g. Toyota Prius is nickel-metal hydride (NiMH) batteries while the PHEV typically uses Li-ion batteries.

The lithium-ion technology offers high energy and power densities, long life time and fast recharging compared to e.g. lead-acid and NiMH battery technologies. Li-ion is a family name including many different cathode and anode materials that use lithium ions for transport between the electrodes. On the commercial market today there are a number of different electrode materials for Li-ion batteries. The lithium cobalt oxide (LCO), LiCoO₂, was the first one introduced on the market by Sony in the 1990s. By mixing the cobalt with other materials a variety of cobalt based oxides is possible. Typically nickel, manganese or aluminum are used forming e.g. nickel manganese cobalt oxide (NMC), LiNi_xMn_yCo_zO₂ and nickel cobalt aluminum oxide (NCA), LiNi_xCo_yAl_zO₂, where $x+y+z=1$. There are also cathode materials without cobalt, e.g. lithium manganese oxide (LMO), LiMn₂O₄. Phosphates are also used as cathode material [2] and the most widely used today is lithium-iron phosphate (LFP), LiFePO₄. Commercial anode materials for Li-ion batteries are dominated by carbon materials, e.g. natural and synthetic graphite, but lithium titanate oxide (LTO), Li₄Ti₅O₁₂, is also used by some manufacturers. There are many potential electrode materials for use in Li-ion batteries and there are intensive research activities within this area, e.g. cells with higher voltage and for use in higher temperatures as well as the Li-air battery. Theoretically the Li-air battery, which uses air (oxygen) as cathode, can reach an energy density more than 10 times higher than today's Li-ion batteries but several major

challenges must be overcome, including safety aspects and the Li-air battery is not likely to be commercialized within 20-30 years [3].

Today Li-ion batteries are widely used in different applications. They have been used for a long time in consumer products such as laptops, mobile phones, digital cameras and power tools. The automotive industry has more recently started to use Li-ion batteries in xEVs and with increasing yearly volumes. The high energy density of Li-ion cells gives batteries with low weight and volumes which have had a major impact on product development and design. However, the Li-ion technology has some drawbacks regarding safety aspects compared to other battery technologies, e.g. lead-acid and NiMH. Lithium-ion batteries have a high cell voltage due to the use of lithium which enables the high energy density but this can also give safety problems and incidents and accidents have happened, some of them with a large media interest [4-7].

Li-ion cells cannot use water based electrolytes due to the high cell voltage, typically 3.7 V (the value varies for different cell chemistries), and use instead organic electrolytes which are volatile and flammable. The electrolyte consists of organic solvents, a Li-salt and additives. Typical solvents used are ethylene carbonate (EC), diethyl carbonate (DEC) and dimethyl carbonate (DMC). The Li-salt commercially used today is lithium hexafluorophosphate, LiPF_6 . A number of different additives are used to achieve various properties, e.g. flame retardants, voltage stabilizers and additives intended to increase life time. The electrolyte and particularly the additives are each cell manufacturer's secret and very rarely disclosed. Lithium metal itself is very reactive, however, the lithium is in form of Li^+ and intercalated in electrodes, which is a much more stable state, with little free lithium metal as a result of e.g. aging effects, overcharge or overcurrent during low temperatures.

A Li-ion cell must be kept within a certain range of temperature, voltage and current in order to be stable. In case these limits are exceeded the result might be any or a combination of these effects: swelling of the cell due to increased gassing/pressure, release of these gases by cell venting which can occur relatively slowly or rapidly (disassembling or even an explosion) and a fire might start. The type of abuse situation and the Li-ion cell chemistry and cell design affect the cell reaction. In case of an excessive internal cell temperature, a thermal runaway can occur. A thermal runaway is a rapid temperature increase, where the heat generation is greater than the heat dissipation to the cell surrounding. The onset temperature of the runaway depends on the cell chemistry, and for a typical cobalt cell it starts at relatively moderate temperatures, 120-150 °C [8]. The first step in a typical thermal runaway is the breakdown of SEI (solid electrolyte interface) layer, followed by a reaction between electrolyte and anode which is exothermic which further accelerates the process and

increases the temperature enabling the third step of the reaction between electrolyte and cathode, which is even more exothermal. The reactions can be sustained by its own oxygen whereas different cathode materials release different amounts of oxygen. The LFP chemistry is considered as the most thermally stable cathode material available at the market today with no oxygen release at those temperatures [8-11]. The thermal response of a LFP cell is thereby dominated by the electrolyte and anode.

In case of mechanical abuse, e.g. deformation and penetration, internal short circuits are created inside the cell which thereby increases the cell temperature. An internal short circuit can also originate from particle contamination or from dendritic bridges formed during cycling (discharge/charging) of the cell. Forming of a dendritic bridge used to be a problem earlier but is nowadays a relatively small problem. However, cell failures in the field, “field failures”, are often seen as internal short circuits, with a low probability on cell level, less than 1 ppm [5,12]. Electrical abuse situations like overcharge, overdischarge and external short circuit can also cause problems. In case of external heating abuse, e.g. a fire close by or a Li-ion battery of a mobile phone lying in a car window a sunny day, a thermal runaway can also be initiated.

In order to evaluate cell response in case of abuse situations, abuse testing can be used. United Nations has a test manual [13] for transportation demands of Li-ion batteries classifying them as dangerous goods and specifies test that the cells and batteries needs to undergo before they can be transported in resting state. In addition UNECE released its addendum 99 to regulation No. R100 [14] including safety tests for battery used on wheeled vehicles, tests that included cycling of the batteries within certain temperature ranges etc that a vehicle might be exposed to. There are several international standards for abuse testing [15-17], many of which have been updated recently. The abuse tests standards for Li-ion is however, not yet complete, e.g. regarding toxic fluoride emissions. Besides, with the fast Li-ion technology development there is also a natural process of updates to follow the technology progress and abuse tests standards are thereby likely to continually be updated for at least some time.

Li-ion cells and battery systems containing multiple cells are equipped with various safety mechanisms [18-23]. Cylindrical cells have e.g. a safety vent, which, if it is properly designed and fully functional, can protect the cell from explosion, by releasing excessive cell pressure before critical pressure levels have been build-up. In case of pouch prismatic cells which have soft packaging (coffee bags) explosion risks due to high pressure are not likely due to the weak packaging.

The released gases contain a complex mixture of possible components, which vary with the abuse situation, e.g. if the cell is on fire or not. The gases can be both flammable and toxic. Vaporized solvents are typically released together with e.g. CO, CO₂, H₂ [24-26]. The fluorine content, from the Li-salt and also from possible use of some binders (e.g. PVdF), is a source for the formation of toxic fluorine compounds. Hydrogen fluoride (HF) is very toxic [27] and has gained most interest so far. Phosphorous oxyfluoride, POF₃, and phosphorus pentafluoride, PF₅, are two other gases that may be emitted [28-30]. The toxicity of POF₃ is unknown but it can potentially be more toxic than HF as is the case for its chlorine analog, HCl/POCl₃ [31]. Besides HF, POF₃ and PF₅ other complex components can be formed [32-34].

The assessment of the overall safety of a battery with Li-ion cells is complex and determined by many factors; cell chemistry, cell design, battery system design, cooling system, safety mechanisms, mechanical deformation protection, etc. Abuse testing is a valuable tool to evaluate safety characteristics under a broad variety of situations. This licentiate thesis demonstrates this and gives insight into the safety issues with Li-ion batteries based on these tests.

2 PAPER I: ARE ELECTRIC VEHICLES SAFER THAN COMBUSTION ENGINE VEHICLES?

The aim of Paper I is to discuss the safety of an electrified vehicle, e.g. EV and PHEV, compared to a vehicle with only a combustion engine for gasoline or diesel. The paper gives a general introduction and description about battery systems, battery types, different hazards associated with electrified vehicles and some incidents that have occurred as well as outlooks for the future.

METHOD

In form of an e-book chapter that is updated regularly (living document) based on new research findings and technology development.

MAIN FINDINGS

- Electrified vehicles have the potential to be safer than combustion engine vehicles, simply due to that they are not carrying or carrying less amount of flammable gasoline/diesel, which will remove/lower the risk for fire and explosions.
- New risks might be introduced by electric vehicles

- New technologies can always mean new unknown risks which might take time to learn to handle.
- The electrical hazard in electric vehicle is low with correct handling.
- Too few electrified vehicles are yet on the roads today to have any reliable statistics of accidents/incidents.

3 PAPER II: ENERGY STORAGE SYSTEM SAFETY IN ELECTRIFIED VEHICLES

The aim of Paper II is to study the thermal runaway response of commercial Li-ion cell with the physical cell size of type 18650, i.e. 18 mm in diameter and 65 mm long. External heating is used to initiate a thermal runaway since safety devices such as PTC and CID inside the cells cannot protect from this type of abuse. Commercial 18650 Li-ion cells from Samsung, Sanyo and K2 Energy were tested. The cells from Samsung and Sanyo had cobalt based cathodes and are typically used in laptop computers, while the cell from K2 Energy has a LFP cathode.

METHOD

The cells were fully charged (100% SOC) and heated up in a thermostated oven. The cells were tested one at the time, fastened on a brick which was centrally placed in the oven. The air in the oven was circulated with its built-in fan in order to achieve a uniform temperature around the cell. The cell surface temperature was measured with four type K thermocouples. The oven was set on 300 °C with continuous heating and was not stopped until the effect of the thermal runaway had completely finished.

MAIN FINDINGS

- The thermal runaway from Samsung and Sanyo cells with cobalt based cathodes showed similar thermal reactions, with a temperature rise of 18-25 °C/sec.
- The LFP cell from K2 Energy had a thermal runaway but it was significantly less energetic compared to the cells from Samsung and Sanyo, with temperature rise of 0.6 °C/sec.
- The thermal runaway temperatures for all cells were around 200 °C, see Figure 1.

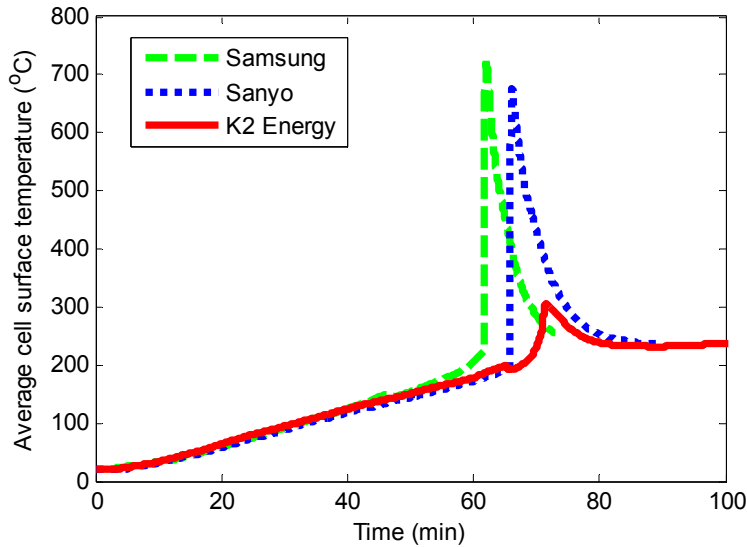


Figure 1 Temperature development for three 18650 lithium-ion cells during external heating test.

4 PAPER III: ABUSE BY EXTERNAL HEATING, OVERCHARGE AND SHORT CIRCUITING OF COMMERCIAL LITHIUM-ION BATTERY CELLS

The aim of Paper III is to study cell response of four types of commercial Li-ion cells under three types of abuse; external heating, overcharge and short circuit. The focus is on LFP cells from EiG and European Battery. 18650 Samsung laptop cells are also studied but during external heating only, since their safety devices (e.g. PTC, CID) would stop overcharge and short circuit situations making them non-interesting for this study.

METHOD

The external heating abuse tests are conducted using the oven and procedure discussed in paper II, with the exception that both a continuous and a step-wise temperature increase was used. For the step-wise increase, the oven temperature was first set to 80 °C and thereafter increased in steps of 10 °C every 15 min until either any thermal runaway had occurred or the maximum temperature of the oven (300 °C) was reached. Cells were fully charged (100% SOC) prior to the tests.

The overcharge abuse tests started with fully charged cells which were then charged beyond their limits. For the EiG power cell a current of 10 C-rate (70A) was used and for the

European Battery energy cell a current of 2 C-rate (90A) was used. Cell voltage, current and temperature (by several type K thermocouples) were measured with 1 Hz.

The short circuit abuse tests were conducted using 50 mm² copper cables and a high current contactor enabling a low resistance short circuit. The current was measured by a current core and the cell surface temperatures measured with several type K thermocouples.

MAIN FINDINGS

- The external heating of the 18650 laptop cell resulted in a rapid thermal runaway, with a rate of temperature increase close to 5000 °C/min, a pressure wave, squirting of ignited cell materials and immediate fire.
- The corresponding energy release from of 300 kg battery pack in an electric vehicle build by the 18650 cells would be approximately 70 MJ, corresponding to the combustion of 2 litre of gasoline. However, our results are up to six times lower than that of other studies.
- LFP cells are less energetic than cobalt based cells. However, variations between LFP cells from different cell manufacturers as well as between different cell design versions from the same manufacturer were found.
- For the 7 Ah LFP cell from EiG, it was found that the newer cell design have a significantly lower, close to undetectable, thermal runaway peak compared to an older cell design, see Figure 2. Even though both cell designs use the safest currently available commercial cathode material, LFP, this shows that the development for safer Li-ion cells is still improving but also underlines that the cathode material is only one of the important components for safety assessment.
- Overcharge of LFP cells resulted in relatively low temperatures, less than 80 °C was measured, which is lower than the thermal runaway onset temperature. One LFP cell did however unexpectedly catch fire during the overcharge, see Figure 3. This fire event was not repeated in the following three tests. This highlights the possibility of field failures of batteries, in that there is a probability for these things to happen.
- The short circuit currents of a single Li-ion cell can be high, around 1000 A was measured, see Figure 4.

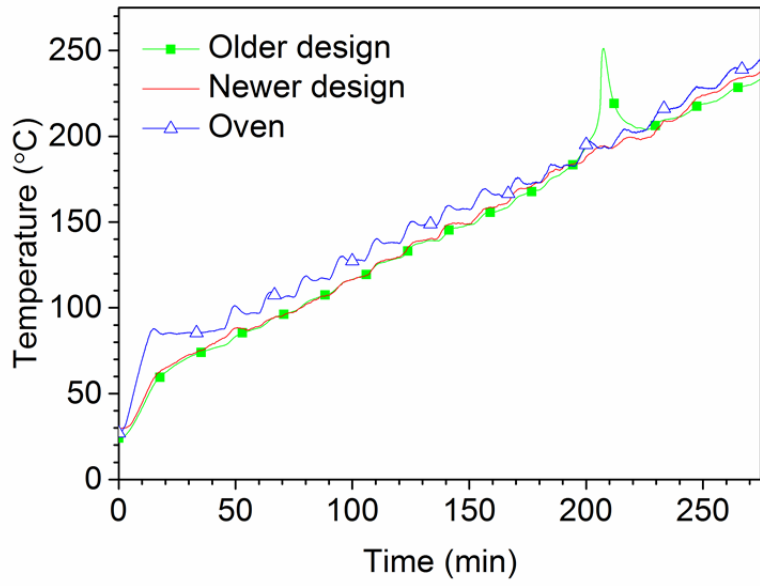


Figure 2 Temperature development during external heating of EiG cells of newer and older cell design.

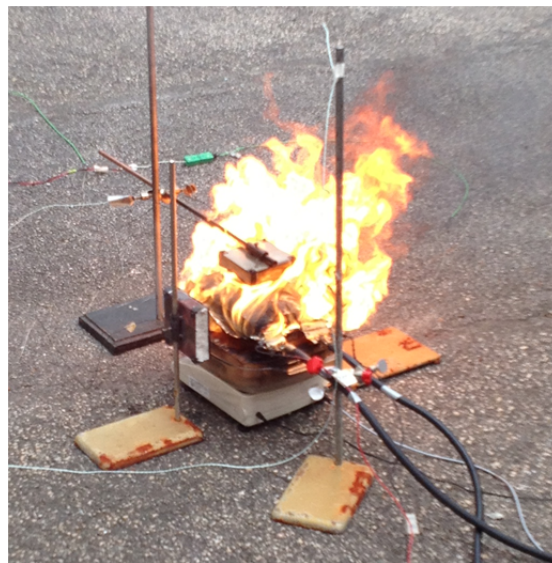


Figure 3 One of the overcharge test, by 2 C-rate (90A), of a European Batteries cell resulted in a fire.

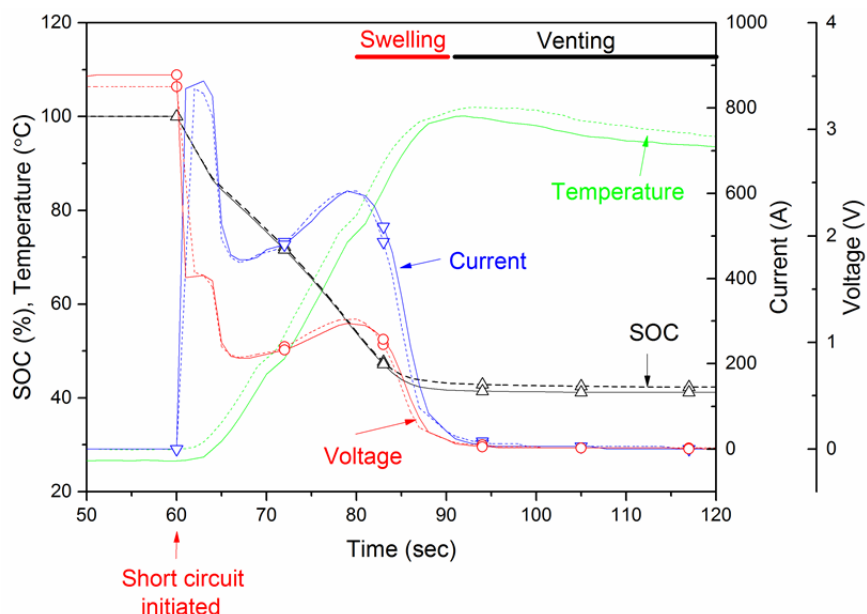


Figure 4 Short circuit of EiG cell of newer design (dashed lines) and EiG of older design (solid lines).

5 PAPER IV: USING FTIR TO DETERMINE TOXIC GASES IN FIRES WITH LI-ION BATTERIES

The aim of Paper IV is to study toxic emissions of HF, POF_3 and PF_5 from samples containing LiPF_6 electrolytes. Tested electrolyte solvents were dimethyl carbonate (DMC), 1,2-dimethoxyethane (DME) and polypropylene carbonate (PC).

METHOD

The FTIR was first quantitatively calibrated for HF, POF_3 and PF_5 . Electrolyte fire tests were performed in a Cone calorimeter using radiative heating. Tests were conducted on pure LiPF_6 salt and LiPF_6 dissolved in PC and DME during both evaporation and ignition by an electric spark.

Electrolyte fire tests were also performed using a custom experimental setup-up with a propane burner and needles to introduce solvents/water into the flames. The amounts of solvents were measured by a flow-meter. DME with 0.4 M LiPF_6 and DMC with 0.4 and 1.0 M LiPF_6 were studied. Water was introduced in the flames in two tests.

MAIN FINDINGS

- It was possible to calibrate the FTIR to be used in fire tests on electrolytes to measure HF, POF_3 and PF_5 .

- HF and POF_3 emissions were measured from LiPF_6 and the solvents PC, DME and DMC, e.g. see Figure 5 and Figure 6.
- PF_5 is highly reactive and thereby difficult to calibrate and no PF_5 was found in the fire tests.
- POF_3 is produced with a concentration of approximately 5-40% of the HF concentration.
- Some of the spectral peaks found correspond to unknown substances.

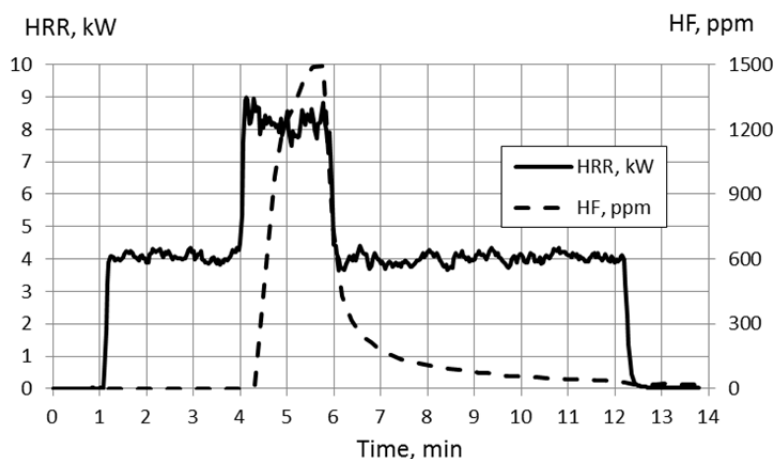


Figure 5 Heat release rate (HRR) and HF concentration during burning of 1 M DMC injected as a spray (18 ml/min) into a 4 kW propane burner during two minutes.

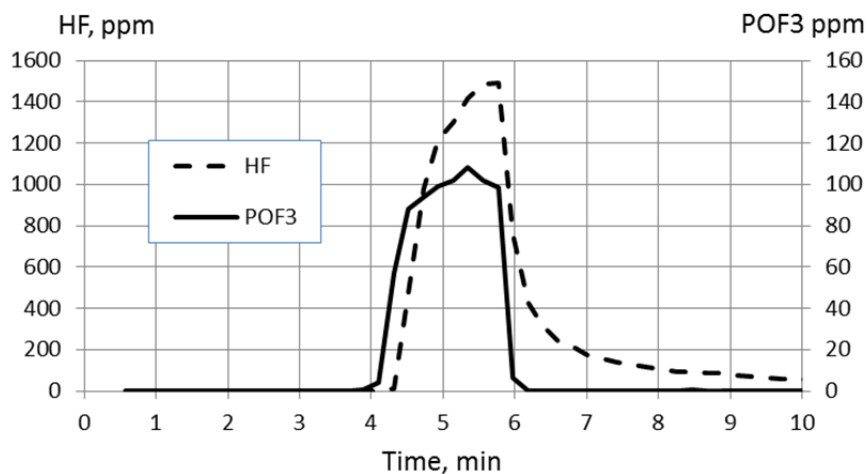


Figure 6 Concentrations of HF and POF_3 during burning of 1 M DMC injected as a spray (18 ml/min) into a 4 kW propane burner during two minutes.

6 PAPER V: CHARACTERISTICS OF LITHIUM-ION BATTERIES DURING FIRE TESTS

The aim of Paper V is to study the fire characteristics and gas emissions of Li-ion batteries in case of an external fire. The heat release rate (HRR), total heat release (THR), battery temperature and voltage were measured. The production of toxic emissions was measured in real-time. Hydrogen fluoride (HF) was quantitatively detectable while phosphorous oxyfluoride (POF_3) was not detectable in this setup, but was probably present in the released emissions.

Seven tests were performed of 3 battery types; EiG 7 Ah, K2 Energy and conventional Lenovo laptop battery packs. The study included SOC levels of 100%, 50% and 0% for EiG cells as well as one test where water mist was applied in order to study possible influence on emissions.

METHOD

The tests were performed using the measurement and gas collection system of a Single Burning Item (SBI) apparatus. The battery was placed on a wire grating and a 15 kW propane burner beneath was used. Five EiG cells were tested at the time, fastened together with steel wire. The nine cells from K2 Energy were placed inside a box with steel net as protection from potential projectiles. The two laptop battery packs were also enclosed by a steel net in order to avoid projectiles.

The HRR and THR were measured using the oxygen consumption method corrected for CO_2 . The O_2 was measured by a paramagnetic analyser and CO_2 by a non-dispersive infrared (NDIR) sensor. The toxic gas emissions were measured in real-time (one spectra every 12 seconds) by Fourier transform infrared spectroscopy (FTIR) and by post analysis of any fluorine contained in the FTIR primary filter. The temperature and cell voltage of the mid cell of the EiG 5-cell pack were measured with 1 Hz.

MAIN FINDINGS

- Cells with 100% SOC are significantly more reactive than cells with lower SOC values and showed energetic outbursts, see Figure 7 and Figure 8.
- The HRR peak values varied between 13 and 57 kW for batteries with approximately 100 Wh energy capacity.
- Emissions of POF_3 and PF_5 were not detected but should have been present according to the theory. POF_3 emissions were probably below the detection limit.

- HF was detected well above the detection limit and varied with SOC, see Figure 9. The total HF emissions varied between 15 and 124 mg/Wh, where lower SOC values gave higher HF values.
- Application of water mist, see Figure 10, above the battery resulted in close to double the momentary HF production, see Figure 9. However, the total amount of HF released was similar to the case without water mist.
- Extrapolation of the HF emission based on the EiG cell to a 10 kWh battery for a PHEV results in a total HF release between 400-1200 g.
- A hypothetical case in which all HF is released and contained inside a PHEV passenger compartment of 5 m³ results in HF concentrations of 80-240 g/m³, which are magnitudes above acceptable short time exposure levels.

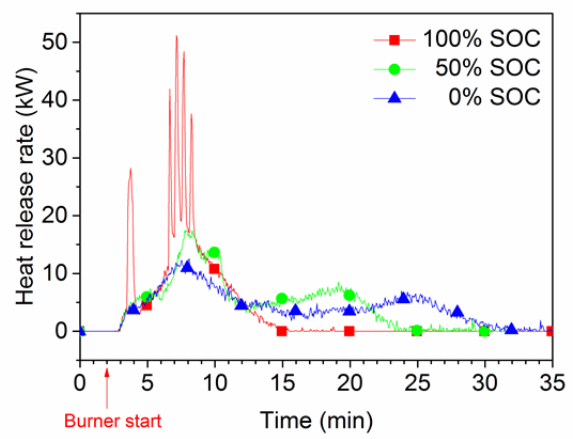


Figure 7 Heat release rate for EiG cells of 0%, 50% and 100% SOC during 15 kW propane burner test (the HRR of the burner is subtracted).

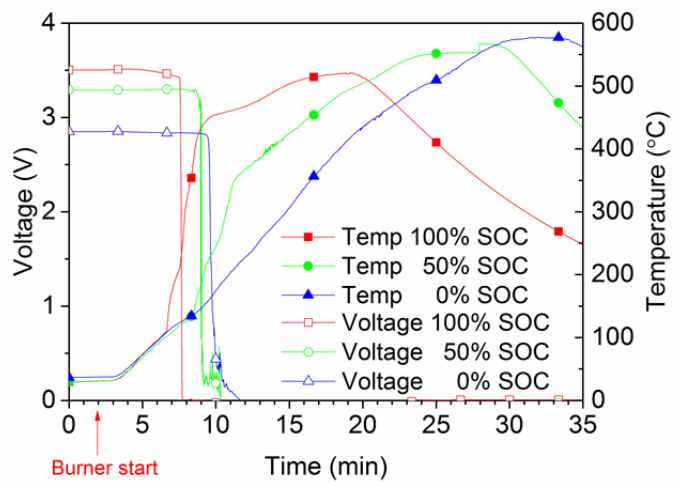


Figure 8 Mid cell temperature and voltage for EiG cells with 0%, 50% and 100% SOC during 15 kW propane burner test.

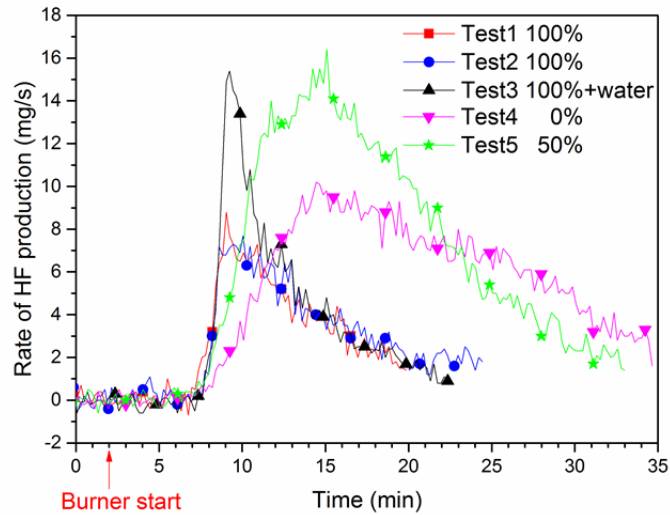


Figure 9 HF mass flow for EiG cells with different SOC (indicated by % in figure legend) in tests 1-5.

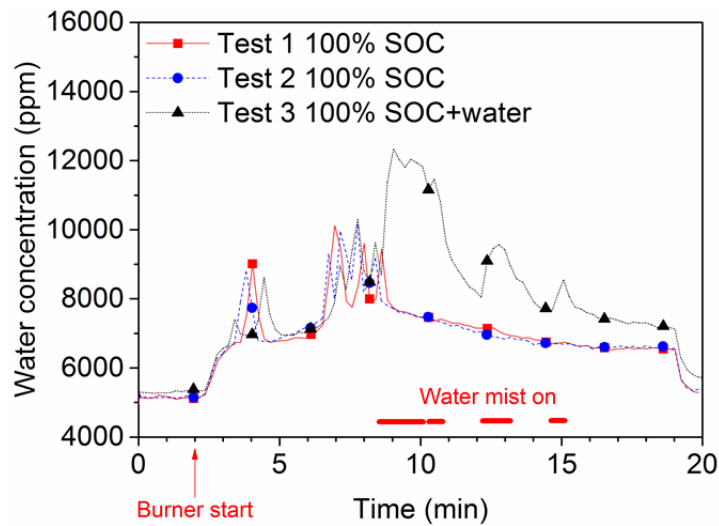


Figure 10 Water concentrations measured in test 1-3. The increased water level in test 3 due to water mist application is clearly seen

7 CONCLUSIONS

Abuse testing is used to evaluate the safety characteristics beyond the design parameters. Different Li-ion cell design and chemistry give diverse reactions to abuse, where LFP is significantly less energetic than cobalt based cells. LFP cells which are considered as the safest Li-ion battery chemistry available today can still catch fire, as shown in one of the overcharge tests.

State of charge impacts the reaction response during the fire tests and the heat release rate is higher with higher SOC values. When a Li-ion cell is short circuited, large currents of e.g. 1000 A can be found. Overcharging tests utilising 2 C-rate and 10 C-rate of LFP cells resulted in swelled cells with gas released but relative low temperatures, below the onset of thermal runaway.

Toxic gas emissions of HF and POF_3 pose a possible critical risk for Li-ion batteries and especially for large Li-ion battery systems. POF_3 is in our limited study found to be produced with about 5-40% of the HF production. The toxicity of POF_3 is unknown but it is possibly even more toxic than HF. It was not possible to draw any clear conclusions on the impact of water as an extinguishing medium in these limited studies but a temporarily increased HF production rate was indicated at the application of water mist, however, further studies are required to make any firm conclusions.

Extrapolation of the total HF emissions from cell-testing to a 10 kWh battery pack, typically used in a PHEV, results in 400 – 1200 g HF that could be released. This might pose a serious threat to humans near a car fire. A hypothetical case in which all HF is released and contained in a 5 m² passenger cabin give HF concentrations that are orders of magnitude over the acceptable short term exposure levels. Further studies are needed also in this case.

8 REFERENCES

- [1] Government Offices of Sweden, "En sammanhållen klimat- och energipolitik", Regeringens proposition 2008/09:162, 2008.
- [2] A. K. Padhi, K. S. Nanjundaswamy, J. B. Goodenough, *J. Electrochem. Soc.*, 144, 1188, 1997.
- [3] G. Girishkumar, B. McCloskey, AC Luntz, S. Swanson, W. Wilcke, *J. of Phys. Chem. Letters*, 1(14), 2193–2203, 2010.
- [4] B. Smith, "Chevrolet Volt Battery Incident Overview Report", National Highway Traffic Safety Administration (NHTSA), DOT HS 811 573, Washington, 2012.
- [5] D. Lisbona, T. Snee, *Process safety and environmental protection*, 89, 434-442, 2011.
- [6] C. Mikolajczak, M. Kahn, K. White, R. T. Long, "Lithium-ion batteries hazard and use assessment", Fire Protection Research Foundation, Quincy, MA, USA, Doc no 1100034.000 A0F0 0711 CM01, 2011.
- [7] <http://edition.cnn.com/2013/07/12/world/europe/uk-heathrow-airplane-fire/>, 2014-06-30.
- [8] D. Doughty, E. P. Roth, *The Electrochem. Soc. Interface*, summer 2012, 37-44, 2012.
- [9] K. Zaghbi, J. Dubé, A. Dallaire, K. Galoustov, A. Guerfi, M. Ramanathan, A. Benmayza, J. Prakash, A. Mauger, C. M Julien, "Lithium-ion cell components and their effect on high-power battery safety", Chapter 19 in *Lithium-Ion Batteries: Advances and Applications*, edited by G. Pistoia, Elsevier, Amsterdam, The Netherlands, p. 437, 2014.
- [10] G. Chen, T. J. Richardson, *J. of the Electrochem. Soc.*, 156 (9), A756, 2009.
- [11] G. Chen, T. J. Richardson, *J. of Power Sources*, 195, 1221, 2010.
- [12] Q. Wang, P. Ping, X. Zhao, G. Chu, J. Sun, C. Chen, *J. of Power Sources*, 208, 210, 2012.
- [13] UNT / UN Manual of Tests and Criteria, Part III, Sub-Section 38.3 for lithium-ion batteries, fifth edition, United Nations, 2009.

- [14] Addendum 99: Regulation No. 100, Revision 2, E/ECE/324/Rev.2/Add.99/Rev.2, E/ECE/TRANS/505/Rev.2/Add.99/Rev.2, United Nations, 2013.
- [15] D. H. Doughty, C. C. Crafts, "FreedomCAR electrical energy storage system abuse test manual for electric and hybrid electric vehicle applications", Sandia report SAND2005-3123, Sandia National Laboratories, USA, 2006.
- [16] UL 1642, UL Standard for safety Lithium Batteries, Fifth Edition, Underwriters Laboratories, Inc., 2012.
- [17] D. Doughty, "SAE J2464 Electric and hybrid electric vehicle rechargeable energy storage system (RESS) safety and abuse testing procedure", SAE Technical Paper 2010-01-1077, doi:10.4271/2010-01-1077, 2010.
- [18] P. G. Balakrishnan, R. Ramesh, T. P. Kumar, *J. of Power Sources*, 155, 401, 2006.
- [19] J. Jeevarajan, "Safety of commercial lithium-ion cells and batteries" In: G. Pistoia (ed) *Lithium-Ion Batteries Advances and Applications*, Elsevier, Amsterdam, The Netherlands, p. 387, 2014.
- [20] Z. Zhang, P. Ramadass, W. Fang, "Safety of lithium-ion batteries" In: G. Pistoia (ed) *Lithium-Ion Batteries Advances and Applications*, Elsevier, Amsterdam, The Netherlands, p. 409, 2014.
- [21] K. Zaghbi, J. Dubé, A. Dallaire, K. Galoustov, A. Guerfi, M. Ramanathan, A. Benmayza, J. Prakash, A. Mauger, C. Julien, "Lithium-ion cell components and their effect on high-power battery safety" In: G. Pistoia (ed) *Lithium-Ion Batteries Advances and Applications*, Elsevier, Amsterdam, The Netherlands, p. 437, 2014.
- [22] S. S. Zhang, *J. of Power Sources*, 162, 1379, 2006.
- [23] G. Nagasubramanian, K. Fenton, *Electrochimica Acta*, 101, 3, 2013.
- [24] T. Ohsaki, T. Kishi, T. Kuboki, N. Takami, N. Shimura, Y. Sato, M. Sekino, *J. of Power Source*, 146, 97-100, 2005.
- [25] E. P. Roth, C. J. Orendorff, *The Electrochem. Soc. Interface*, summer 2012, 45, 2012
- [26] E.P. Roth, *ECS Transactions* 11 (19) 19-41, 2008.
- [27] Documentation for Immediately Dangerous To Life or Health Concentrations (IDLHs) for Hydrogen fluoride (as F), The National Institute for Occupational Safety and Health (NIOSH), USA, 1994.
- [28] H. Yang, G. V. Zhuang, P. N. Ross Jr, *J. of Power Sources* 161, 573-579, 2006.
- [29] T. Kawamura, S. Okada, J.-i. Yamaki, *J. of Power Sources* 156, 547-554, 2006.
- [30] P. Andersson, P. Blomqvist, A. Lorén, F. Larsson, "Investigation of fire emissions from Li-ion batteries", SP Report 2013:5, SP Technical Research Institute of Sweden, Boras, Sweden, ISBN 978-91-87461-00-2, 2013.
- [31] A. Middelman, "Hygiensiska gränsvärden AFS 2011:18", Hygieniska gränsvärden Arbetsmiljöverkets föreskrifter och allmänna råd om hygieniska gränsvärden, ISBN 978-91-7930-559-8, ISSN 1650-3163, Swedish Work Environment Authority, Sweden, 2011.
- [32] A. Hammami, N. Raymond, M. Armand, *Nature* 424, 635-636, 2003.
- [33] C. L. Campion, W. Li, W. B. Euler, B. L. Lucht, B. Ravdel, J. F. DiCarlo, R. Gitzendanner, K. M. Abraham, *Electrochem. and Solid-State Letters*, 7 (7) A194-A197, 2004.
- [34] C. L. Campion, W. Li, B. Lucht, *J. of the Electrochem. Soc.*, 152 (12), A2327-A2334, 2005.

Paper I

4

ARE ELECTRIC VEHICLES SAFER THAN COMBUSTION ENGINE VEHICLES?

Fredrik Larsson

Department of Applied Physics, Chalmers University of Technology*
SP Technical Research Institute of Sweden**

Petra Andersson

SP Technical Research Institute of Sweden***

Bengt-Erik Mellander

Department of Applied Physics, Chalmers University of Technology*

* Division of Solid State Physics

** Division of Electronics

*** Division of Fire

Chapter reviewers: Fredrik Hedenus, Physical Resource Theory, Energy and Environment, and Pontus Wallgren, Design & Human Factors, Product and Production Development, Chalmers

INTRODUCTION

Replacing conventional vehicles using internal combustion engines with electrified vehicles (EV) is a challenge in many respects. Introduction of new technical solutions, especially those produced for a mass market, may substantially change and possibly increase the risks associated with the products. On the other hand, electric vehicles have other clear advantages concerning safety as they do not carry conventional fuels onboard such as petrol or diesel, both of which are flammable and toxic. Without a combustion engine onboard, the risks of fire and explosion are thus minimized. Therefore, the introduction of electric vehicles promises a transition to a clean, non-polluting, healthy and safe means of transportation (see also Chapter 6 on life cycle environmental impact).

While there is a potential for electric vehicles to be safer than conventional ones we still need to consider what other risks this technological transition will bring as the risks associated with conventional vehicles are well known to most people and thus easily dealt with in daily life. What risks are associated with a large onboard chemical energy storage? Will the hazardous traction voltage of the electrical

system pose a danger to the passengers or to rescue personnel in case of an accident? How can eventual risks be diminished in traffic, when vehicles are parked and maintained? All these aspects and more need to be considered when designing the vehicle.

Safety issues for electric vehicles considered here include mainly battery powered vehicles, vehicles which have the battery as the only means to store energy (BEVs) or range extended vehicles where the battery is still the main source of energy but an extended range can be obtained using a combustion engine, for example plug-in hybrid vehicles (PHEVs). Another type of electric vehicle is the fuel cell powered car, using hydrogen gas as fuel. In this case, safety aspects mainly concern the safe handling and storage of hydrogen. While EVs are on the market in rapidly increasing numbers today, the fuel cell car has not reached true commercial introduction yet. Compared to conventional fuels hydrogen has both advantages and disadvantages, but again the risks are different to those we are familiar with and other safety practices are needed. We will, however, not include fuel cell safety issues in this chapter.

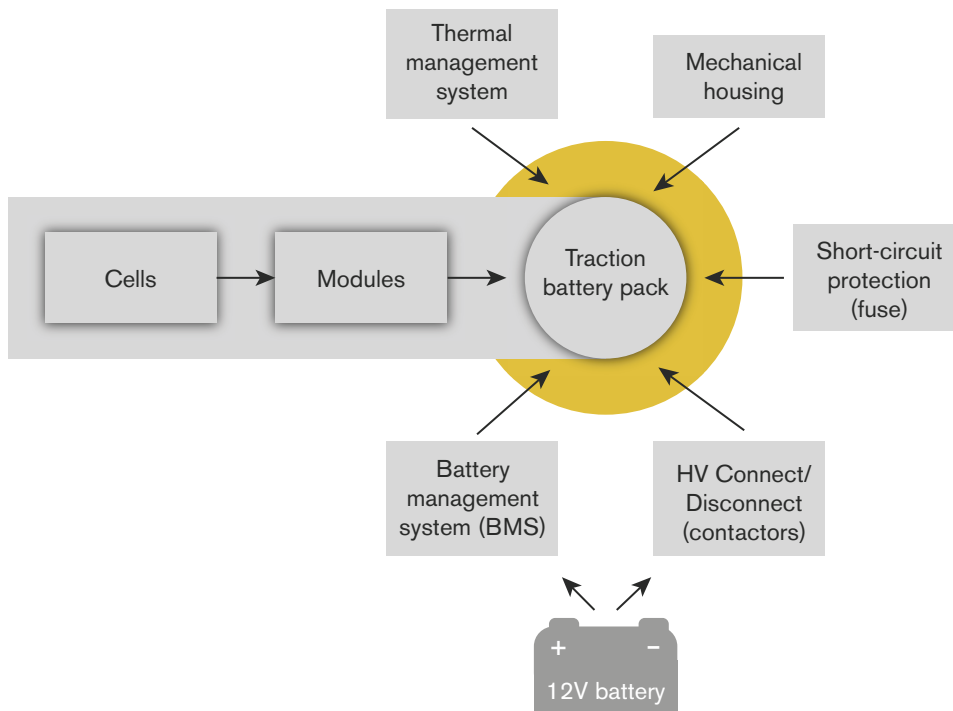
Lithium-ion (Li-ion) batteries have high energy and power densities that make it possible to build BEVs and PHEVs with acceptable electric driving range with zero tail pipe emissions. This type of battery has therefore become the preferred choice for manufacturers of these types of vehicles. In this chapter we focus primarily on the lithium-ion battery while other battery types are discussed more briefly. Other technologies for energy storage, e.g. flywheels, compressed air and supercapacitors might be used in future electric vehicles. Presently, they are used to a very limited extent and are therefore not included.

BATTERY SYSTEM DESCRIPTION

The traction battery system in an electric vehicle consists of many parts. Figure 4.1 shows the principle layout for a traction battery system. The basic building block in the battery pack is the battery cells. The cells are connected in series in order to increase the voltage. Cells can also be connected in parallel, in order to increase capacity. Typically a battery pack for an electric vehicle consists of 100-400 cells.

A number of cells form a module, which is typically kept under 60V at present (2013) and is thus not a particular electrical hazard. A battery pack usually consists of several such modules. To monitor and control cells, modules and pack each battery system has a master Battery Management System (BMS), often in combination with one or several slave management systems (e.g. one per module). The BMS has a number of functions essential for safe operation of the battery system: (i) Parameters such as cell voltage, current and temperature are monitored in order to ensure that the battery operates within the allowed limits, (ii) balancing of cells is performed in order to keep all cells on the same level regarding state of charge (SOC), (iii) contactors placed inside the battery pack in order to connect and disconnect the battery to the rest of the vehicle are controlled, (iv) the status of the electrical insulation of the traction voltage system is monitored and (v) the BMS communicates with the other parts of the vehicle as well as supplies information to the driver. As an independent means of electrical safety the battery often

has one or several fuses, for short-circuit protection. Furthermore, the thermal management system of the battery could both heat and cool the cells in order to maintain a temperature within an efficient and safe temperature range. A mechanical housing, the battery box, is used to enclose and protect the battery pack. It has several functions and a suitable tightness-class.



Figur 4.1 The traction battery system overview.

Typically the battery pack uses an external 12V supply from the vehicle's 12V-battery, e.g. a conventional lead-acid battery. The 12V supply is used to power up the BMS and to close the contactors. In principle, the battery could supply its own 12V by an internal DC/DC converter but an external supply is a simple solution that is commonly used.

BATTERY TYPES

Lead-acid batteries (PbA) have been used for more than 150 years and are still produced in large quantities as 12 V and 24 V vehicle batteries. There are several types, e.g. free ventilated or recombination cells (e.g. AGM, GEL). Compared to Nickel-metal-hydride and Li-ion batteries, they have lower power and energy densities and a significantly shorter cycle lifetime. Lead-acid batteries also require a long charging time, typically 10 hours. Since this should be seen as a fully mature technology it has been cost optimized. Due to its high weight and large volume it is not a real option for PHEVs or EVs, even though it was used experimentally in EVs during the 1990s. Presently lead-acid batteries are considered only for micro-hybrid electric vehicles (start and stop techniques). The safety concerns are small and related mainly to the risk of hydrogen gas production during operation. Hydrogen gas can potentially ignite and explode but the buoyancy of hydrogen gas makes it relatively easy to ventilate the battery in order to avoid the formation of

an ignitable mixture with air. Since lead acid batteries is a mature technology the battery design is very well developed to avoid these problems.

Nickel-metal-hydride batteries (NiMH) are presently dominating the HEV-market; they are used in the Toyota Prius for instance. NiMH offers significantly improved energy and power densities compared to lead-acid batteries. Further, it offers a high cycle life time and safety concerns are small. They do not, however, have the same energy storage capacity as Li-ion batteries.

Lithium-ion is the dominant battery technology today for PHEVs and EVs due to its high energy and power densities, combined with a long life time. The safety concerns are however larger than for NiMH and lead-acid batteries. This is basically due to the chemistries used for these cells but the large size of the battery systems needed for these types of vehicles also makes the consequences of a malfunction potentially more serious. We will therefore devote most of this chapter to describe safety aspects of Li-ion batteries.

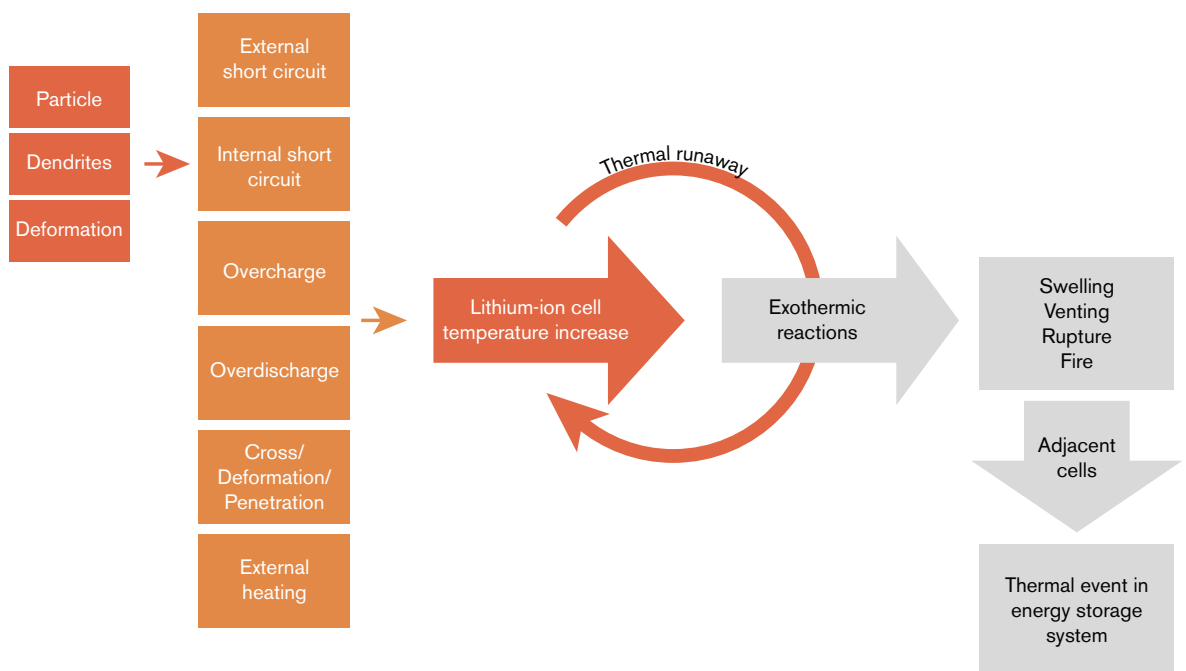
A lithium-ion cell consists essentially of anode, electrolyte, separator and cathode. The lithium ion is shuttled back and forth between the anode and cathode through the electrolyte. Even though a large number of different lithium-ion chemistries are possible there are today (2013) only a few lithium-ion chemistries that are used commercially. The anode and cathode are intercalated lithium compounds. Typically the anode is based on graphite, lithium titanate oxide (LTO) can also be used. The cathode is composed of lithium cobalt oxide (the most common type for small consumer cells), mixed oxides (manganese, nickel, cobalt, and aluminum) or phosphates (mainly iron-phosphate). The electrolyte typically consists of organic solvents, lithium salt and additives. The exact composition differs between the manufacturers and is usually a commercial secret, especially regarding the additives. The separator is a porous polymer where the pores are filled with the electrolyte; its primary function is to avoid direct contact between anode and cathode. In some cases the separator may also have the function of shutting down the ion transport in case of overheating.

The risks involved with the use of lithium-ion batteries are closely related to the chemistries used, the design of cell and system, the handling of the battery when in use and the quality of the production. The choice of cell chemistry is, in turn, determined by the demands regarding energy and power density, cost and safety for the specific application. Small size lithium-ion batteries have been used for more than a decade in consumer products, such as laptop computers and mobile phones. During this time, battery fire incidents have been reported in laptops, iPods, cargo planes and electric vehicles.¹ However, the conditions and requirements for lithium-ion batteries in automotive applications are different and more demanding than those for consumer electronics. Lithium-ion cells for the automotive industry are, for example, characterized by increased quality, safety and life time compared to that of small consumer cells, and generally use more advanced materials with higher degree of purity.

¹ Wang, Q., Ping, P., Zhao, X., Chu, G., Sun, J., and Chen, C., "Thermal runaway caused fire and explosion of lithium ion battery", *Journal of Power Sources*, 208 (2012) 210-214.

Lithium-ion batteries have many advantages but the window of stability is relatively small (both regarding temperature and voltage). The cells must therefore be monitored and controlled by the BMS. Overheating may cause a severe malfunction; if the temperature exceeds typically 120-150 °C, exothermic reactions within the cell can start. The exothermic reactions will increase the temperature further, which can trigger additional exothermic reactions. If the overall cell reaction creates a rapid temperature increase, it could result in a so called thermal runaway. A thermal runaway consists usually of one or a combination of the following events: rapid gas release, electrolyte leakage, fire, rapid disassembling/explosion.

The reason for the initial overheating may be an external short-circuit, overcharge, over-discharge, deformation of the battery by external forces, external heating or an internal short-circuit. The latter may be caused by dendrite growth, unwanted particles in the cell etc. If the overheating spreads to adjacent cells a large part of the battery system may be affected. Figure 4.2 shows how a thermal event on the cell level could develop to the system level. In order to obtain a high level of safety such a chain of events must be hindered.



Figur 4.2 Potential chain of events for a thermal event on the cell level developing to system level.

The outcome of these reactions varies with cell design and chemistry, particularly with the electrode and electrolyte composition. The combination of reactive materials and flammable components in the cell pose a risk, the electrolyte is flammable and the oxide materials may release oxygen at elevated temperatures, thus both fuel and oxidant needed for a fire might be present inside the cell.

In order to meet the demand of the automotive industry, improved battery materials have been produced. The selection of the active electrode materials (anode and cathode) strongly affects the thermal runaway and its onset temperature. Lithium iron phosphate (LFP) is for example a more stable cathode material than the

cobalt-based lithium oxides that are commonly used in consumer Li-ion batteries. Other electrode materials, for example mixed oxides with cobalt in combination with other metals (e.g. Ni, Mn, Al), have been developed in order to improve safety and other aspects (e.g. life time, cost, energy and power densities).²

The electrolyte composition and its additives, e.g. flame retardants, redox shuttles and gas release controllers, are also very important for the overall safety of the battery. The organic solvents involved, e.g. ethylene carbonate (EC) and dimethyl carbonate (DMC) are volatile and flammable. The mechanical packaging, cylindrical, soft or hard prismatic can or pouch-prismatic, also affects the cell behavior during a thermal event. For example, a cylindrical can cell could build up a much higher pressure than a pouch cell.

There are both pros and cons associated with each type of cell packaging. For example, with a cylindrical cell it can be easier to control the venting direction but higher internal cell pressure build up can be potentially more dangerous. Thus, there are a number of safety mechanisms that can be included into a lithium-ion cell construction by its manufacturer depending both on the chemistry and physical design of the battery.

It takes a long time to develop new battery technologies, typically more than 20 years. Potential future battery storage technologies is a very active field of research and one of the most interesting future battery technologies is the *lithium-air battery*, which has a huge potential compared to Li-ion batteries, e.g. the energy density is projected to be more than 10 times that of Li-ion batteries. There are, however, several challenges to be solved for the lithium-air technology, e.g. regarding life time and safety. One safety concern is how to prevent air from reaching the free lithium-metal. Li-air batteries are, however, not likely to be commercialized within at least 20-30 years.³

VOLTAGES, CURRENTS AND ELECTRICAL HAZARDS

An electrified vehicle still contains electrical energy in the battery when it is shut-down and parked. The manufacturer has constructed the vehicle in such a way that the hazardous traction voltage is kept inside the battery pack and insulated from the rest of the vehicle. In other words, all parts except the inside of the battery system can be considered as voltage free (provided there are no electrical insulation failures). It is important to understand that also an “empty” battery, meaning fully discharged, 0% SOC, still has a considerable voltage. For an electric vehicle this is still to be considered as a hazardous voltage. The definition of hazardous voltage is that it is potentially dangerous for humans, and it is usually stated as > 60 VDC (although this limit varies in different countries).

Vehicles with internal combustion engines have had a remarkable increase in vehicle safety during the last 10-20 years. Active safety is now starting to be introduced in some cars, e.g. lane departure warnings. The passive safety, e.g.

² Wang, Y., Jiang, J., Dahn, J., “The reactivity of delithiated $\text{Li}(\text{Ni}_{1/3}\text{Co}_{1/3}\text{Mn}_{1/3})\text{O}_2$, $\text{Li}(\text{Ni}_{0.8}\text{Co}_{0.15}\text{Al}_{0.05})\text{O}_2$ or LiCoO_2 with non-aqueous electrolyte”, *Electrochemistry Communications*, 9 (2007) 2534-2540.

³ G. Girishkumar, B. McCloskey, AC Luntz, S. Swanson, W. Wilcke “Lithium- air battery: Promise and challenges” *Journal of Physical Chemistry Letters* 2010, Vol. 1(14), p. 2193–2203.

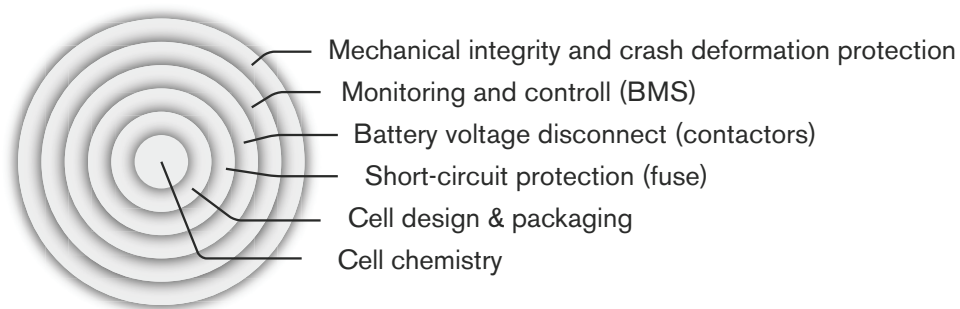
crash protection, has evolved greatly over the years with e.g. the NCAP testing. Computer simulations and crash tests have fostered the development of crash deformation structures significantly and increased crash and collision protection.

Electrified vehicles are likely to have the same level of passive and active safety as conventional vehicles. In order to ensure this, the safety techniques must be adapted for this new technology, e.g. during a crash, crash detection sensors inside the vehicle, also used for activation of airbags, can disconnect the traction voltage from the battery before the crash is complete. This means, that even if the electrical insulation of the traction voltage, containing the hazardous voltage, would be damaged, this voltage will be turned off. Of course, in severe crashes, there is always a risk that this might not be the case.

Presently (2013), car manufacturers crash protect the battery pack so that no short-circuit may occur in its electronics and that no lithium-ion cell can be deformed during pre-defined crash scenarios. In principle, this is done by putting the battery inside a crash protected box. This adds weight, volume and costs. In the future, it is likely that the battery pack instead becomes a part of the crash structure. Battery packs of today can handle some small deformation; this is a matter of design, which today varies depending on cell chemistry, cell design and packaging. In the future, it is likely to have safer lithium-ion cells and battery systems which could to a higher level stand a deformation. In that case the battery can to a larger extent be used in the vehicle's crash structure. The deformation protection design criteria are given by load-cases. This means that for a severe crash, which is outside the design criteria, a deformation which is larger than expected can occur. It is unrealistic and just not possible to design the crash protection for all types of extreme collisions.

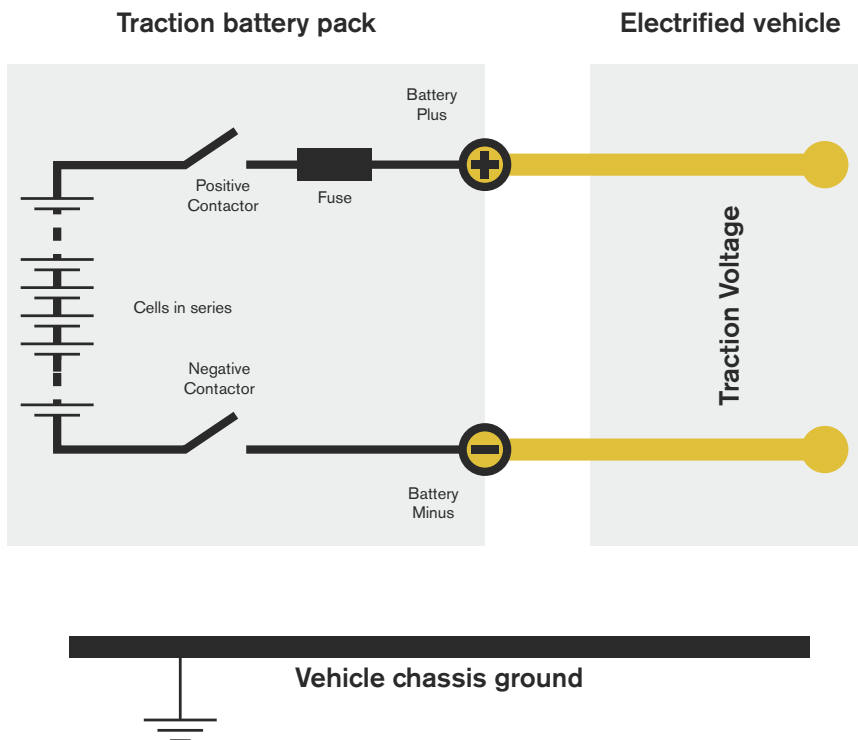
The electrical drive train is made safe by several means. In general the battery cells presently used are in general very safe since judicious choice of Li-ion technology ensures that an unsafe lithium-ion cell would not be chosen. The voltage of each lithium-ion cell is in general monitored and balanced with respect to the other cells. This requires quite advanced electronics and electro-components such as fuses and contactors are used in the battery pack. The electronic parts (electrical components, processors, circuit-boards etc.) of the battery pack are similar to the parts used in conventional vehicles by a large part of the industry. In case of errors in the electronics or sensor failures an unsafe situation could occur. However, the manufacturers work with functional safety (e.g. ISO26262) in order to minimize these risks.

The battery safety is ensured by the manufacturer by adding layer by layer of safety, schematically shown in Figure 4.3. Deformation of the battery cell can result in a thermal event. Therefore the battery is usually placed outside the deformation zone. For a passenger car, this generally results in a battery placement inside or beneath the passenger compartment.



Figur 4.3 An example of battery safety layer by layer.

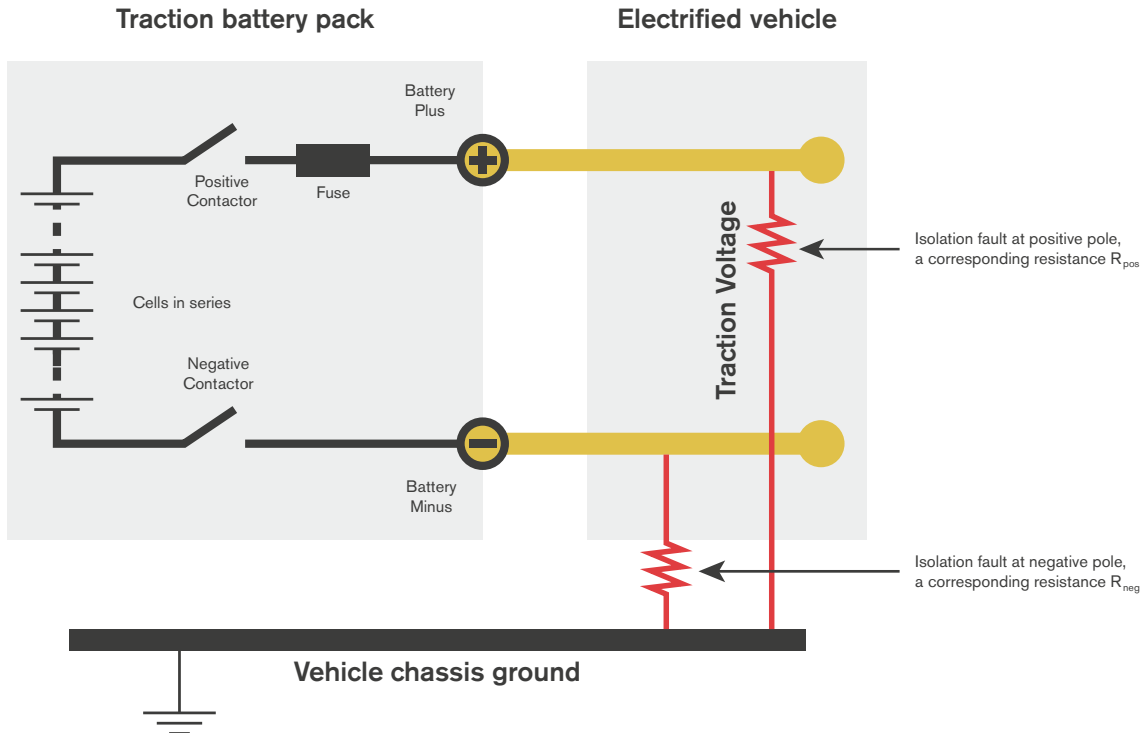
The components and traction voltage cables carrying a high voltage are usually very well insulated and protected. The risk that a human, e.g. driver, passenger, rescue personnel or firefighter, would be exposed to an electrical shock is in general very low. The traction battery has a so called floating ground, meaning that there is no electrical connection between the traction battery poles and the vehicle chassis ground. The 12V/24V vehicle battery on the other hand (for both conventional ICE vehicles and EVs) uses the vehicle chassis ground as the current return path to the negative 12V/24V pole. The principle of the floating ground and the current path of the traction battery are shown in Figure 4.4.



Figur 4.4 Traction battery pack current path and the floating ground principle. If there are no insulation fault(s), there are no electrical connections between vehicle chassis ground and the battery poles.

Both DC (direct current) and AC (alternating current) voltages are present in EVs (see also Chapter 3). The DC voltage comes from the traction battery and the AC voltage is used by the power electronics and electric motor. Both pose a danger for humans in case of an electric shock caused by either a direct touch of the battery poles, or indirectly by touching the metal chassis. In order for such exposure

to occur, two insulation faults are required (one at each pole of the battery) and the victim must touch metallic parts with the different potentials at the same time. Figure 4.5 shows the principle of a double insulation fault.



Figur 4.5 Principle figure that shows a double insulation fault. This means one insulation fault at the plus and one at the minus pole. They are shown as two resistances, R_{pos} and R_{neg} , connected to ground. This creates a current path between battery plus and battery minus.

The vehicle chassis ground is usually constructed to electrically act as one pole of the 12/24 V system by having most metal parts connected to each other. In the situation of a double insulation fault there will be a short-circuit through the chassis. Since the current takes the easiest path (i.e., the conducting path with the lowest resistance), the human body will hardly be affected by touching the chassis ground. On the other hand, there could be a potential risk for service personnel repairing a damaged electric vehicle, since they can, during disassembly, have two chassis ground, one with the negative battery potential (minus) and the other with positive battery potential (plus). There are however, protection means for this, e.g. insulation measurements, electrically insulated gloves (typically marked for safe use up to 1000V), and knowledgeable maintenance staff should be able to minimize this risk.

It could be mentioned that hazardous voltages, both DC and AC, inside the components in an EV, sometimes are referred to as “high voltage”. From the automakers perspective, this term conveniently separates the 12/24V system (“low voltage”) and the 300-600 V system (“high voltage”) for the electric drivetrain and the traction battery. However, to name the hazardous traction voltage as “high voltage” is somewhat misleading since there is already a definition and a long time tradition to use the term “high voltage” within the mains (electricity grid), for voltages over 1000 VAC or over 1500 VDC. The term “HV” is actually in automotive industry sometimes interpreted as “hazardous voltage” (instead of “high voltage”).

FIRES, GASES AND EMISSIONS

The energy stored in the battery in an electric vehicle is essentially released once you connect the two poles while the energy in a conventional vehicle requires the fuel to be mixed with air at the right proportion and pressure and then the gas mixture needs to be ignited by a spark or by exposure to high temperatures; the spark could for example be created by the starter engine. The higher voltages and currents used in an electric vehicle may be a risk for fires and lithium-ion batteries pose a special risk as the electrolyte is combustible, with properties similar to gasoline or LPG. Furthermore, the battery might progress into thermal runaway as described previously. One of the safety mechanisms used in these cells to prevent a more severe incident to occur is venting. The gases released in a venting situation are, however, highly toxic and flammable. In particular, a venting cell would release hydrogen fluoride (HF) which is highly toxic. Venting would also release many other fluorinated substances that have a potential of being toxic, but the toxicity of these has not yet been publically investigated.

If a fire starts, many of these substances might be consumed in the fire but the knowledge in this field is still limited and more research is needed regarding evolved gases from battery fires. HF is a gas that evolves in many different types of fires. Recently INERIS in France set two different electric vehicles and two similar conventional ICE vehicles on fire and measured the heat release rate during the fire and also gases evolved including HF. They found that the heat release rate was of the same order of magnitude, independent of vehicle type. High concentrations of HF were emitted in the beginning of the fire for all four vehicles. This might have been caused by the air-conditioning system. Some HF also evolved later in the fire for EVs, but the concentration was less than that of the first spike of HF and distributed over a longer time period.⁴

Anecdotal evidence exists that electric vehicles burn fiercely and that the fire is difficult to extinguish. The INERIS experiment does not confirm this burning behavior but the fire was started by a gas burner in one of the seats in these experiments. Other means of starting the fire might give another result but there are at present a very limited number of investigations, if any, available on this topic.

Extinguishment of a fire is an area where there still are questions to be answered. The advice from manufacturers is often to let the vehicle burn or to use water or sand. Letting the vehicle burn is not a viable option in e.g. a garage, a ferry or in a tunnel. Research for fire-fighters has until now mainly focused on extrication of people from crashed cars and not on extinguishment. In general, water is an excellent extinguishing medium that has a very high extinguishing power per mass. However, when it comes to potential live electric parts the advice is often to avoid using water. Research is therefore needed on how to attack a fire in a battery. Would it be safe to use water both in terms of the risk of electric shock and when it comes to gases evolved? Should other methods be used to respond to a fire? In addition a fire in the battery system might be difficult to reach. It is only just recently that a first extinguishing study was available. This study was conducted by

⁴ A. Lecocq, M. Bertana, B. Truchot and G. Marlair "Comparison of the Fire Consequences of an Electric Vehicle and an Internal Combustion Engine Vehicle" Proceedings of FIVE 2012, Chicago, 27-28 September 2012

DEKRA in Germany where batteries were extinguished using water and different additives.⁵ They conclude that more water was needed for the EV fires than for vehicles with conventional internal combustion engines.

The EV users would like to be able to charge their vehicle fast in some situations, similar to filling fuel into a conventional vehicle, or at least have a significantly shorter charging time than that of overnight charging. Systems for fast charging are therefore under development. Fast charging requires high currents and one would therefore intuitively associate this with larger fire risks. The high current would result in a higher risk of overheating or other malfunctions in the charging station or in the vehicle itself and thus careful design is important. These risks are well known and when the number of fast charging stations will grow actions will be taken to minimize associated risks.

INCIDENTS

Despite the manufacturers efforts to produce safe batteries some events have occurred that have reached media attention. One of the major media events in June 2011 was the fire that started in a GM Chevrolet Volt car three weeks after a crash test. The incident was thoroughly investigated by NHTSA and the chain of events was reproduced. The reason was found to be that the cooling media had leaked over the battery and then dried; leaving crystals that finally short-circuited the battery through the metallic belt around it. Changes have since been made to the design, e.g. to avoid leakage of cooling media.

Another event that has drawn some media attention is the fires that occurred after hurricane Sandy hit the Atlantic coast in the New York area in November 2012. At the harbor of Newark, New Jersey, thousands of parked vehicles were flooded. The cars were brand new shipped in from abroad. The water wave that followed Sandy immersed the parked vehicles in 1.5-2.5 meters of seawater during several hours. It has been reported that sixteen Fisker Karma PHEVs and a few Toyota Prius HEV and PHEV burned. Unconfirmed statements from Fisker and Toyota blame the fires on short-circuits in the 12V vehicle electronics. NHTSA and Fisker have started an investigation to find the cause of the fires. To be submersed in 1.5-2.5 meter deep seawater for several hours is a very severe test for an electrical system in general which can only be met with IP68 class or equal water-tightness level. Seawater is a good electrical conductor and can cause short-circuits, for both low voltage (e.g. 12/24V vehicle voltage) systems and for the traction voltage in electrified vehicles.

Apart from these events there are some other events that have not reached media interest. Focus on battery safety has to a large extent been on the cells as such and much progress has been made in this respect. The traction voltage parts of the system are also subject to many protection steps in many cases. It is important, however, to take into account that the cells are part of a large system with a lot of electronics that needs to be functioning in a harsh environment as vehicles are subject to many different situations.

⁵ Electric car batteries 'at least as safe as combustion cars' (2012)

OUTLOOKS FOR THE FUTURE

Safety issues are of major concern in any introduction of a new product into the market as negative publicity might have a negative impact of general public's perception of a product and the products potential to succeed. Key aspects here are to design safe products and be very open about events that have occurred as ample correct information is the best way to avoid rumors. One threat to a safe introduction could be home-converted vehicles as these, with their limited budget, would have difficulties reaching the same high safety levels as commercially built vehicles.

Lithium-ion batteries for automotive use have shown an increased safety regarding fire and explosion through e.g. improved electrode and electrolyte materials. Therefore, the focus of lithium-ion safety research has moved increasingly towards the safety aspects associated with released gases and smoke, as well as other electrical aspects.

The choice of material for future batteries is a fundamental issue including possible scarcity problems. Further, the choice of different additives to obtain sufficient safety, e.g. flame retardants, or other necessary battery characteristics can result in life-cycle issues which will be untenable. New technologies are necessary which will no doubt pose new risks which will need to be addressed.

The number of EVs on the road is still low so reliable statistical studies of incidents and accidents are not possible yet, anyhow, the numbers are increasing steadily and with that also the possibility to conduct different safety studies as the price per vehicle is lowered and the vehicles are commercially available and not only leased etc. It is therefore likely that we will see an increasing number of studies on different safety aspects that still need to be resolved which will foster the development of safer EVs.

Paper II

Energy storage system safety in electrified vehicles

Fredrik Larsson^{1,2} and Bengt-Erik Mellander²

¹SP Technical Research Institute of Sweden AB, Borås, Sweden

²Applied Physics, Chalmers University of Technology, Göteborg, Sweden

ABSTRACT

The environmental challenges with CO₂ emissions and a diminishing oil reserve drive the need of a broad introduction of electrified vehicles. The relatively new lithium-ion battery technology offers batteries with increased energy and power densities. Li-ion technology requires a monitoring system since its safety window is lower than many other battery technologies. In an energy storage system for electrified vehicles safety aspects thus have to be taken into serious consideration. In this paper fire as a consequence of malfunction or abuse of the energy storage system is discussed.

KEYWORDS: energy storage system, electrified vehicle, lithium-ion, battery, safety, thermal runaway, fire

INTRODUCTION

An electrified vehicle has a traction system which can be either pure electric or a combination of electric and some other source (e.g. fossil fuel). New battery technologies, e.g. lithium-ion, makes it possible to build electric vehicles (EV) and plug-in hybrid vehicles (PHEV) with acceptable driving range with zero emissions. The Li-ion cells offer high energy and power densities and are constructed with advanced materials. There are however, still aspects to consider for these new technologies and electrified vehicles. A drawback is that the window of stability is relatively small (both regarding temperature and voltage region) and the lithium-ion cell materials are volatile and flammable. Safety is thus an important issue due to the combination of the reactive nature of the cell materials and the presence of hazardous voltages in the vehicle.

LITHIUM-ION BASICS AND THERMAL EVENTS

Lithium-ion cell technologies have been used for more than 10 years in consumer products, such as laptop computers and mobile phones. During the years, there have been fire incidents with these batteries. The last 5 years, reports have been made regarding battery fire incidents in e.g. laptops, iPods, cargo planes and electric vehicles [1].

Lithium-ion cells consists of different layers, essentially; anode, separator, cathode and electrolyte. The electrolyte consists of organic solvents, lithium salt and additives. The electrolyte recipe is every cell manufacturer's secret, especially regarding the additives. The organic solvents, e.g. ethylene carbonate (EC) and dimethyl carbonate (DMC) are flammable. Lithium is a reactive metal while the lithium-ion is more stable. Lithium metal can however be formed during normal and abusive use.

Under abuse or malfunction conditions, the lithium-ion cell temperature can increase. If the temperature reaches typically 120-150 °C, exothermic reactions within the cell starts. The exothermic reactions will further increase the temperature, which could start additional exothermal reactions. If the overall cell reaction creates a rapid temperature increase, it could result in a so called thermal runaway, which could consist of one of or a combination of the following; rapid gas release, electrolyte leakage, fire, rapid disassembling/explosion.

Figure 1 shows an overview of the potential chain of events for a thermal runaway. On the left side in the figure, the sources of a cell temperature increase are shown. Furthermore, one cell could affect the

adjacent cells. In a worst-case scenario the thermal events from one of several cells could spread and affect the complete energy storage system.

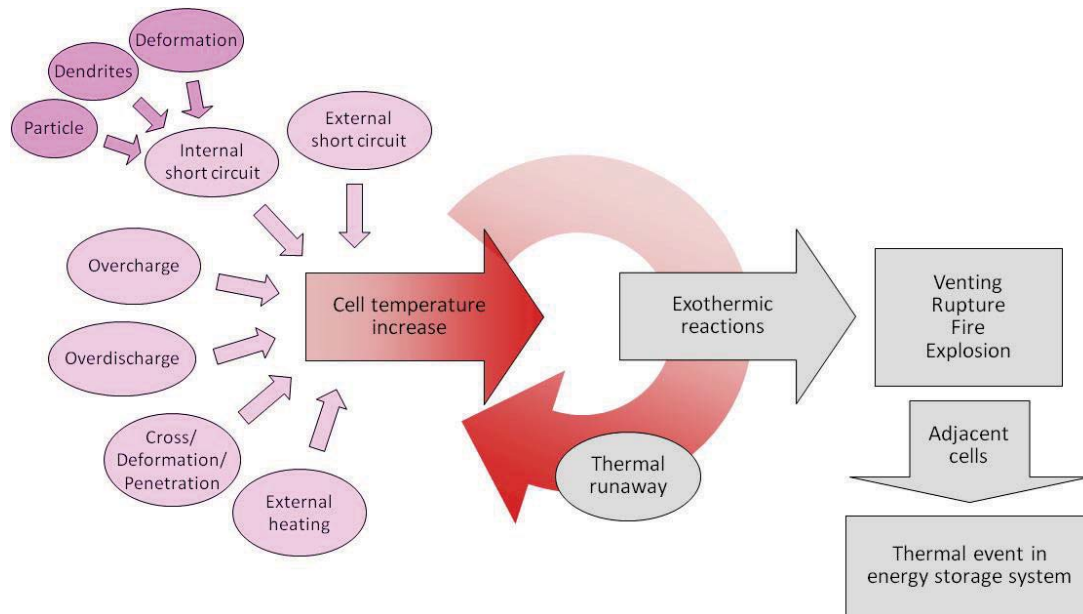


Figure 1. Potential chain of events for a thermal event on the cell level developing to system level.

LI-ION FOR AUTOMOTIVE USE

The conditions and requirements put on lithium-ion batteries in automotive applications are different from those in consumer electronics. Basically, Li-ion batteries for consumer products do not meet the needs of the automotive industry. The safety aspects, which are discussed in this paper, are just one on many aspects which must be considered in a different perspective.

In order to meet the demand of the automotive industry, new lithium-ion battery materials have been developed. Lithium iron phosphate (LFP) is a more stable cathode material than the mainly cobalt-based lithium oxides that are commonly used in consumer Li-ion batteries. Researchers has also developed other electrode materials, for example mixed cobalt with other materials (e.g. Ni, Mn, Al) in order to improve safety and other aspects (e.g. life time, energy and power densities) [2].

The cell design, both chemical and mechanical, affects safety. The cell manufacturer can influence the electrolyte composition and its additives [3], e.g. flame retardants, redox shuttles and gas release controller. The selection of the active electrode materials (anode and cathode) also affects the thermal runaway and its onset temperature. The mechanical packaging, e.g. cylindrical, soft or hard prismatic can or pouch prismatic, also affects the cell behavior during a thermal event. For example, a cylindrical cell could build up a much higher pressure than a pouch cell. There can be both positive and negative aspects on each cell packaging. For example, with a cylindrical cell it can be easier to control the venting direction. There are thus a number of safety mechanisms that can be included into a lithium-ion cell construction, by its manufacturer [4].

Lithium-ion batteries for automotive use have shown an increased safety regarding fire and explosion. Therefore, the focus of the lithium-ion safety have drawn more and more towards the safety aspects of released gases and smoke, as well as other electrical aspects, e.g. electromagnetic compatibility (EMC).

EXPERIMENTAL

In order to experimentally study thermal runaways in lithium-ion cells three cells of size 18650 were thermally abused in a thermostated oven. Two of the cells were standard laptop batteries from Samsung and Sanyo with unknown cathode composition, most likely cobalt mixed oxides. The third

18650 cell was manufactured by K2 Energy and had a lithium iron phosphate (LFP) cathode. The cell was fastened on a brick and centrally placed inside the oven. The oven was equipped with a fan system to circulate the air to achieve a uniform temperature. The cells were tested one at a time with continuous heating from ambient temperature up to the onset of thermal runaway or to max 300 °C, without any ramping or stops. Prior to the test, the cells were fully charged to 100% SOC according to each manufacturer's charging instructions. Each cell was equipped with four thermocouples, placed uniformly with two sensors on the top and two sensors on the bottom of the cell. Figure 2 shows the average cell surface temperature for the three tested cell types.

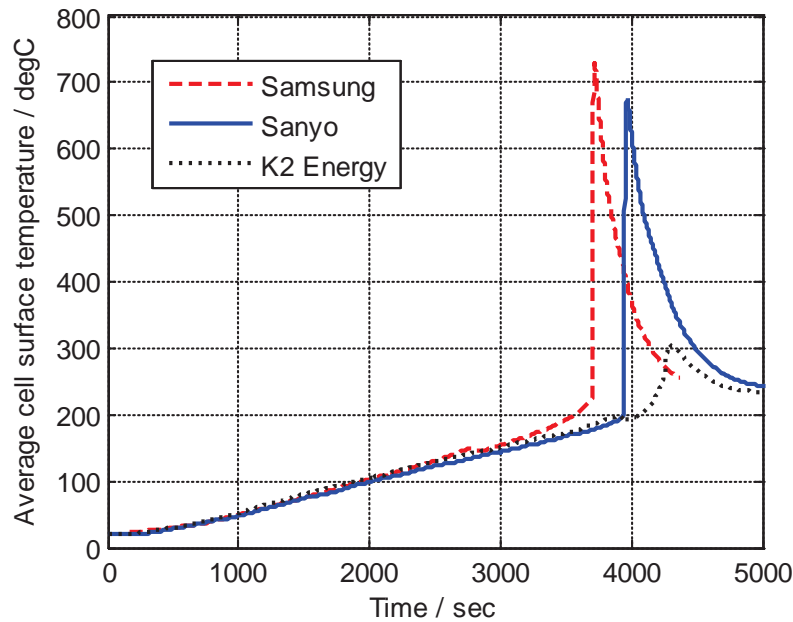


Figure 2. Temperature development for three 18650 lithium-ion cells during thermal abuse tests.

All cells vented and got into thermal runaway. The cells from Samsung and Sanyo with the cobalt mixed oxide showed a very rapid temperature increase at the onset of thermal runaway. The LFP based cell from K2 Energy also entered thermal runaway but with a more modest temperature increase. Both Samsung and Sanyo cells started to burn during the thermal runaway while the K2 Energy cell did not burn. Table 1 shows basic cell data and extracted thermal runaway results where the rise time is the time between the onset and peak temperature of the runaway. The temperature rise is the difference between onset and peak temperatures of the runaway and the temperature rise rate is the ratio between temperature rise and rise time. As seen from the results the cell with the LFP cathode demonstrates a more safety performance than the laptop cells with a lower temperature rise rate and no fire.

Table 1. Basic data for tested cells and extracted results from the thermal runaway.

Cell type	Cell data		Thermal runaway results			
	Nom voltage (V)	Nom capacity (Ah)	Onset temperature (°C)	Temperature rise (°C)	Rise time (sec)	Temperature rise rate (°C/sec)
Samsung ICR18650-24F	3.6	2.4	227	503	20	25.2
Sanyo UR18650F	3.7	2.2	198	477	26	18.3
K2 Energy LFP18650E	3.2	1.25	213	91	157	0.6

LITHIUM-ION BATTERY FIRE DEVELOPMENT

When discussing fire in an energy storage system, two main fire types should be considered. The first type is the reaction within the lithium-ion cell material itself, that is, reactions between electrolyte and electrodes. The special properties in this case are; an accelerated process due to exothermic reactions and self-supply of oxygen due to oxygen released by the reactions itself. Therefore, this fire is difficult to control and extinguish. In theory, the thermal runaway reactions could be stopped by cooling the cell below the onset temperature of the reaction. In practice, as seen in Figure 2, the temperature development is so rapid that simultaneous cooling is difficult to achieve after the onset of the thermal runaway, a more viable option is to make sure that the onset temperature is not reached.

The second type is a more traditional fire, that is, a fire which requires oxygen from its surroundings. It could be fires in e.g. plastics, cables and housing inside the energy storage system as well as in parts of the cell. Free electrolyte from cells or fire in plastic insulation and separator on a cell-level may be part of this type of fire. Furthermore, a fire of the first type, involving a thermal runaway inside a cell could start a fire of the second type, and vice versa.

The design of the energy storage system is important in order to make it possible to stop or retard additional cells from going into thermal runaway. As always with batteries, adding additional safety is a compromise that adds negative consequences, e.g. adds weight, volume and costs to the system. However, the access of fire fighting media to be applied on the cell surfaces inside an energy storage system is usually very limited due to the packaging design of energy storage systems and electrified vehicles. A lithium-ion cell which undergoes thermal runaway or other severe conditions (e.g. overtemperature) will react with swelling and could release gases, smoke and particles. The gases released during cell venting are flammable and could thereby be ignited by a spark in the vicinity. Regarding the electrified vehicle and the integration on the energy storage systems as well as the hazardous voltage systems in the vehicle, the design for crash safety is vital.

THE OVERALL SAFETY OF THE ENERGY STORAGE SYSTEM

The overall safety of a complete electric vehicle and energy storage system will not only be a function of the cell safety but also of many other parameters on the system level. The battery management system (BMS) is very important in order to e.g. monitor and prohibit critical situations, alerting the driver in case of a thermal event, activate potential available counter-actions and controlling the shut-down procedure of the system, which should be constructed under consideration of the complete safety of the electrified vehicle. The cooling system and the mechanical housing and structures are other important parameters. The positioning of the cells within the battery pack is also essential, and should e.g. consider cell venting properties.

In order to obtain a safe system, all components and its properties must be considered. One of the key design parameters to understand when designing an energy storage system for electrified vehicles are the mechanisms for spreading of gases, smoke, fire and heat from components (e.g. battery cells) to battery system and to the complete electrified vehicle.

ACKNOWLEDGEMENTS

The authors would like to thank the support from Swedish Energy Agency and the FFI-program.

REFERENCES

1. Wang, Q., Ping, P., Zhao, X., Chu, G., Sun, J., and Chen, C., "Thermal runaway caused fire and explosion of lithium ion battery", *Journal of Power Sources*, 208 (2012) 210-214.
2. Marom, R., Amalraj, S.F., Leifer, N., Jacob, D. and Aurbach, D., "A review of advanced and practical lithium battery materials", *Journal of Materials Chemistry*, 2011, 21, 9938.
3. Zhang, S.S. "A review on electrolyte additives for lithium-ion batteries", *Journal of Power Sources*, 162 (2006) 1379-1394.
4. Balakrishnan, P.G., Ramesh, R., Prem Kumar, T.P., "Safety mechanisms in lithium-ion batteries", *Journal of Power Sources*, 155 (2006) 401-414.

Paper III



Abuse by External Heating, Overcharge and Short Circuiting of Commercial Lithium-Ion Battery Cells

Fredrik Larsson^{a,b,z} and Bengt-Erik Mellander^a

^aDepartment of Applied Physics, Chalmers University of Technology, Goteborg SE-412 96, Sweden

^bSP Technical Research Institute of Sweden, Boras SE-501 15, Sweden

Lithium-ion batteries offer great energy and power densities but the thermal stability is an issue of concern compared to other battery technologies. In this study different types of abuse testing have been performed in order to compare the battery safety for different types of commercial lithium-ion battery cells. The results show large differences in abuse response for different cells. Exposed to external heating laptop cells with cobalt based cathode developed a thermal runaway resulting in pressure release, fire and temperatures over 700°C. Lithium iron phosphate (LFP) is known to be a very thermally stable cathode material and LFP-cells showed a significantly lower thermal response, a thermal runaway could, however, be detected for some of the cells in the external heating test. The overcharge tests of LFP-cells were in most cases uneventful but in one case the test resulted in a violent fire. The short circuit tests showed modest temperature increases of the cells in spite of high currents peaking at around 1000 A. Although the development of safer lithium-ion battery cells has been successful thermal runaway events may still occur under extreme conditions. © 2014 The Electrochemical Society. [DOI: 10.1149/2.0311410jes] All rights reserved.

Manuscript submitted April 28, 2014; revised manuscript received June 4, 2014. Published July 11, 2014.

The high energy and power density of lithium-ion batteries have made them the preferred type of battery for battery electric vehicles as well as for plug-in hybrid electric vehicles. Lithium-ion batteries have many advantages but the reactive, volatile and flammable materials present in the battery are a concern and may be a threat to safety. Lithium-ion batteries are produced in large quantities, mainly for small consumer products such as cellular telephones and other portable electronic devices. Using them in electric vehicles poses another situation since the large size of the battery as well as the environmental conditions that the battery is exposed to in terms of temperature, vibrations etc have an influence on the safety. In addition, requirements such as long life time and the possibility for a fast recharge of the battery calls for other demands on the cells. All these aspects have an effect on the safety of the vehicle, including the safety for people inside and outside the vehicle, for service personnel involved in maintenance and of rescue personnel in case of an accident.

Lithium-ion batteries have a limited window of stability regarding temperature and voltage. Overheating may start exothermal reactions that release even more heat which in turn can lead to an accelerated process called a thermal runaway. A thermal runaway can be devastating if it spreads to a complete battery system, releasing large amounts of energy. Such a process could start due to overcharge, overdischarge, mechanical deformation, external heating or an external or internal short circuit, see Figure 1. The heat generated by any of these events may start exothermal reactions in the battery that in turn could lead to cell venting, fire or explosion.

These risks are well known¹⁻⁸ and are not only associated with the heat and high temperatures that may develop, the emission of harmful or poisonous gases also pose a danger that has been emphasized in literature,^{9,10} but also other gases which can be flammable may be emitted.¹¹⁻¹³ The reactions during overheating are typically due to the decomposition of the solid electrolyte interphase (SEI) layer, anode and cathode as well as electrolyte decomposition and combustion.^{5,14} These reactions are exothermal. In addition to this separator melting, an endotherm event, may occur. Oxygen may be released at the positive electrode during decomposition; this oxygen can provide the oxidant for the combustion of the electrolyte. Large efforts have been spent on improving the safety of Li-ion cells, e.g. by replacing the cobalt based electrode by lithium iron phosphate¹⁵ which is more thermally stable and has long life time and high power density but lower energy density.¹⁶ Another common practice for commercial cells is to use a number of additives to the electrolytes to improve safety, e.g. including fire retarders.¹⁷⁻²⁰

Incidents involving lithium-ion batteries have been reported in small as well as large battery systems, see for example Wang et al.²¹

and Mikolajczak et al.²² Abuse tests of batteries are therefore of prime importance in order to evaluate and improve the level of safety for these types of battery systems. In this article results from abuse tests of commercial Li-ion batteries of different type, chemistry and size are presented to illustrate the problems that may arise under abnormal operating conditions.

Experimental

Four types of commercial cells were tested; a Samsung 18650-cell, i.e. a cylindrical cell 18 mm in diameter and 65 mm long, typically used in laptops; two EiG cells of pouch-type with lithium iron phosphate (LiFePO₄) cathode, and a carbon-based anode (a newer and an older cell design); a European Batteries cell of pouch-type with lithium iron phosphate cathode and graphite anode. A summary of the cell specifications is provided in Table 1. The EiG cells were optimized for power application while the European Batteries cell as well as the laptop cell was optimized for energy applications. All cells were fully charged, 100% State of Charge (SOC), according to the manufacturer's instructions.

Three types of abuse tests were performed; external heating, overcharge and short circuit tests. All measurements were performed in a similar but not identical condition as described in international test standards for batteries such as FreedomCAR²³ or SAE J2464.²⁴ Cells of different sizes, packaging, chemistries and manufacturers were tested. Most tests were repeated in order to account for the variations between individual cells. The tests presented in this paper are a selection of representative examples of these tests. For the Samsung 18650 cell only results from external heating tests are presented since overcharge and short circuit tests would not be of interest due the built-in cell protection mechanisms in the cell.

External heating test.— In the external heating test, the cells were heated to excessive temperatures in order to examine their thermal stability. This test is sometimes referred to as thermal ramp test. The tested cell was placed inside a thermostatically controlled oven, Binder FED 115. The oven has a microprocessor control and a PT 100 temperature sensor for internal regulation of oven temperature. The oven's internal fan was set on full speed in order to circulate the oven air to obtain a uniform temperature around the tested lithium-ion cell. The cells were placed on one or two bricks in the center of the oven and tested one at a time, see Figure 2. For the pouch cells the oven temperature was first set to 80°C and thereafter increased in steps of 10°C every 15 min until either any thermal runaway had occurred or to the maximum temperature of the oven (300°C). For the 18650 cell the oven was set to the maximum temperature (300°C) with continuous maximum heating. Both heading procedures were relatively slow.

^zE-mail: vegan@chalmers.se

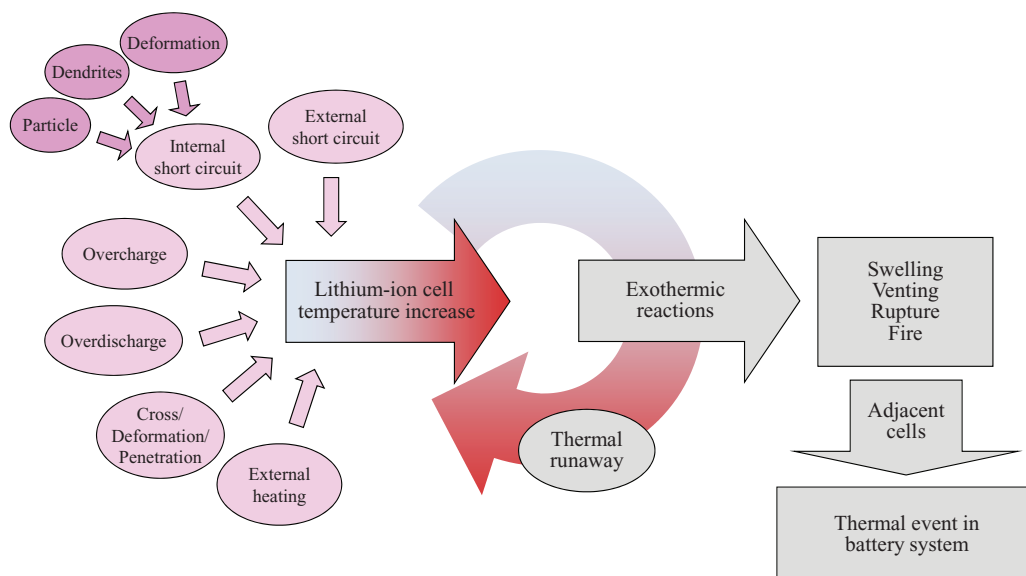


Figure 1. Lithium-ion thermal runaway overview from cell event to potential system event.

Table I. Basic data of tested cells.

Cell type	Cell packaging	Nominal voltage (V)	Nominal capacity (Ah)
Samsung ICR18650–24F	Cylindrical	3.6	2.4
EiG ePLB-F007H <i>In article referred as “older design”</i>	Pouch	3.2	7
EiG ePLB-F007A <i>In article referred as “newer design”</i>	Pouch	3.2	7
European Batteries EBattery 45 Ah v1.4	Pouch	3.2	45

With the continuous heating method it took around 90 min for the oven to reach 200°C.

The cell voltage and the cell surface temperature were measured with a sample rate of 1 Hz with a data logger, Pico Technology ADC-24. There were up to five type K thermocouples evenly distributed on both sides of the cell’s surface and one additional thermocouple measuring the oven temperature.

Overcharge test.— In the overcharge test, the lithium-ion cells were abused by being charged beyond their limits. The charger was limited to the preset maximum current of each experiment and up to max 15.3 V. The 7 Ah EiG cell was charged with 70 A (corresponding to 10 C-rate) considering that the cell is optimized for power applica-

tions while the 45 Ah European Batteries cell was overcharged with 90 A (corresponding to 2 C-rate) due to its optimization for energy applications. The cell surface temperature was measured with five type K thermocouples; one of the sensors was directly attached to the cell surface while four were so called plate-thermometers, that is a thermocouple attached to a 10 × 10 cm metal plate. The plate-thermometers were distributed around the cell, one directly under the cell, the others placed with an air gap from the cell. The current was measured using a current shunt (accuracy 0.5%). Cell voltage, current and temperature were measured with a sample rate of 1 Hz with a data logger, Pico Technology ADC-24.

Short-circuit test.— EiG and European Batteries cells were short circuited using 50 mm² copper cables and a high current contactor, Telemecanique LC1F630, with a low internal resistance of 40 μΩ. The short circuit current was measured by a current core, Hitec 6000E Topacc 1.0, which can measure currents up to 6000 A. The cell surface temperature was measured with eighteen type K thermocouples equally distributed on both sides of the cell surface. The cell voltage, current and temperature were measured at 1 Hz using two data loggers, Pico Technology ADC-24 and Fluke Hydra Series II, as well as by a Tektronix TDS 3034 oscilloscope.

Results

External heating test.— Figure 3 shows the results of an external heating test on the 18650 cell. At 220°C, a very rapid temperature increase occurs when the cell catches fire and a pressure wave is observed. The maximum average temperature at the cell surface reaches 743°C which is higher than the melting temperature of aluminum, 660°C. The maximum cell surface temperature measured by a single sensor was 775°C, the temperature of the cell interior was thus probably even higher. Based on the average surface temperature increase, the corresponding energy released from the thermal runaway

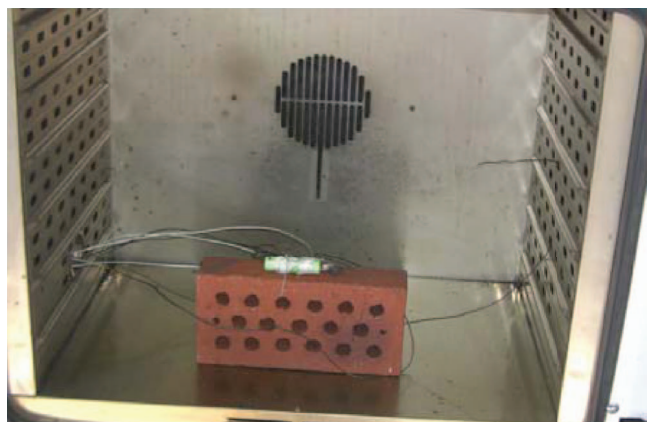


Figure 2. Photo of oven set up, showing a cylindrical 18650 cell fastened onto a brick with steel wire.

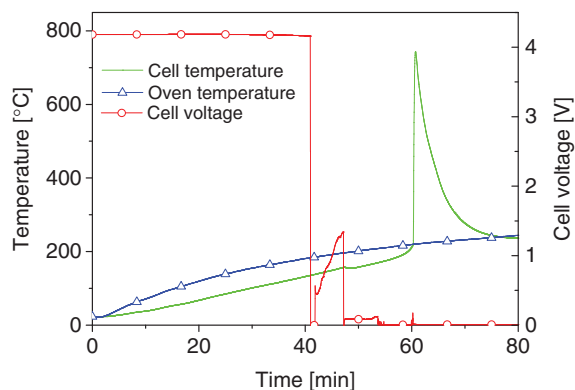


Figure 3. Temperature and cell voltage development during external heating of a Samsung 18650 cell.

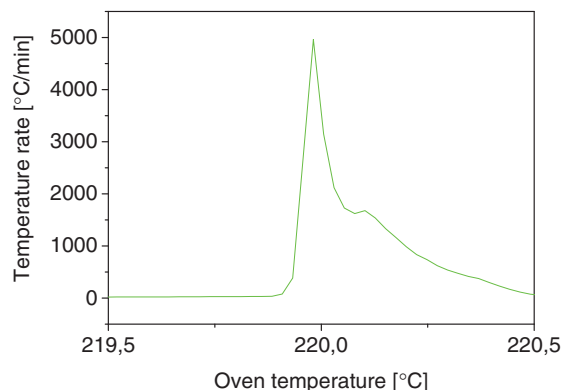


Figure 5. The rate of the cell surface temperature for the Samsung 18650 cell in the temperature region of the thermal runaway peak.

can be roughly estimated since the cell is likely to be under adiabatic conditions during the short duration of the thermal runaway, approximately 20 seconds. The specific heat capacity of a complete cell varies between cylindrical and pouch cell packaging and is also dependent on size, energy/power optimization etc. In the estimations we use an approximate value of $700 \text{ J/kg}^\circ\text{C}$ based on published values for different cell types.^{5,25-29} Using the measured temperature increase of 523°C the energy released can be estimated to 15.6 kJ (4.33 Wh). The calculated released energy is thus about half of that of the electrical energy available in the cell, 8.64 Wh . It may also be noted that just prior to the runaway, burning electrolyte is squirting out of the cell seen in Figure 4, which releases energy which is not included in the above value for the energy release calculation. Figure 5 shows the derivative of the average cell surface temperature; the figure shows that the thermal runaway temperature is 220°C and that the rate of temperature increase is very high, initially close to 5000°C/min .

Cells with lithium iron phosphate (LFP) cathode have an enhanced thermal safety compared to cells with cobalt oxide based cathode. Figure 6 shows the results for two LFP-cells during external heating. The old cell design shows a clear but relatively small thermal runaway event while the new cell design shows no obvious signs of thermal runaway. Actually, a minor exothermic event, hardly visible in Figure 6, can be detected in the same temperature region as the thermal runaway in the old cell design also for the new cell design. The chemical and/or physical changes in the cell design are not known or studied in this report. Complementary experiments where the temperature was continuously increased also resulted in a similar behavior as that in Figure 6. The time to reach the thermal runaway temperature was approximately 90 minutes for the test using continuous heating and approximately 200 minutes for the test using temperature-ramping.



Figure 4. Samsung 18650 cell at the beginning of thermal runaway releasing ignited material.

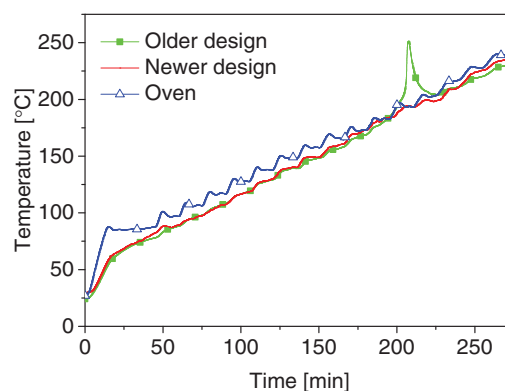


Figure 6. Temperature development during external heating of EiG newer and older cell design.

Figure 7 shows the results of the European Batteries cell during external heating. A moderate thermal runaway is detected also for this LFP-cell, with temperatures reaching well above 300°C . The runaway temperature was 183°C within $\pm 1^\circ\text{C}$ for these cells, this value is close to the value observed for the older design EiG cell, 189°C . The runaway temperature was thus somewhat lower than for the laptop-type cell. The energy released at the detected thermal runaway estimated using the same method and specific heat capacity value as for the Samsung cell above is also much smaller than for the laptop cell. While the ratio of energy released to the electric energy stored in the fully charged battery is of the order of 50% for the laptop battery it is

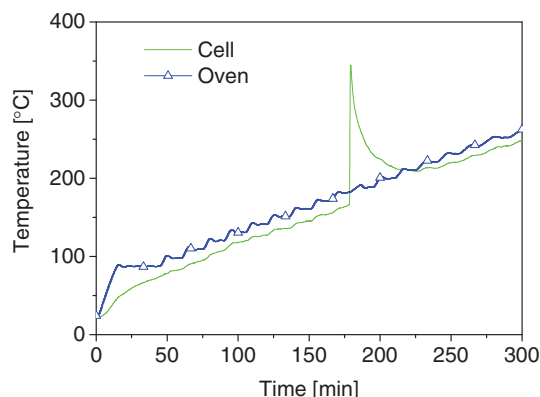


Figure 7. Temperature development during external heating of European Batteries cell.

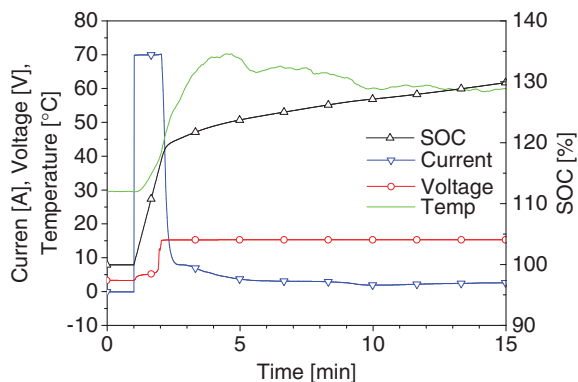


Figure 8. Overcharge of EiG cell of newer design.

between 10 and 30% for the LFP-type cells that showed a thermal runaway. The rates of temperature increase at the thermal runaway for the LFP-cells were 500°C/min for European Battery cell and 60°C/min for EiG older design while the rate was not detectable for EiG newer design. The 18650 cell lost 30% of its weight in the external heating tests while the LFP cells lost between 16–26%, the EiG new design had the lowest weight loss of 16%.

Overcharge test.— Figure 8 shows the result from an overcharge test of the EiG cell of newer design. The cell surface temperature reached a moderate temperature of 70°C. An almost negligible weight loss was measured, probably due to minor venting of electrolyte. The overcharge test for one of the European Batteries cells is shown in Figure 9. After approximately 5 minutes of charging at a state of charge level of 115%, the cell suddenly caught fire, as seen in Figure 10. The temperature reached 855°C for a sensor placed in the center of the top surface of the cell. During the fire, the top layer of the cell was blown away so the cell temperature presented in Figure 9 may include the temperature of the flames and does not reflect the cell temperature after this event.

The overcharge test on the European Batteries cells was repeated three more times without any occurrence of fire and Figure 11 shows the results of one of the repeated tests. The surface temperature reached a maximum of 79°C, a value comparable to that of the EiG cell. It may be noted that all overcharged cells were swollen with a thickness increase after the test ranging from 350 to 850% of the initial thickness.

Short-circuit test.— The results from short circuit tests for EiG cells of both newer and older design are shown in Figure 12. There were no significant differences between the two types of cells. Be-

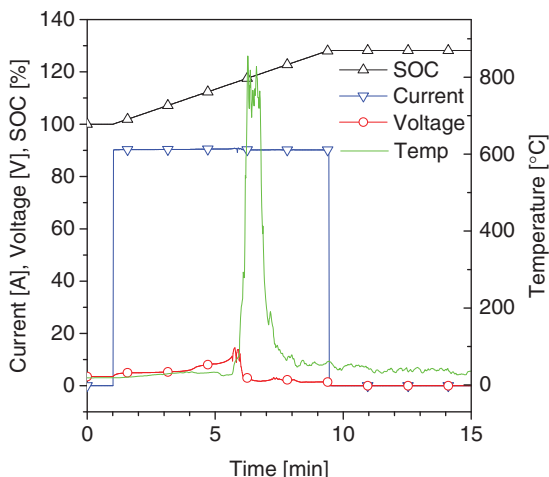


Figure 9. Overcharge of a European Batteries cell resulted in fire, in this case the charger was manually stopped at 9.5 min due to the fire.

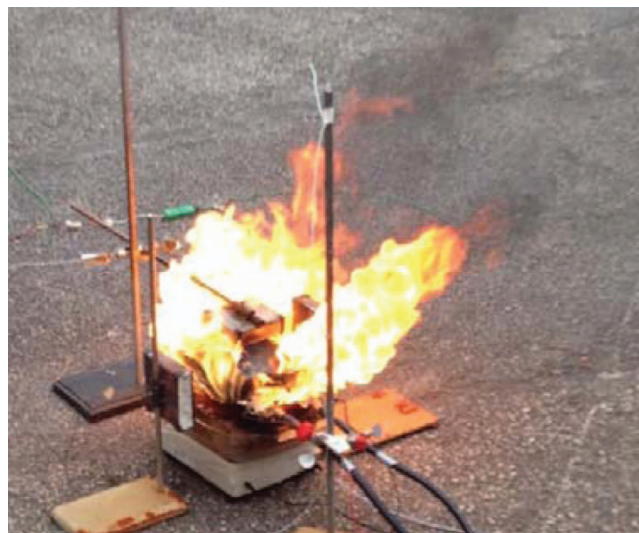


Figure 10. Overcharge of a European Batteries cell resulted in fire.

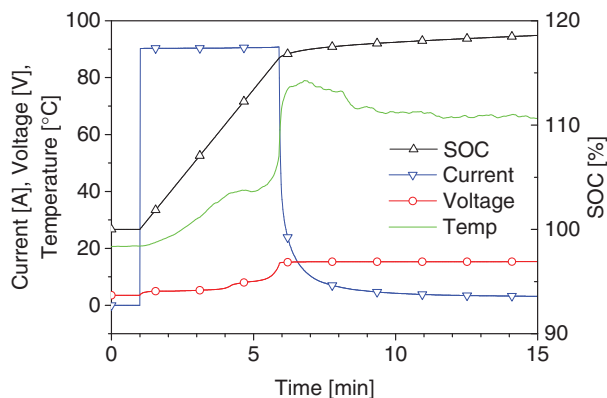


Figure 11. Overcharge of a European Batteries cell that did not result in a fire.

tween 20 and 30 seconds after the start of the short circuit the cell swelled up quickly. The following 2 minutes the cell vented (with no visual smoke) and swelling decreased considerably. The following 5 minutes the cell contracted further to a thickness close to that of the untested cell. The peak current reached almost 900 A which corresponds to a discharge rate of 128C. The maximum cell surface

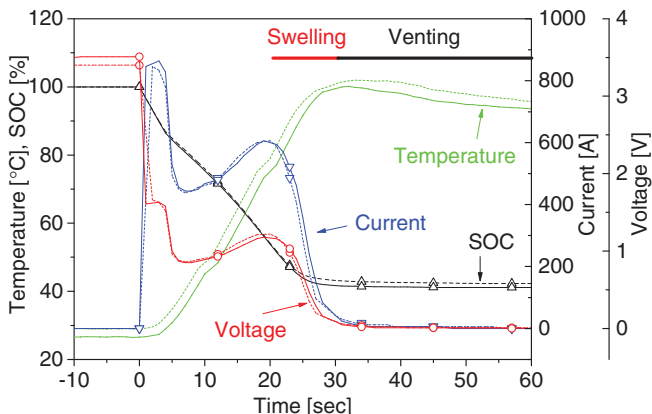


Figure 12. Short circuit of EiG cell of newer design (dashed lines) and EiG of older design (solid lines).



Figure 13. Short circuit of European Batteries cell, photo (left) showing the flame and smoke from the burnt off positive terminal tab, the photo (right) after the test shows the burnt off tab.

temperature was about 100°C and both types of cells were discharged to about 43% SOC.

In the short circuit test of the European Batteries cell the positive tab of the cell burnt off, which stopped the short circuit current, see Figure 13. The current just before this event was 1084 A and due to the very short time for the short circuit the cell temperature and SOC changed very little, less than 6°C and 4% respectively.

Discussion

When the Samsung 18650 laptop cell was exposed to external heat, the open circuit voltage remained stable until about 135°C, measured on the cell surface, as seen in Figure 3, then it falls abruptly. The melting points of typical shutdown separator materials, polyethylene and polypropylene, are about 130 and 165°C, the measured values are thus reasonably close to these values, where the final voltage drop occurs at about 158°C. The difference may be due to a delay in the temperature measurement due to the slow heat transfer in the interior of the cell. The runaway temperature, 220°C, and the temperature increase during the thermal runaway, 532°C, is in the same order as reported in our previous study.³⁰ The rate of temperature increase in the initial phase of the thermal runaway is extremely high, close to 5000°C/min. Jhu et al.²⁸ found for a similar cell a peak value of about 37000°C/min with a more sensitive technique, and in another study by Jhu et al.²⁹ temperature rates beyond 70000°C/min were found. The state of charge can have a strong influence on the cell behavior during abuse situations and the influence may vary with different types of abuse. Jhu et al.^{28,29} and Doughty et al.¹⁷ showed that lower SOC gives lower energy release during external heating.

A comparison of the results of the external heating tests for the 18650 laptop cell (Figure 3) and the LFP-cells (Figure 6 and Figure 7) shows that the behavior is much less dramatic for the LFP-cells. Two of the three LFP-cells still go into thermal runaway but the energy released is much less than that from a cell with cobalt-based cathode. This is well-known from other studies^{2,13,20,31-36} and attributed to the stability of the olivine structure of LiFePO₄. The electrode influence on the thermal stability of a LFP-cell is therefore dominated by the anode material. Swelling and venting occurred for all pouch-type cells while the laptop cell vented with a rapid release of gas, accompanied by a pressure wave and immediately followed by fire.

The runaway temperature for the LFP-cells was lower than for the laptop cell, 189°C for the EiG older design and 183°C for the European Batteries cell. The thermal runaway in the external heating test for the new design of EiG is significantly reduced compared to that of the older design. It may be noted that the EiG cell is designed

to target electrified vehicles in the automotive sector and is currently in use there. The rates of temperature increase at runaway differ considerably for the different cells; 5000°C/min for the Samsung laptop cell, 500°C/min for European Battery cell and 60°C/min for EiG older design. This highlights the large differences for Li-ion cells and particularly underlines the importance of thermal stability.

Cell venting is an important safety factor to protect a Li-ion battery from reaching too high pressure, especially in the case of cylindrical or hard prismatic cell packaging. In fact, cell manufacturers may include so called shutdown additives in the electrolyte in order to activate cell venting at a pre-designed stage by gas generation from polymerizing of the additive molecules, before the cell reaches extreme conditions.²⁰ Upon heating of a cell, ventilation is also unavoidable since the electrolyte typically consists of a Li-salt dissolved in volatile organic solvents. Even in cases when fire or explosion does not occur, emitted flammable and toxic gas can be a serious problem as mentioned in the introduction.

Abuse by overcharging and external heating adds energy to the system due to the input of electric power or heat, while in a short circuit test no energy is added to the cell. Therefore, the overcharge and external heating test can theoretically be seen as a more severe abuse due to the addition of external energy to the cell. In the overcharge tests presented the additional charged energy is between 20–30% in terms of battery capacity. The energy released in the external heating tests presented in this paper is calculated based on the change of the cell surface temperature and are of the order of 50% or less of the electrical energy within the cell. Those values do not represent the total energy release and neither the possible maximum energy release during the most severe abuse situations when the cell materials are allowed to fully combust. During the external heating, part of the electrolyte, and particularly low boiling components (e.g. dimethyl carbonate), can evaporate due to venting and cell opening. However, some electrolyte is still present since thermal runaway does occur. For example, for the 18650 cell, electrolyte is squirting out of the cell prior to the thermal runaway as seen in Figure 4, releasing energy which is not included in the calculations. Besides, several other parameters also affect the results e.g. abuse test methods, cell chemistry, capacity size, cell design and cell venting characteristics. Values typically found in the literature show a released energy of 2–3 times the electrical energy.^{1,38} The results presented in this article are lower presumably due to the reasons discussed above. However, the energy release, 15.6 kJ, of the thermal runaway for the 18650 cell in the external heating test can be compared to 19.2 kJ measured for a similar 18650 cell.²⁸

10 C-rate overcharge tests of the EiG newer design did not result in a thermal runaway and the peak surface temperature reached

a moderate 79°C. A similar result was obtained for one of the European Batteries cells, seen in Figure 11. However, one of the European Batteries cells that was overcharged ignited with a resulting fire. This behavior was not reproduced in three other tests. Excluding the ignited cell, no thermal runaway could be detected even though all cells were heavily affected by large swelling and venting. Hund and Ingersoll³⁸ studied 1 C-rate overcharge of LiFeBatt 10 Ah LFP cells which resulted in a significantly higher temperature of 160°C but no fire or sparks. He et al.³⁹ used 2 Ah LFP cells and found a temperature peak of 90°C without fire during 1 C-rate overcharging. The incident of the fire in our test is interesting but we can only speculate on the reason. It could be a bad cell due to errors in the manufacturing process or induced by some small variety in the test setup. An event like this in the field could be referred to as a field failure, but field failures rarely happens on cell-level, the probability is typically less than 1 ppm.^{21,22} For an overcharge situation to occur in a battery system a failure of the Battery Management System (BMS) is required allowing the cell to be charged above its limits. Secondly, as we have seen above, the cell itself does not necessarily go into thermal runaway because it is overcharged. Studies have, however, shown that LFP-cells have a smaller margin with respect to the amount of overcharged capacity compared to other common Li-chemistries, although the exothermal response for LFP is significantly lower.²

The tested large-sized LFP pouch automotive cells have low internal resistance, enabling high short circuit currents known from other studies.⁴⁰ The short circuit current of the EiG cells was close to 900 A, corresponding to a 128 C-rate. These cells are power optimized and capable of delivering 20–30 C-rate in normal use. The short circuit current for the six times larger capacity European Batteries cell is close to 1100 A, i.e. a 24 C-rate. The European Batteries cell is energy optimized and made to deliver up to 4 C-rate in normal use. The cell voltage seen in Figure 12 drops quickly due to the short circuit, but does not reach 0 V instantly even if it is a hard short circuit with low connection resistance. The current curve in Figure 12 quickly rises and then falls to about half the value and then increases again. This behavior could be explained by the fact that the extreme current cannot be sustained due to limitations of the transport process of the lithium ion in the cell resulting in a current drop, while the cell is quickly heated due to the ohmic losses. The increased temperature finally enables a higher transportation of lithium ions resulting in an increased current. The time frame for these phases is less than 30 seconds as seen in Figure 12. No thermal runaway is observed, however the cell temperature increases fast during a short period of time.

The short circuit test of the European Batteries cell resulted in that the positive terminal tab burnt off as seen in Figure 13 which stopped the short circuit. In one perspective this can potentially be seen as positive for the safety since the tab functioned as a “fuse” that stopped the short circuit at an early stage. However the flame can be a potential source of ignition of e.g. vented and flammable battery gases or other easily ignitable materials inside a battery system.

Lithium-ion cells can be equipped with a variety of reversible and irreversible safety mechanisms.⁴¹ The 18650 cells typically have protection for short circuit, by the use of for example CID (current interrupture device) and PTC (positive temperature coefficient), the latter causing the cell resistance to increase rapidly at increased temperature reducing the current going through the cell. Many of these safety mechanisms were developed specifically for the Li-ion consumer battery. The use of Li-ion batteries in other applications such as within automotive give rise to more and different demands on the safety as well as other aspects, e.g. cost, life time, energy and power density. The environmental conditions in automotive applications are different to those in consumer products; vibrations, extreme temperatures and varying humidity can be challenging. The risks involved in case of electric vehicle crash deformations must also be taken into consideration. In the automotive industry large capacity cells are required and typically hundreds of these are connected in series. Safety mechanisms within the cell used in commercial Li-ion battery systems do not always give the same protection in e.g. automotive applications. A first example is the shutdown separator which can give an increased

safety for some cell abuse situations. However, the use of shutdown separators in a large battery pack with higher voltage due to hundreds of cells connected in series might not give the same safety due to e.g. voltage breakdown of the separator.^{42,43} A second example is the PTC which has a relative low voltage tolerance in cell-strings, potentially as low as 30 V, which can result in spontaneous ignition in case of overvoltage.⁴⁴ Besides the safety concern the PTC also add parasitic resistance in a large battery pack. A third example is the CID which cannot offer the same safety in case of higher voltage systems.⁴⁴

The battery module design as well as the rate of energy release and the total energy release from a thermal runaway in one cell determines if neighboring cells are effected or not. From a safety perspective it is essential to minimize the probability for a thermal event to occur but also to minimize the consequences of such an event and prevent damage to neighboring cells, avoiding the potential propagation of a thermal runaway from cell to system-level as shown in Figure 1.

Conclusions

The abuse tests conducted on various types of Li-ion cells give valuable information regarding diverse aspects of the cell safety. Risks associated with thermal runaway situations; fire, smoke and gas emissions are especially important for the use of Li-ion batteries in automotive applications. The external heating test of the 18650 laptop cell resulted in a rapid thermal runaway accompanied with a pressure wave and immediate fire. In large battery packs using multiple cells in series and/or parallel the effect of a propagation scenario in this is a concern. Safer chemistries like the LFP-cells are in general significantly less energetic. Nevertheless our results show that LFP-cells can still go into a thermal runaway event even though the tested LFP cells showed various results. During external heating up to 300°C a LFP-cell with a newer design did not show any substantial thermal runaway while older design LFP cells showed a moderate thermal runaway. Overcharge of the newer designed LFP-cell did not result in thermal runaway either. However, overcharge of another LFP pouch cell did result in a fire, even if that event could not be reproduced in this study.

The energy released during a thermal runaway based on the results reported above for a 18650 cobalt-based cell can be used to estimate how much energy may be released in a thermal runaway of a 300 kg battery system for an electric vehicle. The answer is perhaps somewhat surprising, the calculation shows that the energy released could be in the order of 70 MJ, corresponding to the combustion of about 2 liters of gasoline. However, our estimate is low, as described above, and using the highest value reported earlier one can expect a value up to six times that calculated here. This is still considering the battery type that has the largest energy release while other more safe chemistries, e.g. LFP will have lower values. The presented results thus show that although the safety aspects of Li-ion batteries are still a concern, the safety is improving with safer chemical components and design improvements.

Acknowledgments

The authors thank the Swedish Energy Agency and the FFI-program for its support.

References

1. G. G. Eshetu, S. Grugeon, S. Laurelle, S. Boyanov, A. Lecocq, J.-P. Bertrand, and G. Marlair, *Phys. Chem. Chem. Phys.*, **15**, 9145 (2013).
2. D. Doughty and E. P. Roth, *The Electrochem. Soc. Interface: summer* **2012**, 37 (2012).
3. E. P. Roth and C. J. Orendorff, *The Electrochem. Soc. Interface: summer* **2012**, 45 (2012).
4. D. Lisbona and T. Snee, *Process Safety and Environmental Protection*, **89**, 434 (2011).
5. R. Spotnitz and J. Franklin, *J. of Power Sources*, **113**, 81 (2003).
6. P. Biensan, B. Simon, J. P. Pères, A. de Guibert, M. Broussely, J. M. Bodet, and F. Pertont, *J. of Power Sources*, **81–82**, 906 (1999).

7. F. Larsson, P. Andersson and B.-E. Mellander, "Are electric vehicles safer than combustion engine vehicles?", Chapter 4 in Systems perspectives on Electromobility, edited by B. Sandén, *Chalmers University of Technology*, Goteborg, Sweden, ISBN 978-91-980973-1-3, p. 31 (2013).
8. Z. J. Zhang, P. Ramadass, and W. Fang, "Safety of lithium-ion batteries", Chapter 18 in *Lithium-Ion Batteries: Advances and Applications*, edited by G. Pistoia, Elsevier, Amsterdam, The Netherlands, p. 409 (2014).
9. A. Hammami, N. Raymond, and M. Armand, *Nature*, **424**, 635 (2003).
10. H. Yang, G. V. Zhuang, and P. N. Ross Jr, *J. of Power Sources*, **161**, 573 (2006).
11. T. Ohsaki, T. Kishi, T. Kuboki, N. Takami, N. Shimura, Y. Sato, M. Sekino, and A. Satoh, *J. of Power Sources*, **146**, 97 (2005).
12. D. P. Abraham, E. P. Roth, R. Kostecki, K. McCarthy, S. MacLaren, and D. H. Doughty, *J. of Power Sources*, **161**, 648 (2006).
13. E. P. Roth, *ECS Trans.*, **11**(19), 19 (2008).
14. C. Arbizzani, G. Gabrielli, and M. Mastragostino, *J. of Power Sources*, **196**, 4801 (2011).
15. A. K. Padhi, K. S. Nanjundaswamy, and J. B. Goodenough, *J. Electrochem. Soc.*, **144**, 1188 (1997).
16. K. Zaghib, A. Guerfi, P. Hovington, A. Vijn, M. Trudeau, A. Mauger, J. B. Goodenough, and C. M. Julien, *J. of Power Sources*, **232**, 357 (2013).
17. D. H. Doughty, E. P. Roth, C. C. Craft, G. Nagasubramanian, G. Henriksen, and K. Amine, *J. of Power Sources*, **146**, 116 (2005).
18. S. S. Zhang, *J. of Power Sources*, **162**, 1379 (2006).
19. G. Nagasubramanian and K. Fenton, *Electrochimica Acta*, **101**, 3 (2013).
20. K. Zaghib, J. Dubé, A. Dallaire, K. Galoustov, A. Guerfi, M. Ramanathan, A. Benmayza, J. Prakash, A. Mauger, and C. M Julien, "Lithium-ion cell components and their effect on high-power battery safety", Chapter 19 in *Lithium-Ion Batteries: Advances and Applications*, edited by G. Pistoia, Elsevier, Amsterdam, The Netherlands, p. 437 (2014).
21. Q. Wang, P. Ping, X. Zhao, G. Chu, J. Sun, and C. Chen, *J. of Power Sources*, **208**, 210 (2012).
22. C. Mikolajczak, M. Kahn, K. White, and R. T. Long, "Lithium-ion batteries hazard and use assessment", Fire Protection Research Foundation, Quincy, MA, USA, Doc no 1100034.000 A0F0 0711 CM01 (2011).
23. D. H. Doughty and C. C. Crafts, "FreedomCAR electrical energy storage system abuse test manual for electric and hybrid electric vehicle applications", Sandia report SAND2005-3123, Sandia National Laboratories, USA (2006).
24. D. Doughty, "SAE J2464 Electric and hybrid electric vehicle rechargeable energy storage system (RESS) safety and abuse testing procedure", SAE Technical Paper 2010-01-1077, (2010).
25. L. Fan, J. M. Khodadadi, and A. A. Pesaran, *J. of Power Sources*, **238**, 301 (2013).
26. J. Yi, U. S. Kim, C. B. Shin, T. Han, and S. Park, *J. of the Electrochem. Soc.*, **160**(3), A437 (2013).
27. W. Wu, X. Xiao, and X. Huang, *Electrochimica Acta* **83**, 227 (2012).
28. C.-Y. Jhu, Y.-W. Wang, C.-Y. Wen, C.-C. Chiang, and C.-M. Shu, *J. Therm. Anal. Calorim.*, **106**, 159 (2011).
29. C.-Y. Jhu, Y.-W. Wang, C.-M. Shu, J.-C. Chang, and H.-C. Wu, *J. of Hazardous Materials*, **192**, 99 (2011).
30. F. Larsson and B.-E. Mellander, *Conference proceedings of Fires in vehicles (FIVE) 2012*, edited by P. Andersson and B. Sundstrom, SP Technical Research Institute of Sweden, Sweden, p. 303 (2012).
31. M. Takahashi, S. Tobishima, K. Takei, and Y. Sakurai, *Solid State Ionics*, **148**, 283 (2002).
32. A. Yamada, S. C. Chung, and K. Hinokuma, *J. of the Electrochem. Soc.*, **148**(3), A224 (2001).
33. H. Joachin, T. D. Kaun, K. Zaghib, and J. Prakash, *J. of the Electrochem. Soc.*, **156**(6), A401 (2009).
34. K. Zaghib, J. Dubé, A. Dallaire, K. Galoustov, A. Guerfi, M. Ramanathan, A. Benmayza, J. Prakash, A. Mauger, and C. M. Julien, *J. of Power Sources*, **219**, 36 (2012).
35. G. Chen and T. J. Richardson, *J. of the Electrochem. Soc.*, **156**(9), A756 (2009).
36. G. Chen and T. J. Richardson, *J. of Power Sources*, **195**, 1221 (2010).
37. E. P. Roth, "Lithium ion cell and battery safety", *Tutorials E in Conference proceedings in Advanced Automotive Battery Conference (AABC)*, AABC Europe 2011, Mainz, Germany (2011).
38. T. D. Hund and D. Ingersoll, "Selected test results from the LiFeBatt iron phosphate Li-ion battery", Sandia report SAND2008-5583, Sandia National Laboratories, USA (2008).
39. Y.-B He, G.-W. Ling, Z.-Y. Tang, Q.-S. Song, Q.-H. Yang, W. Chen, W. Lv, Y.-J. Su, and Q. Xu, *J. Solid State Electrochem.*, **14**, 751 (2010).
40. F. V. Conte, P. Gollob, and H. Lacher, *World Electric Vehicle J.*, **3**, 1 (2009).
41. P. G. Balakrishnan, R. Ramesh, and T. P. Kumar, *J. of Power Sources*, **155**, 401 (2006).
42. E. P. Roth, D. H. Doughty, and D. L. Pile, *J. of Power Sources*, **174**, 579 (2007).
43. C. J. Orendorff, *The Electrochem. Soc. Interface: summer* **2012**, 61 (2012).
44. J. Jeevarajan, "Safety of commercial lithium-ion cells and batteries", Chapter 17 in *Lithium-Ion Batteries: Advances and Applications*, edited by G. Pistoia, Elsevier, Amsterdam, The Netherlands, p. 387 (2014).

Paper IV

Using FTIR to determine toxic gases in fires with Li-ion batteries

Abstract

Batteries and in particular Li-ion batteries are seen as an alternative to fossil fuels in the automotive sector. Li-ion has however some safety issues including possible emissions of toxic fluorine containing compounds during fire and other situations. This paper demonstrates the possibilities to use the Fourier Transfer Infrared Technique to access these gases. The study is conducted in the Cone Calorimeter on different solvents used in Li-ion batteries. The measurements show that, apart from HF with a known high toxicity, also POF_3 is emitted. The toxicity of POF_3 is not yet established but has the potential of being very toxic.

Petra Andersson^{a,*}, Per Blomqvist^a, Anders Loren^a, Fredrik Larsson^{a,b}

^aSP Technical Research Institute of Sweden, Brinellgatan 4, SE-501 15 Borås, Sweden

^bDepartment of Applied Physics, Chalmers University of Technology, SE-412 96 Göteborg, Sweden

*Corresponding author: petra.andersson@sp.se

Introduction

Batteries are used in more and more applications and are seen as an important alternative to fossil fuels as energy carrier in the automotive sector. Several types of batteries are used today and more are developed over time. One of the most common types of batteries today is lithium-ion (Li-ion) batteries due to their high energy and power densities. Li-ion batteries have, however, some safety drawbacks with their organic based flammable electrolyte. Compared to many other battery technologies, Li-ion batteries also have a smaller temperature and voltage region of stability. Outside this region, Li-ion batteries can undergo a thermal runaway resulting in gassing and fire, and potentially even explosion [1,2]. A thermal runaway can be the result if a Li-ion cell is exposed to increased temperatures, i.e. temperatures of 120-150 °C [3]. Other types of abusive conditions, e.g. overcharge or deformation can also result in venting of gasses and thermal runaway reactions.

The electrolyte of a Li-ion cell contains a lithium salt, organic solvents (e.g. ethylene carbonate (EC), diethyl carbonate (DEC), dimethyl carbonate (DMC)) and a number of additives. The far most used Li-salt today is hexafluorophosphate (LiPF_6) due to its attractive performance despite its moderate thermal stability and fluorine content. The fluorine content can under abusive conditions emit fluorine containing compounds, e.g. hydrogen fluoride (HF). Other gases that can pose a danger include the chemical species in the oxidation and thermal breakdown of the initial LiPF_6 salt solution. Most likely phosphorus pentafluoride (PF_5), phosphorous oxyfluoride (POF_3) and HF are of greatest concern but also the fluorinated phosphoric acids [4] can be of interest since they will give HF and phosphoric acid (H_3PO_4) when completely reacted with water. Overheating in a Li-ion battery cell can also result in formation of toxic fluoro-organic compounds [5]. The toxicity of all these gases is not fully established. The Swedish Work Environment Authority has exposure limits for total fluorides, HF and phosphoric acid but lacks data for the rest of the substances [6].

The NGVⁱ for total fluorides are 2 mg/m³ and HF has a TGVⁱⁱ of 2 ppm. NIOSH (National Institute for Occupational Safety and Health, USA) states that HF has a IDLH (Immediately Dangerous to Life and Health) value of 30 ppm. No exposure limits are given for PF₅ and POF₃, however, their chlorine analogues, PCl₅ and POCl₃, have NGV values of 0.1 ppm. The toxicity might, however, differ between the chlorine and fluorine species and there is no general rule like “fluorine is always more toxic”. But, still, the limits are low and gases evolved from battery fires are certainly of great concern to both the fire fighters, people close to a Li-ion battery in e.g. electric vehicles or in the close vicinity of the fire. Other gases emitted from electrolytes, especially under non-fire conditions include e.g. H₂, CO, CH₄, C₂H₆ [7, 8, 9], this paper focuses however on the fluorinated species.

The HF formation in the decomposition of the LiPF₆-based electrolytes under heated but non-fire conditions is complex [10, 11, 12]. When heated in a dry and inert environment LiPF₆ decomposes to lithiumfluoride (LiF) as solid and phosphorouspentafluoride (PF₅) as gas [13]



In contact with moisture/water PF₅ reacts to form phosphorous oxyfluoride and hydrogen fluoride [13]



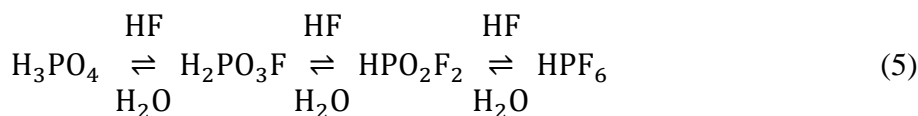
LiPF₆ is highly susceptible to hydrolysis by even trace amounts of moisture [14]. When heated in moisture/water LiPF₆ can directly form LiF, POF₃ and HF [13].



PF₅ also react with HF to form hexafluorophosphoric acid (HPF₆) [15]:



Phosphorous oxyfluoride (POF₃) can react to form several fluorinated phosphoric acids, monofluorophosphoric acid (H₂PO₃F), difluor-phosphoric acid (HPO₂F₂) hexafluorophosphoric acid (HPF₆), and phosphoric acid (H₃PO₄) [4]. The fluorinated phosphoric acids can react with water and yield HF and form phosphoric acid as a final product [4]:



Of these gases it is HF, PF₅ and POF₃ that are of most interest due to their toxicity and potential toxicity and in particular is it interesting to know if and to what extent these three substances are emitted in fire situations. Further the possible effect of different burning conditions and fuel composition on the amount of gases produced is of interest together with if the addition of water, like in an extinguishing situation, would change the amounts produced.

ⁱ ”Nivågränsvärde” Mean value threshold in a working environment

ⁱⁱ ”Takgränsvärde” Maximum allowed concentration in a working environment

There is only limited information available on PF₅ and POF₃ measurement methods. Possible techniques for this were sought for in the literature and it was soon concluded that a possible solution was to use the FTIR (Fourier Transform Infra-Red) technique as all three gases have absorbance in the infrared spectra while no information was found on e.g. suitable fluorescence wavelength for these species. There is only limited information available on determination of PF₅ and POF₃ in gas phase. This study focused on FTIR methodology since it has the advantage of detection of several substances simultaneously without interfering with the chemical equilibria in the gas phase. Wet chemical methodologies followed by chromatography and suitable detection were ruled out due to uncertain kinetics and equilibria.

Both PF₅ and POF₃ are reactive and few measurements have been performed on these gases in the literature. Yang, Zhuang and Ross [13] report measurements of these gases conducted using TGA (Thermal Gravimetry Analysis) and FTIR (Fourier Transform Infra-Red) on pure LiPF₆ salt and salt solved in EC, DMC, PC (polypropylene carbonate), and EMC (ethyl methyl carbonate). Recently Eshetu et.al. [16] published a study on the different solvents used in the electrolytes without the salt with a focus on Heat Release Rate (HRR) from the different solvents and also toxicity of the combustion gases from the solvents. However as no LiPF₆-salt was included in these tests the toxicity was similar to most organic solvents. A recent study by Ribiere et. al. [17] has been performed on pouch cells in the Fire Propagation or Tewarson apparatus where FTIR was used to measure toxic gases including HF but other fluorinated gases were not evaluated.

This paper presents experiments conducted in the cone calorimeter where HRR [18] was measured together with gases emitted including HF, POF₃ and PF₅ in order to investigate possible influence of the burning conditions, fuel composition and water addition on the amounts of HF, POF₃ and PF₅ produced. The measurements were conducted using the FTIR technique and a first step in the study was to demonstrate the suitability of the FTIR technique to be used for measurements of these substances in fire situations. To this end the FTIR equipment was first calibrated for HF, POF₃ and PF₅. Then, tests were conducted on pure salt and LiPF₆ salt solved in different electrolyte solvents at various concentrations. The solvents included in this study were Dimethyl carbonate (DMC) and Dimethoxyethane (DME) and Polypropylene carbonate (PC). The solutions were introduced to a propane flame as a spray at different flow rates or onto a metal plate in the flame in order to achieve different burning conditions and fuel composition.

FTIR instrumentation and calibration

The measurement system used consisted of an FTIR spectrometer, a gas cell, sampling lines, filters for removing particulates before the gas cell and a pump that continuously drew sample gas through the cell. The system is specified in Table 1.

Table 1 Specification of the FTIR measurement system.

Instrumentation	Specification
Spectrometer	Thermo Scientific Antaris IGS analyzer (Nicolet)
Spectrometer parameters	Resolution: 0.5 cm ⁻¹ Spectral range: 4800 cm ⁻¹ – 650 cm ⁻¹ Scans/spectrum: 10 Time/spectrum: 12 seconds Detector: MCT
Gas cell	Volume: 0.2 litres Path length: 2.0 m Temperature: 180°C Cell pressure: 650 Torr
Primary filter	M&C ceramic filter heated to 180 °C
Secondary filter	M&C sintered steel filter heated to 180°C
Sampling tubing	4/6 mm diameter PTFE tubing heated to 180°C. The length of the tubing was 1.5 m + 2.5 m
Pump	Sampling flow: 3.5 l/min

The FTIR used had a calibration for a number of components when delivered from factory. These components included e.g. CO₂, CO and HF. It was seen that the factory calibration for HF was not sufficiently accurate for the intended use of the instrument and the instrument was recalibrated to include more spectral information and a wider concentration range i.e. include the full spectral band of HF and a concentration range from 18 ppm to 1245 ppm. The calibration of HF was made using a dynamic dilution system where a water solution of HF was injected into a heated stream of nitrogen.

The quantification limit (LOQ) for HF with the recalibrated FTIR was determined to 2 ppm. In addition was the FTIR calibrated for PF₅ and POF₃. Calibration gas mixtures were prepared for this purpose by dilution of PF₅ (99%, ABCR) and POF₃ (99%, ABCR) in nitrogen atmosphere using gasbags (Flexfoil, SKC). Extra effort was put into pre-conditioning the bags so they were free of water adsorbed to the walls. This was necessary to be able to prepare the highly reactive PF₅ mixture.

Tests were conducted to record the spectral bands of POF₃ as a basis for calibration of the FTIR. An important part of the calibration work was further to investigate the stability of POF₃. The spectral range of interest of POF₃ (116 ppm) is shown in Figure 1; several distinctive absorption bands can be seen.

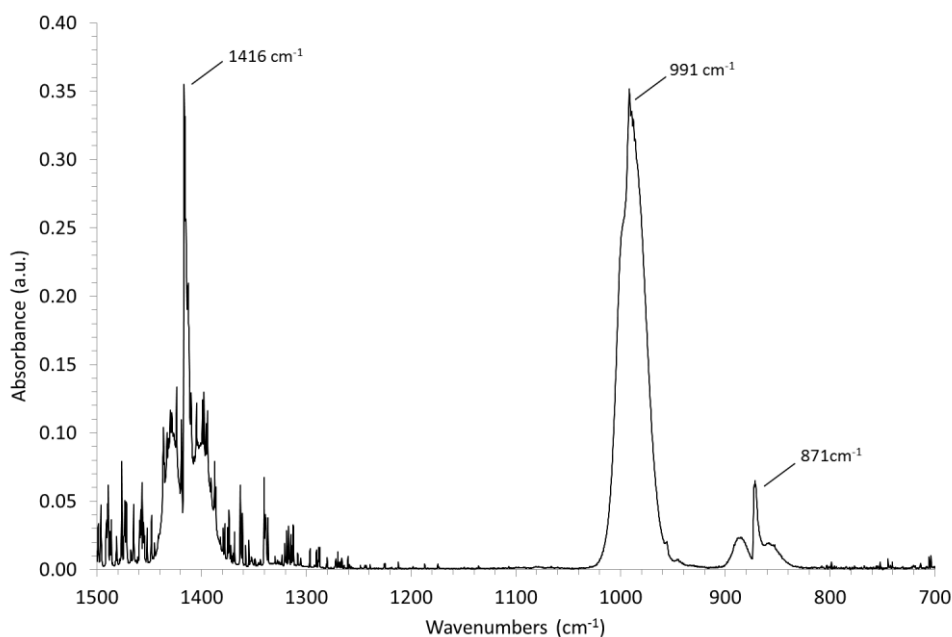


Figure 1 Spectral bands of POF₃.

Three spectral bands are shown centred around the wavenumbers 871 cm⁻¹ (P-F symmetrical stretch), 991 cm⁻¹ (P-F asymmetrical stretch) and 1416 cm⁻¹ (P-O stretch). The two latter vibrations are the strongest. The spectral information of POF₃ is summarized in Table 2.

Table 2 Spectral band positions for POF₃.

Band position (cm ⁻¹)	Absorptivity* (abs/ppm.m)	Type of band [13]
1416	0.0014	P-O stretch
991	0.0014	P-F asymmetrical stretch
871	0.00025	P-F symmetrical stretch

* Calculated from a spectrum of 100 ppm POF₃ (650 Torr, 180 °C).

A quantitative calibration was made for POF₃ using flushed gas bags where known volumes of POF₃ gas were injected into a known volume of nitrogen gas. The concentrations produced for the calibration were: 25 ppm, 100 ppm, 200 ppm, 300 ppm and 416 ppm. Spectral regions around 871 cm⁻¹ and 1416 cm⁻¹ were used for a CLS (classical least squares) calibration and water was included as an interfering component. The calibration was linear and a regression yielded a 0.98 R² fit. The quantification limit (LOQ) for POF₃ was calculated to 6 ppm.

The stability of POF₃ at both room temperature and at an elevated temperature was investigated. It was important to have this information to know that the calibration mixtures prepared in gas bags were stable and to see if any significant decomposition would take place in the heated sampling and measurement system. The investigation showed that POF₃ is very stable at room temperature in a gas bag diluted with N₂, which makes it possible to prepare quantitative calibration standards. Figure 2 shows the spectra of ~200 ppm POF₃ from two different gas bags, stored for 8 and 33 minutes respectively at room temperature before measurement. Any decomposition at room temperature could not be detected from this test.

The half-life for POF_3 in N_2 at $170\text{ }^\circ\text{C}$ ⁱⁱⁱ was about 15 minutes according to the measurements shown in Figure 3, which means that there is no significant self-decomposition taking place in the measurement system during the $\sim 10\text{ s}$ response time of the FTIR measurement set-up.

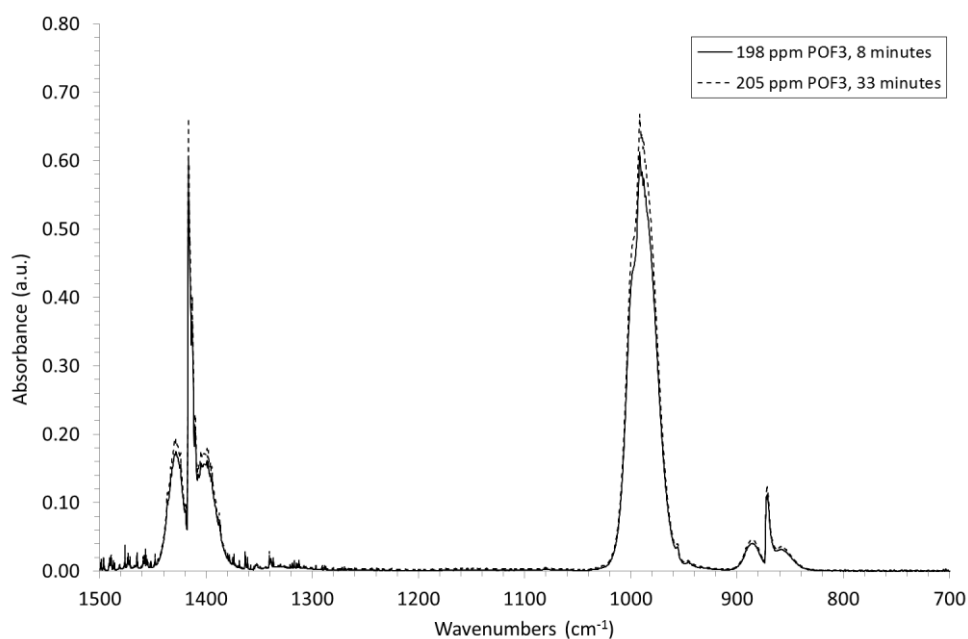


Figure 2 Spectra of $\sim 200\text{ ppm POF}_3$ measured in two separate Flexfoil bags at 8 min and 33 min after preparation.

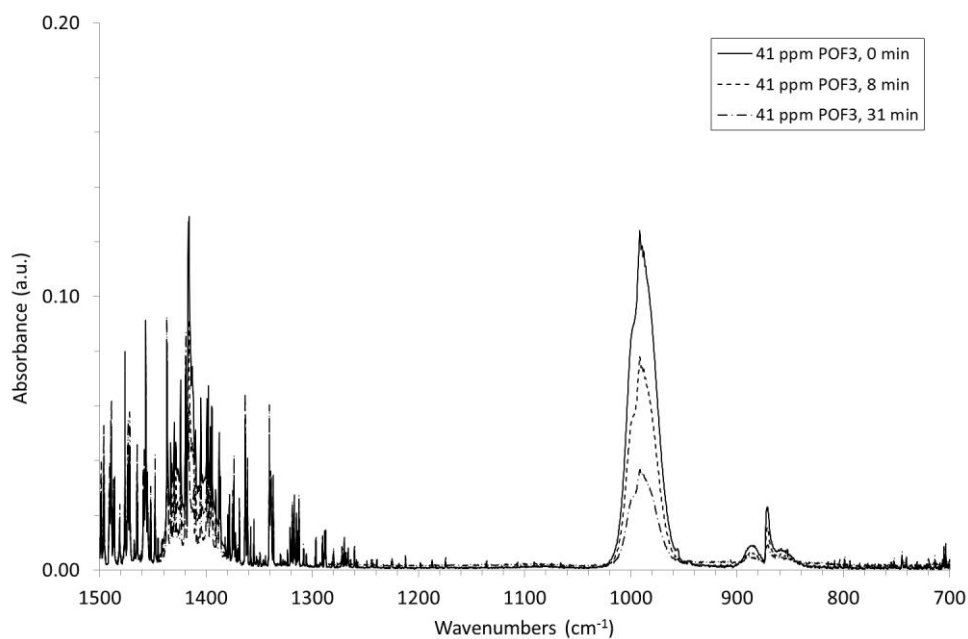


Figure 3 Series of spectra of 41 ppm POF_3 kept at $170\text{ }^\circ\text{C}$ in the FTIR gas cell for different times (0, 8 and 31 minutes).

To prepare PF_5 standard gas blends for calibration it was found that the gas bags used needed to be dried by flushing with N_2 in order to remove any remaining water as otherwise no

ⁱⁱⁱ The investigation of decomposition at an elevated temperature was made with a cell temperature of $170\text{ }^\circ\text{C}$ which was slightly lower compared to the standard cell temperature of $180\text{ }^\circ\text{C}$.

significant spectral bands apart from those of POF_3 and HF could be seen. This is explained by that the PF_5 added to the bag was hydrolysed even by the small amounts of water that was present in the bag, to form the decomposition products POF_3 and HF . The bags were subsequently thoroughly dried before adding PF_5 .

By using flushed bags it was possible to locate the spectral bands of PF_5 [13]. The interesting spectral range for PF_5 of nominally 200 ppm PF_5 in N_2 is presented in Figure 4 with the interesting bands of 1027, 1071, 956 and 946 cm^{-1} . As seen in Figure 4 bands from POF_3 (1416, 991 and 871 cm^{-1}) are also seen despite careful flushing of the bag. PF_5 has two stretching modes according to Yang et al. [13]. These are most probably the bands at 1017 cm^{-1} and 946 cm^{-1} . The remaining two bands found, 1027 cm^{-1} and 956 cm^{-1} , must thus originate from unidentified decomposition products of PF_5 . The bands are listed in Table 3.

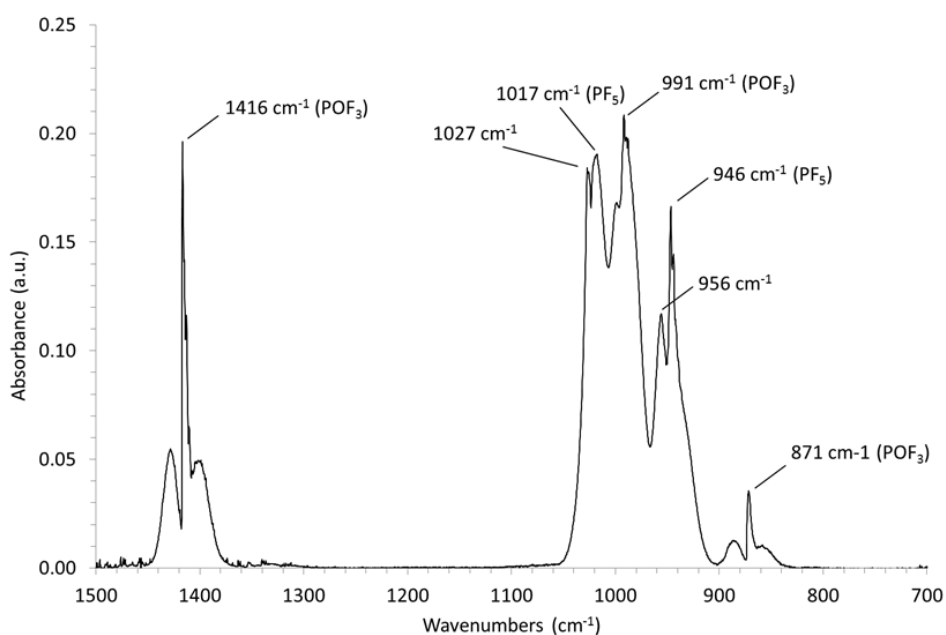


Figure 4 Spectral bands of PF_5 and decomposition products from 200 ppm PF_5 in N_2 . Decomposition occurred although the Flexfoil bag was flushed with dry N_2 prior to standard preparation.

Table 3 Spectral band positions found from PF_5 and decomposition products.

Band position (cm^{-1})	Type of band
1017	PF_5 : PF stretching [13]
946	PF_5 : PF stretching [13]
1027	Band from unknown decomposition product
956	Band from unknown decomposition product
1416	POF_3 : P-O stretch
991	POF_3 : P-F asymmetric stretch
871	POF_3 : P-F symmetric stretch

Heating tests with the Cone Calorimeter

The first step in our study was to investigate whether the same type of decomposition products as Yang et. al. [13] found, could be found in tests where the salt and the salt solved in electrolyte was heated in an open container with radiative heating in a Cone calorimeter, a schematic of the Cone calorimeter is provided in Figure 5. Further, combustion tests were conducted where the vapour was ignited to investigate how combustion would change the type of decomposition products.

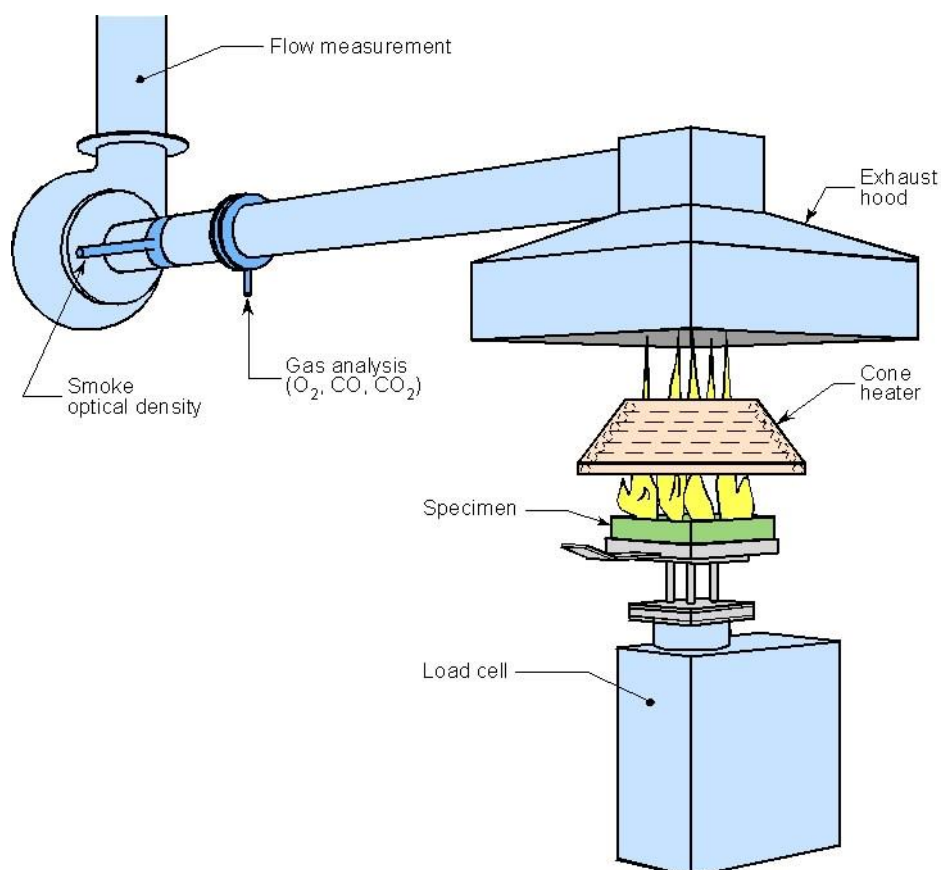


Figure 5 The Cone calorimeter.

The sample was placed in a small (~40 mm diameter) metal bowl which was placed under the heating cone of the Cone calorimeter. The irradiation of the sample was in the range of 10-15 kW/m². The FTIR was connected to the exhaust duct of the Cone calorimeter. Separate tests were conducted with only solvents (DME and PC), the pure LiPF₆ salt, and saturated solutions of LiPF₆ salt and solvents.

Figure 6 show the spectral bands of POF₃ in a test where pure LiPF₆ salt was thermally decomposed in the cone calorimeter. HF was also identified in this experiment. There are no traces of PF₅ or any additional decomposition products apart from POF₃ in the spectral range shown in Figure 6.

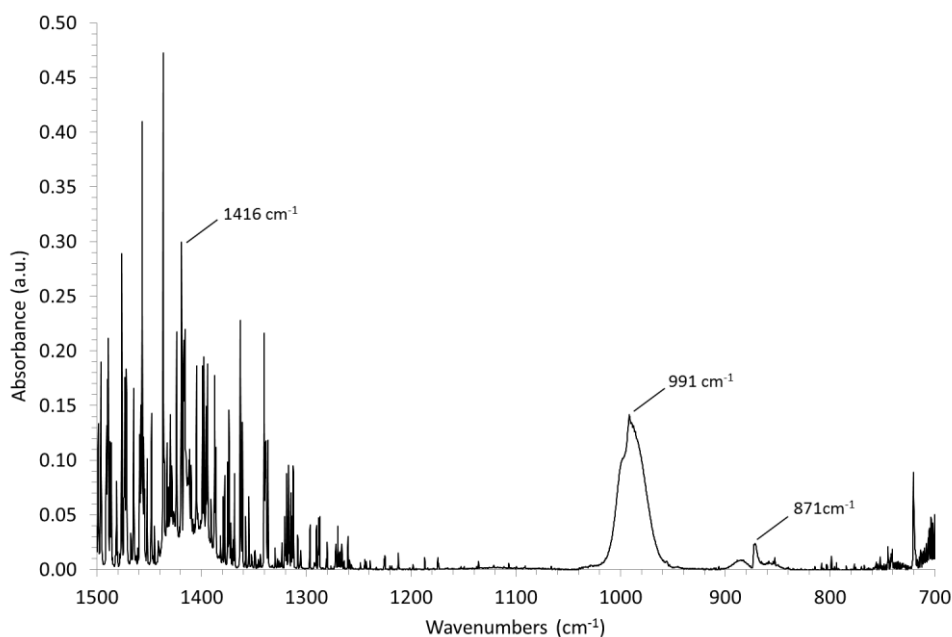


Figure 6 Spectral bands of decomposition products from pure Lithium hexafluoride (LiPF_6) in an evaporation test with the Cone calorimeter.

A spectrum from an evaporation experiment with a saturated solution of LiPF_6 salt in PC is shown in Figure 7. Overlaid in this figure is a spectrum from an evaporation tests with pure PC. The spectral band from the solvent is shown around 1100 cm^{-1} together with the three bands of POF_3 at 871 cm^{-1} , 991 cm^{-1} and 1416 cm^{-1} demonstrating the clear identification of the different substances in the evaporation experiment.

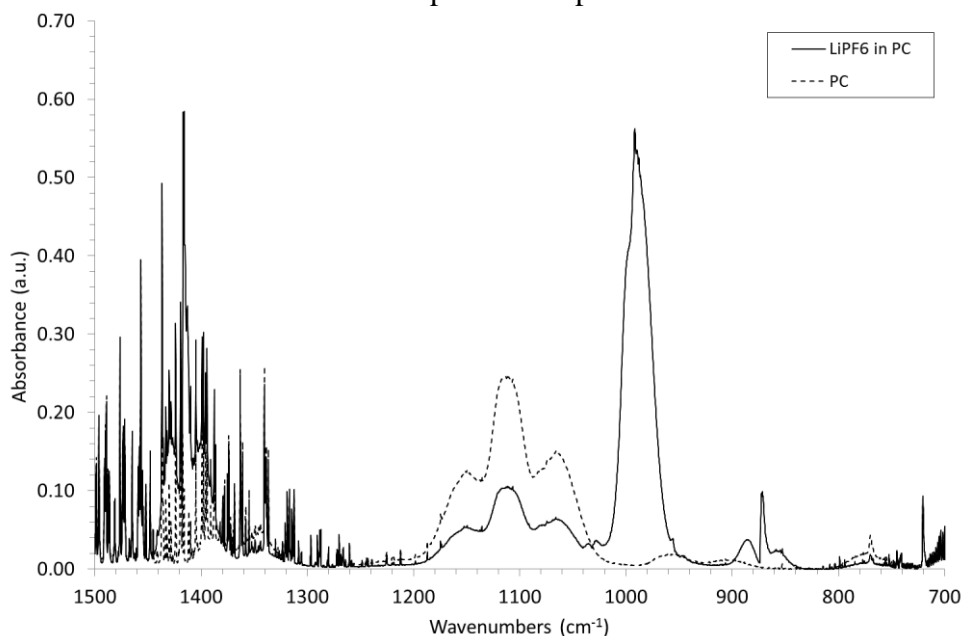


Figure 7 Spectrum from evaporation test with LiPF_6 mixed in Polypropylene carbonate (PC) with overlaid spectrum from evaporation of pure PC.

Similarly Figure 8 shows a spectrum from an evaporation test with a saturated solution of LiPF_6 salt in DME together with an overlaid spectrum from an evaporation experiment with

pure DME. Also here the spectral band from the solvent is seen around 1100 cm^{-1} together with the three bands of POF_3 at 871 cm^{-1} , 991 cm^{-1} and 1416 cm^{-1} .

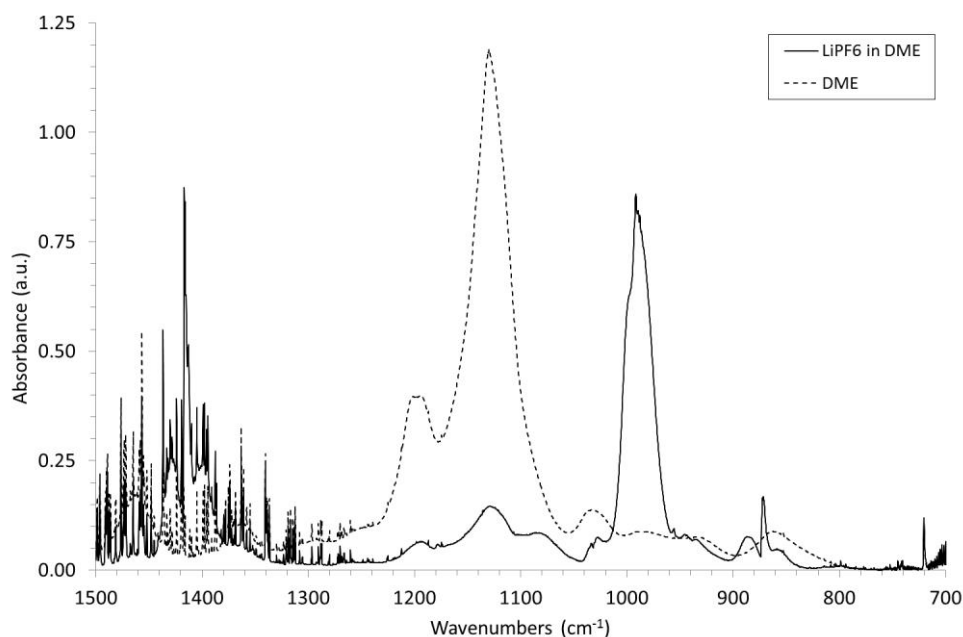


Figure 8 Spectrum from evaporation test with LiPF_6 mixed in Dimethoxyethane (DME) solid line overlaid by spectrum of DME only (dotted line).

Tests were also conducted where saturated solutions of LiPF_6 salt in DME, were ignited by the electric spark igniter in the Cone calorimeter. In these tests the same level of external radiative heat flow was used as for the evaporation tests discussed above ($10\text{--}15\text{ kW/m}^2$). A series of spectra (overlaid) are shown in Figure 9 from the tests with LiPF_6 salt in DME. One can clearly see the characteristic spectral features of POF_3 during the period of combustion (2–95 s). Also HF was seen in the spectrum during this period (not shown in Figure 9). The spectral band from the solvent is shown only in the first spectrum and in the spectrum from 67 s. The combustion efficiency must have decreased at this time but extinction was not recorded until 95 s. Figure 10 shows the spectrum from 54 s with a spectrum of DME from an evaporation test overlaid. Interesting is the two additional peaks, one at 1027 cm^{-1} and one at 1034 cm^{-1} , which do not originate from POF_3 and most probably not from DME. The peak at 1027 cm^{-1} was also found in the calibration tests with PF_5 where PF_5 was partly decomposed (see Figure 4).

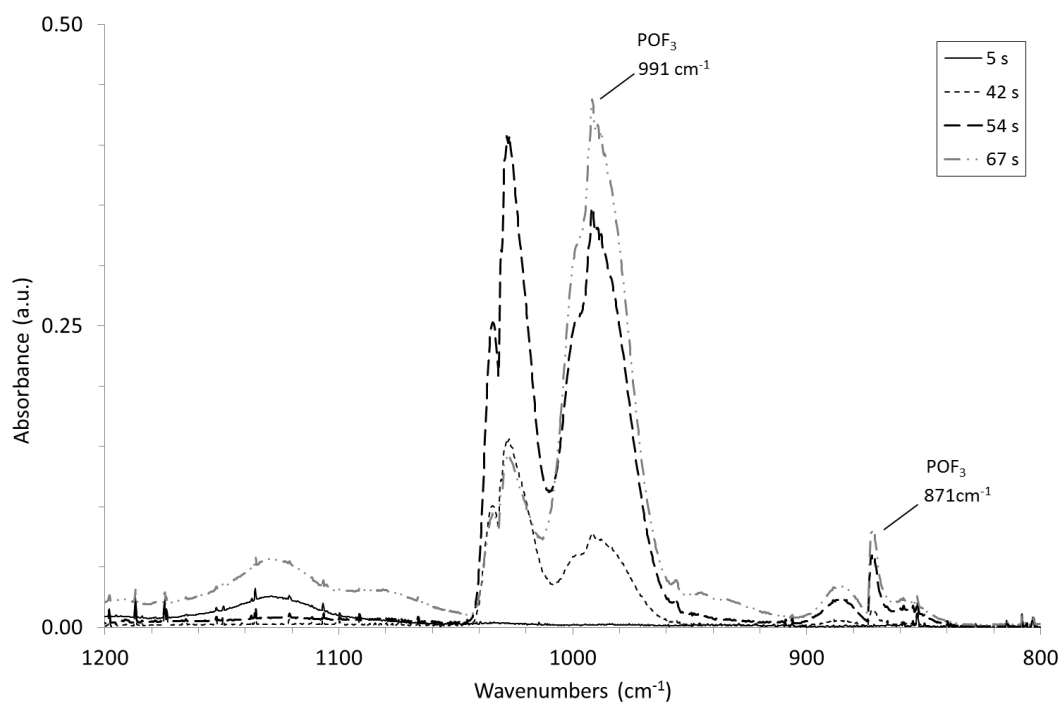


Figure 9 Series of spectra from fire test with LiPF_6 mixed in Dimethoxyethane (DME). Spectra measured at 5 s, 42 s, 54 s and 67 s after start of heat exposure. Ignition at 2 s after start. Flame-out at 95 s.

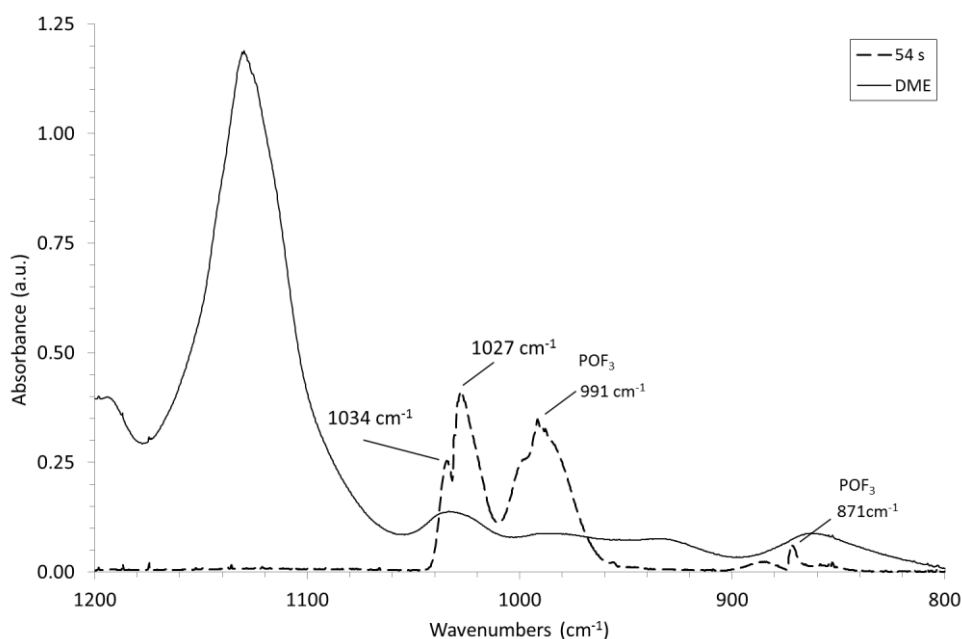


Figure 10 Spectra from the fire test with LiPF_6 mixed in DME at 54 s from start of test. Overlaid by spectra from evaporation test with DME (solid line).

Figure 11 shows a series of spectra (overlaid) from tests with LiPF_6 salt in PC. The spectral bands of POF_3 (the band at 991 cm^{-1} can be clearly seen in the figure) were seen in the spectra during the period of combustion (71-170 s). Also HF was seen as in the spectra during this period (not shown). The spectral band from the solvent is clearly shown in the spectra before ignition.

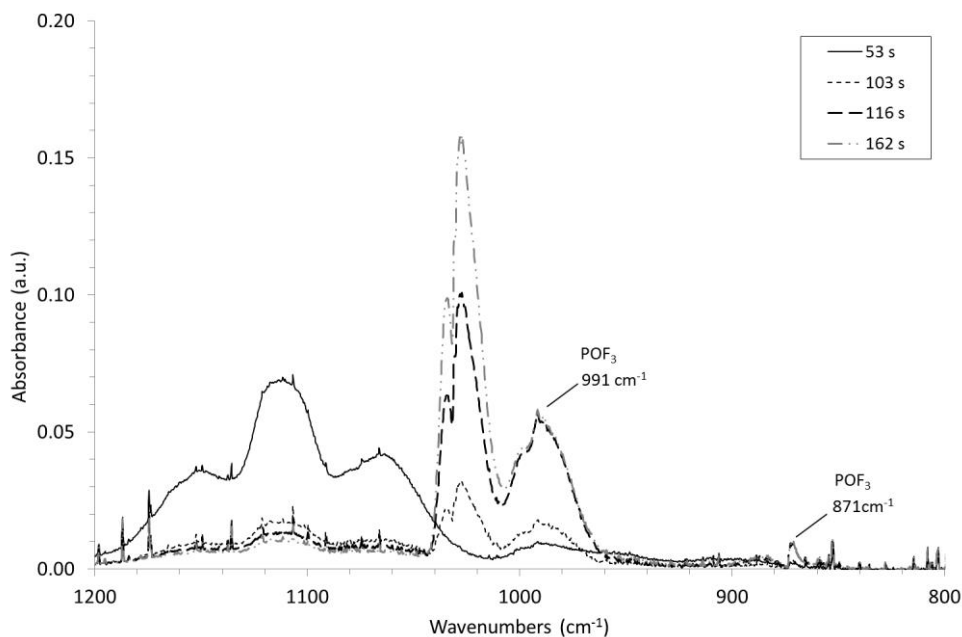


Figure 11 Series of spectra from fire test with LiPF_6 mixed in Polypropylene carbonate (PC). Spectra measured at 53 s (solid line, before combustion), 103 s (during combustion), 116 s (during combustion) and 162 s (during combustion) after start of heat exposure. Ignition at 71 s after start. Flame-out at 170 s.

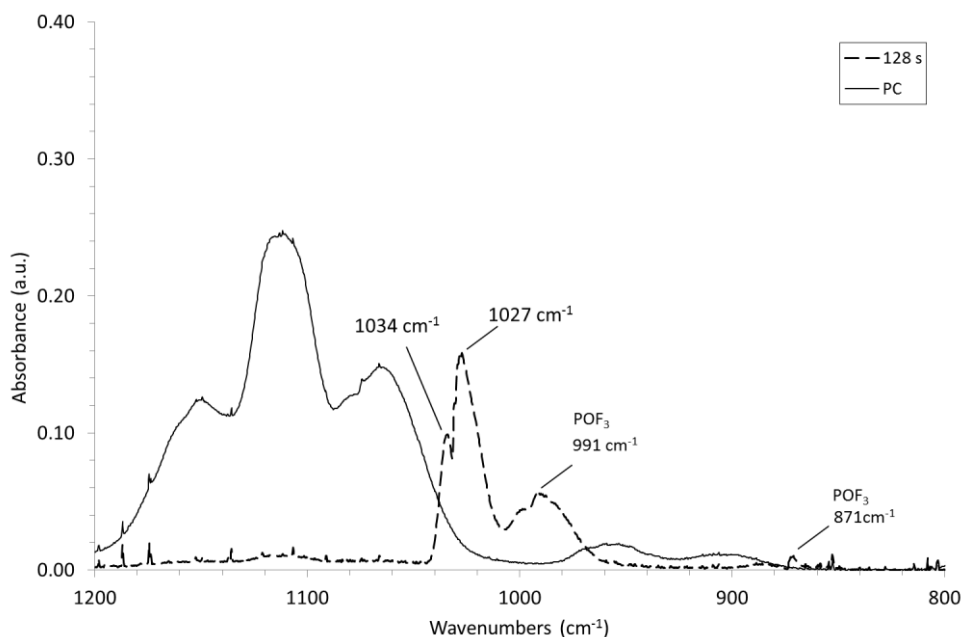


Figure 12 Spectrum from the fire test with LiPF_6 mixed in PC at 128 s from start of test (dotted line). Overlaid by spectrum from evaporation test with PC (solid line).

Figure 12 shows the spectrum collected at 128 s into the combustion test with LiPF_6 salt in PC. A spectrum of pure PC has been overlaid. Also here one can see the two additional peaks which do not originate from POF_3 , one at 1027 cm^{-1} and one at 1034 cm^{-1} .

The combustion tests with electrolyte solvents of LiPF_6 salt showed that HF and also POF_3 are present in the combustion effluents, while PF_5 is not present. Further, unidentified spectral absorption bands indicate the presence of an additional, possibly fluorine containing, decomposition product. The identification of the origin of the unidentified absorption peaks would be important to fully understand the decomposition of LiPF_6 . The presence of POF_3 is an important finding as this emission can be important to include in a toxicity evaluation of the fire effluents.

Burner tests with electrolyte

An experimental set-up, with a simple diffusion propane burner with the possibility to introduce solvent/salt solutions and water into the flame trough needles, was designed in order to be able to vary the salt/solvent concentration and combustion conditions in the test flames. This was done in order to investigate possible effects on toxic gas production from varying combustion conditions and from water used as extinguishing media.

The needle solution was chosen in order to produce a spray into the propane flame to make sure that the total amount of solvent/salt introduced was combusted. The propane burner was a very simple one, about 2 cm in diameter and holes were drilled in the side about 0.5 cm below the rim to introduce the needles, a picture of the burner is provided in Figure 13.

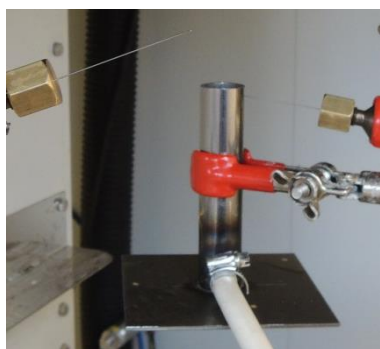


Figure 13 Picture of burner.

The amount of propane inserted was controlled by a variable area flow-meter. The amount of electrolyte inserted was controlled by two HPLC pumps. In the cases where salt was included, the solutions had been prepared before introduction into the HPLC pumps. Solutions of LiPF_6 (99 %, Sigma-Aldrich) were prepared by dilution in dimethylcarbonate (DMC, 99% Sigma-Aldrich) and 1,2-dimethoxy ethane (DME, 99% Sigma-Aldrich). The DMC solutions were 1.0 M and 0.4 M respectively and the DME solution was 0.4 M.

The HRR from the combustion was measured by using Oxygen Consumption Calorimetry on the effluents quantitatively collected in the Cone calorimeter hood. FTIR measurements were made in all tests. Tests were conducted with different propane/solvent ratio. Also the way the solvent and salt were introduced into the flame was varied (either through the needle into the flame or onto a metal plate in the flame) and the amount of salt was varied. A photo of the set-up with the metal plate is available in Figure 14.

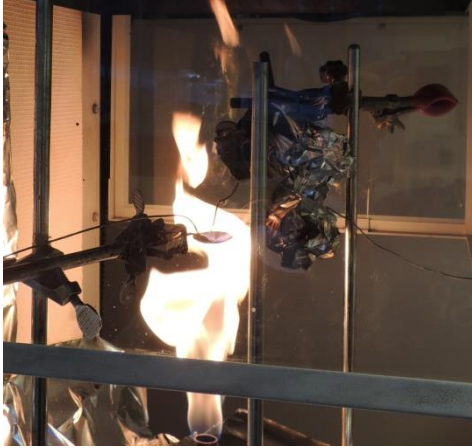


Figure 14 Photo of test where the electrolyte is introduced onto a metal plate in the flame.

Some tests were conducted where water was introduced into the flame. The duration of these tests was however, limited because despite careful design of needles that were custom made for this study we encountered problems with creating a stable spray for long periods of time.

An example of test results using the spray into the flame is presented in Figure 15 and Figure 16 where 18 ml/min with 0.4 M salt solved in DME was introduced in the flame as a spray during 2.5 minutes. A full set of test results is available in Andersson et al [19]. In Figure 15 the HRR is presented on the left hand axis together with the HF concentration in the smoke duct on the right hand axis. The HRR curve includes the HRR from the propane flame also, the timing for the introduction of the electrolyte spray is clearly seen as the HRR increases sharply. In Figure 16 from the same test, HF concentration in the smoke duct is presented on the left hand side and the POF_3 concentration in the duct on the right hand side axis.

When studying the graphs it is important to remember that the concentrations presented are concentrations in the exhaust duct. These depend on the gas flow in the exhaust duct and the amount of salt and electrolyte introduced into the flame. They should not be considered as the concentration in the vicinity of a burning Li-ion battery in an electrified vehicle but are only presented here as concentrations in order to evaluate changes in amount produced due to changes in flame composition etc.

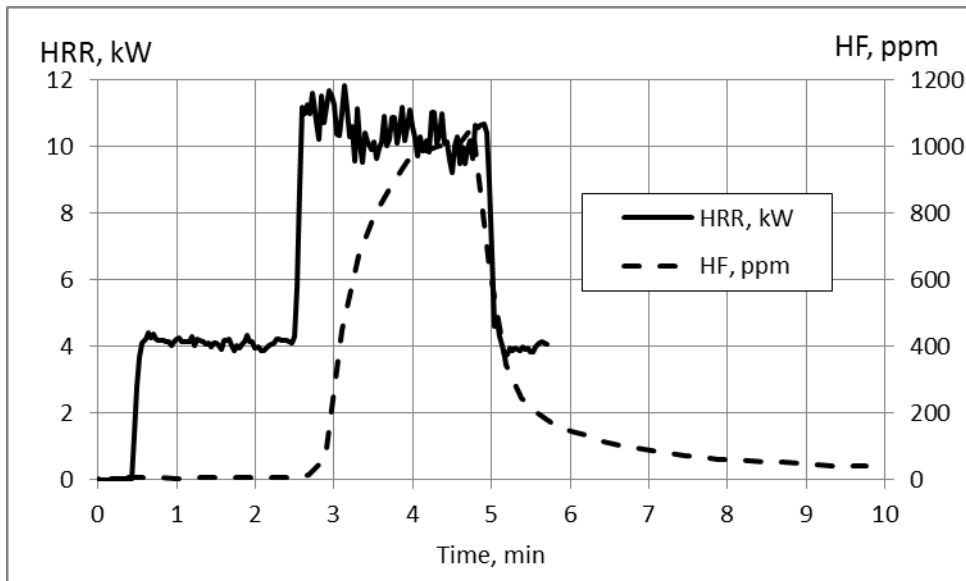


Figure 15 HRR and HF concentration in a test where 18 ml/min with 0.4 M salt solved in DME was introduced in the flame during 2.5 minutes.

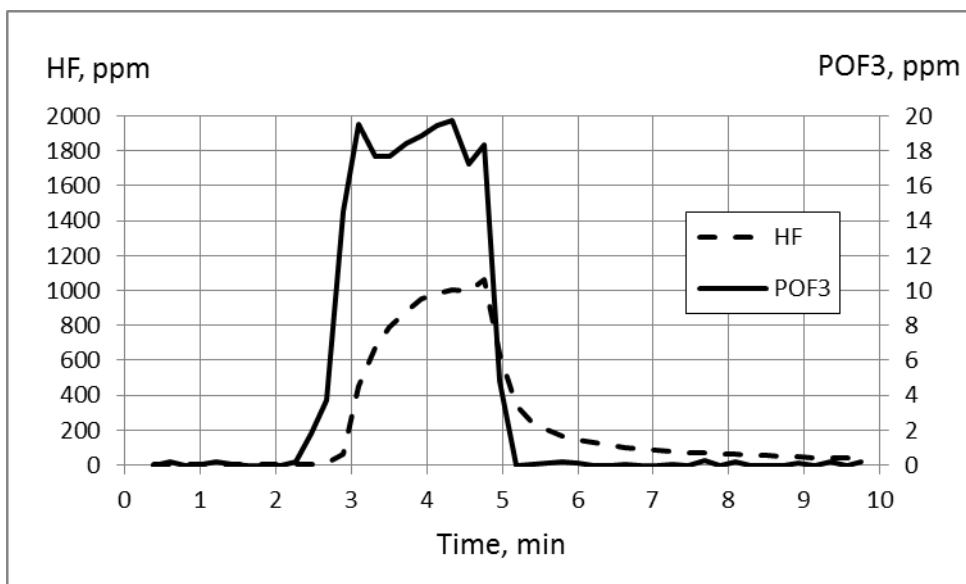


Figure 16 HF and POF₃ concentration as a function of time in a test where 18 ml/min with 0.4 M salt solved in DME was introduced in the flame during 2.5 minutes.

Similar curves for a test where 18 ml/min of 1 M salt in DMC was introduced into the flame as a spray during two minutes are shown in Figure 17 and Figure 18. As seen the results are similar to the case with 0.4 M salt in DME as presented in Figure 15 and Figure 16, i.e. the spray introduction is clearly seen as a sharp increase in the HRR and the HF and POF₃ concentration increases with a slight delay. A difference is however seen in the HF/POF₃ ratio.

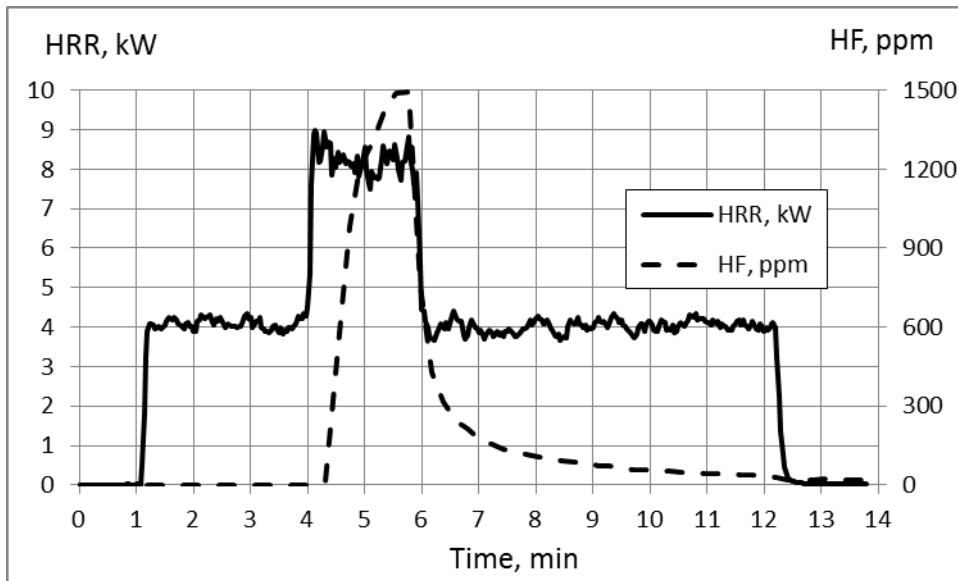


Figure 17 HRR and HF concentration during a test where 18 ml/min of 1 M salt solved in DMC was injected as a spray during two minutes.

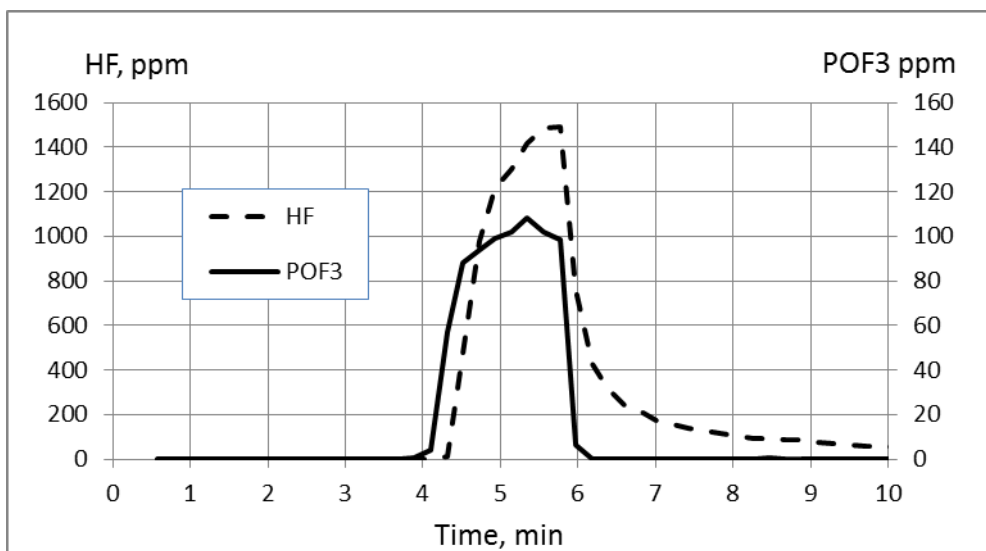


Figure 18 HF and POF₃ concentration as a function of time for a test where 18 ml/min of 1 M salt solved in DMC was injected as a spray during two minutes.

The tests using the spray introduced into the burner all showed that the HRR was increased immediately upon injection of the electrolyte while it seems that the HF and POF₃ concentration increased somewhat delayed. This is caused by the 12 s integrating time of the FTIR analysis equipment and could also be due to delays in the filter and sampling system and to some extent to the delays in the pump system for introducing the salt and solvent.

An example of a result from a test where DMC and salt was introduced into the flame in a much slower pace, i.e. 1.8 ml/min during 5 minutes is given in Figure 19. In this case the electrolyte flow had to be inserted onto a metal plate in the flame as it was not possible to get a spray at this low rate. As only a small amount of electrolyte was introduced into the flame no change in HRR could be observed. Still both HF and POF₃ were detected. The time delay

here is significant; this is due to the long transportation time through the pump system with this small pump flow. Also the delay in HF concentration due to delay in the sampling system is more pronounced here as the amount of HF produced is much lower due to the lower rate of electrolyte introduction.

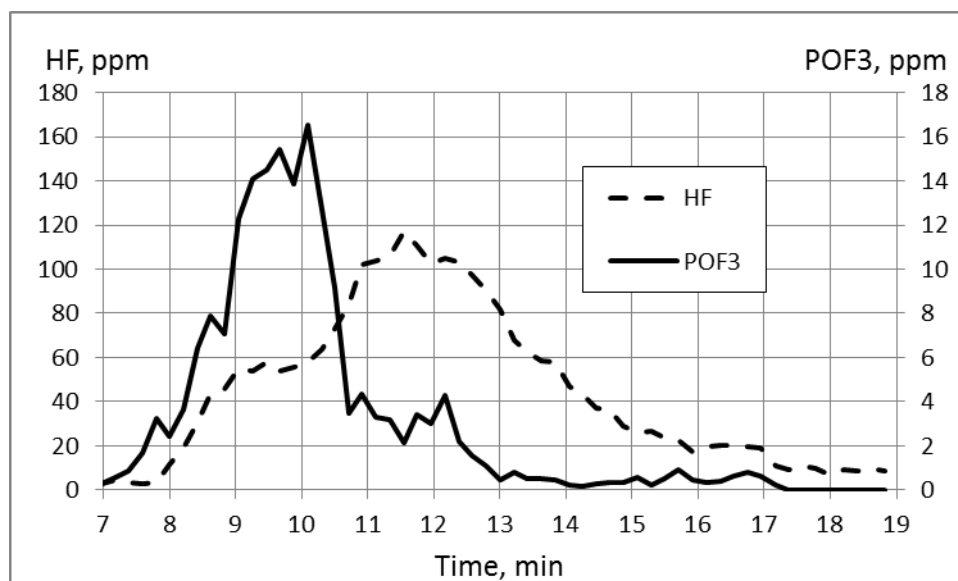


Figure 19 HF and POF₃ measurements from a test where 1.8 ml/min of 1M salt solved in DMC was introduced onto a metal plate in the flame.

The tests conducted are summarized in Table 4 together with the HF/POF₃ ratio. As seen in the table the FTIR measurements showed that both HF and POF₃ were always present in the combustion effluents when electrolytes were burning. The measured concentration of HF was always significantly higher than the measured POF₃ concentration.

Table 4 Tests conducted.

Test	Type	Flow (ml/min)	Salt	Propane HRR	Electrolyte HRR	HF/POF ₃ ratio	Test # in [19]
A	Needle	18	0.4 M in DME	4 kW	6 kW	53	12
B	Needle	18	1 M in DMC	4 kW	4 kW	14	10
C	Needle	18	1 M in DMC	4 kW	4 kW	20	13
D	Metal plate	1.8	1 M in DMC	4 kW		8	15
E	Needle	15	1 M in DMC	5 kW	3 kW	23	22
F	Needle	15	0.4 M in DMC	3.2 kW	2.5 kW	20	23
G	Needle	15	1 M in DMC	5 kW	3.3 kW	12	25
H	Needle, water spray	15	1 M in DMC	5 kW	3 kW	8	26
I	Needle, water spray	15	1 M in DMC	5 kW	2 kW	16	26

Despite careful design of needles it was difficult to obtain a stable spray. The needles were clogged in many cases and tests had to be interrupted. In some cases the measured HRR was lower than anticipated indicating that the flow through the pump was lower than anticipated or that not complete combustion of the electrolyte occurred due to that some electrolyte was released as a beam rather than a spray. Table 4 gives some insights into the uncertainties involved in these measurements e.g. by studying test B and C which repeats the same conditions and results in a HF/POF₃ ratio of 14 and 20 respectively. A similar variation is seen between test E and G with a HF/POF₃ ratio of 23 and 12 respectively.

Studying test B, E and G one sees that test E and G with a larger propane/electrolyte ratio resulted in a HF/PO₃ ratio of 23 and 12 respectively while the ratio was 14 for test B, i.e. varying the propane/electrolyte ratio does not affect the HF/POF₃ ratio.

The test E and G range of 12-23 covers to some extent the results from test H and I where water was sprayed into the flame for some period during the test which resulted in a HF/POF₃ ratio of 8 and 16 respectively. The results from test H are shown in Figure 20 where water was sprayed into the propane/electrolyte flame during time 3 minutes until 3:45. As seen it seems that the water injection causes the POF₃ to increase. The same ratio is also kept initially when the electrolyte injection was stopped and water was let trough the pump and needle in order to clean the needle from time 5 minutes until 7 minutes. However looking into Figure 21 for test I no such effect can be observed and thus it is not possible to make any conclusions concerning the water influence on the fluorinated species generated even if the ratio seems to be on the lower side of the HF/POF₃ ratio measured in the without water case. The reason for the limited effect of the water spray can be the fact that the water sprayed into the flame was limited compared to the amount of water already present due to the combustion products from the propane and electrolyte as seen from the water vapour measurement from the FTIR presented as a dotted line in Figure 20 and Figure 21.

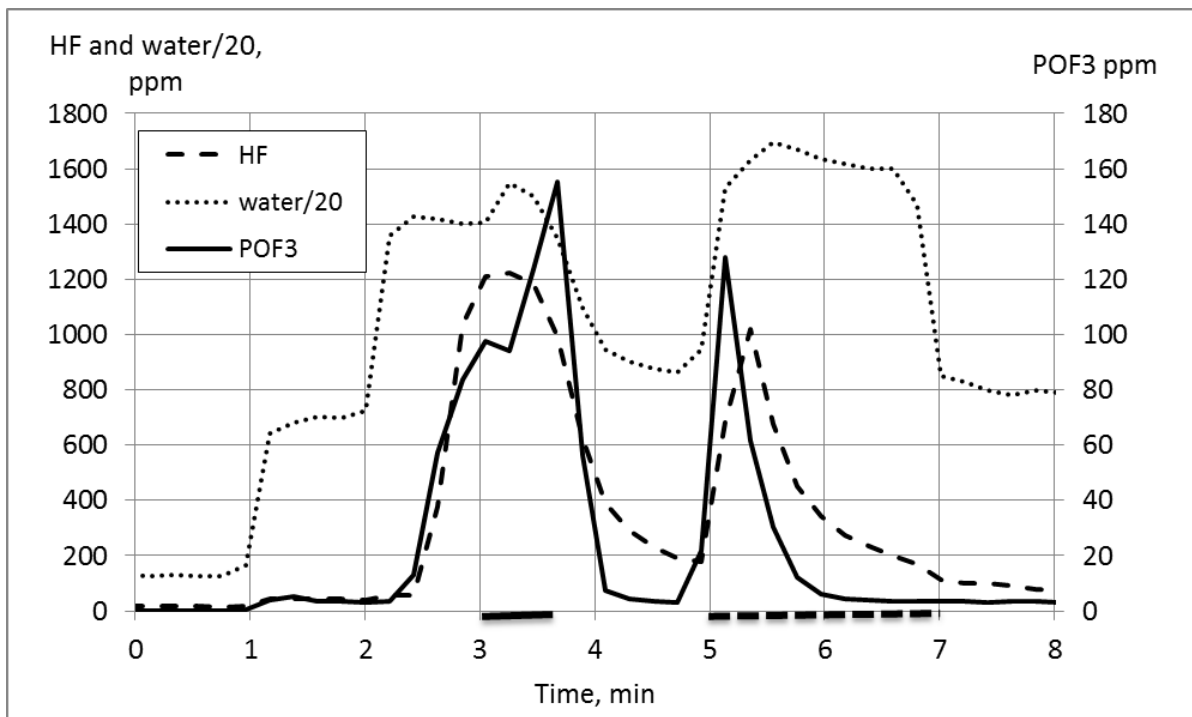


Figure 20 HF and POF₃ concentration for the electrolyte injection during time 2 minutes until 3 minutes 40 and water cleaning of the system during time 5

minutes until 7 minutes. Water was sprayed into the propane/electrolyte flame from time 3 minutes until 3 minutes 40.

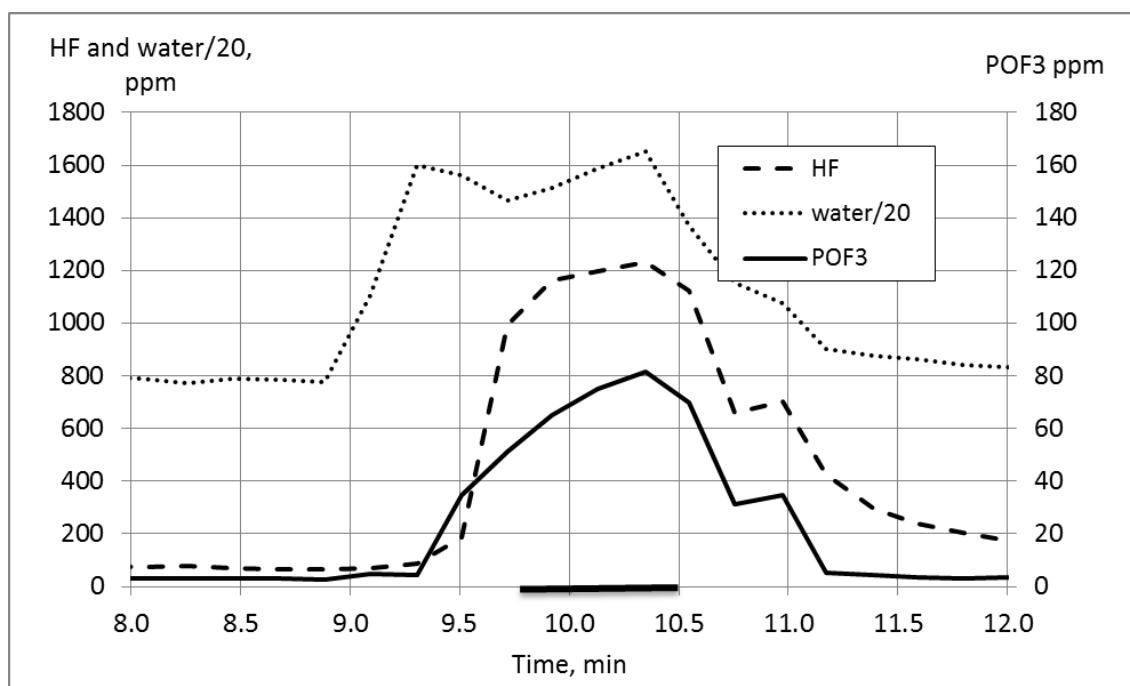


Figure 21 HF and POF₃ concentration for the electrolyte injection during time 9 minutes until 10 minutes 30s. Water was sprayed from time 9 minutes 50 until 10 minutes 30.

A notable difference is however seen between Test A and the other tests. In Test A 0.4 Molar DME was used while DMC was used in all other tests. The HF/POF₃ ratio is 53 in Test A while it differs between 8 and 23 for the other tests. The 53 ratio is especially interesting in the light of Test F where the HF/POF₃ ratio is 20 for a 0.4 Molar DMC solution. Eshetu et. al. [16] indicate that the toxicity of the combustion gases depends on the solvents used when studying unburned hydrocarbons, aldehydes and soot in oxygen lean conditions, i.e. linear carbonate esters results in less toxic gases than cyclic carbonates. Both DMC and DME are linear which gives thus no guidance in this matter, in addition did Eshetu et al [16] not study fluorinated compounds but only the solvents without any salt. DME and DMC differs however significantly when it comes to Heat of combustion where DME has a much higher heat of combustion of almost 28 kJ/g compared to DMC of about 14.6 kJ/g. Also the solubility of the salt differs significantly between DME and DMC.

All tests showed that the POF₃ seems to appear a bit earlier than HF, this was especially apparent in Test D where the electrolyte/salt solution was introduced onto a metal plate at a low flow rate in the flame. It is known that losses of HF occur in the measurement system and especially in the sampling filter [20]. The effect is most significant at measurements of low concentrations as the proportion captured in the filter in such cases is high compared to the total amount HF sampled through the filter. An effect of HF-losses in the filter is an initial increased response time (until the sampling system is saturated) that can be significant especially in measurements of low concentrations. Selected filters used in the measurements were analysed for total fluorine content. The analysis results showed that the amounts lost in the filter were low, normally around 5 % on weight basis.

Conclusions

The study conducted here is limited. In addition, it was not possible to vary all parameters to an as large extent as planned for due to difficulties with creating a stable spray. Further was it difficult to assess some of the variations as the time delays particularly for the HF was significant. Still some important findings were made.

The work presented shows that it is possible to use FTIR to measure HF and POF_3 in real time in Li-ion electrolyte experiments with and without combustion. The detection limit for the equipment used here was found to be 2 ppm for HF and 6 ppm for POF_3 .

Both HF and POF_3 were detected in all experiments. It is an important finding that POF_3 is emitted together with HF also from combustion as this can increase the toxicity of the fire effluents. The amount of POF_3 is shown to be significant, 5-40 % of the HF emissions on a weight basis and demonstrates the importance of finding the toxicity parameters for this substance. The toxicity of POF_3 is not known but halogen analogues (POCl_3) similar to POF_3 are highly toxic, more toxic than their corresponding acid (HCl). More information is needed to resolve this issue especially as POF_3 can be emitted under other cell venting situations and not only fires.

PF_5 could not be detected in any of the tests. The reason for this is probably the high reactivity of this specie. This was demonstrated by the difficulty to produce a calibration gas mixture for PF_5 .

Given the uncertainties involved in the tests it was not possible to determine any impact on gases produced depending on combustion parameters such as solvent/propane ratio, concentration of salt or the way the salt/solvent was introduced into the flame.

A possible difference was however seen in HF/ POF_3 ratio depending on solvent used. This shows that also the solvent might have an impact on the amount of substances emitted in a fire situation. Eshetu et al [16] suggested an evaluation scheme for different solvents considering combustion behaviour and other properties such as viscosity. Considering the combustion parameters DME would be a poor choice. This evaluation scheme does not include fluorinated compound toxicity however. Given the toxicity of HF and possibly also POF_3 , a replacement for the LiPF_6 salt is important to improve the safety for Li-ion batteries which is also concluded by Ribiere et al [17].

Acknowledgments

The authors gratefully acknowledge the Swedish Fire Research Board and the Swedish Energy Agency for the financial support.

References

1. Wang Q, Ping P, Zhoi X, Chu G, Sun J, Chen C. Thermal runaway caused fire and explosion of lithium ion battery. *Journal of Power Sources* 2012; **208**: 210-214.

2. Lisbona D, Snee T. A review of hazards associated with primary lithium and lithium-ion batteries, *Process safety and environmental protection* 2011; **89**: 434-442.
3. Doughty D, Roth P, A general discussion of Li ion battery safety. *The Electrochemical Society Interface*, 2012: 37-44.
4. Kirk-Othmer *Encyclopedia of Chemical Technology*, John Wiley & Sons, 1994, **11**.
5. Hammami A, Raymond N, Armand M. Runaway risk of forming toxic compounds, *Nature* 2003; **424**, 635-636.
6. Hygiensiska gränsvärden AFS 2011:18, Hygieniska gränsvärden Arbetsmiljöverkets föreskrifter och allmänna råd om hygieniska gränsvärden, ISBN 978-91-7930-559-8, ISSN 1650-3163, Swedish Work Environment Authority, Sweden, 2011.
7. Ohsaki T, Kishi T, Kuboki T, Takami N, Shimura N, Sato Y, Sekino M, Satoh A. Overcharge reaction of lithium-ion batteries, *Journal of Power Source* 2005; **146**: 97-100.
8. Abraham DP, Roth P, KostECKI E, McCarthy K, MacLaren S, Doughty D, Diagnostic examination of thermally abused high-power lithium-ion cells, *Journal of Power Sources* 2006;**161**: 648-657.
9. Roth P. Thermal response and flammability of Li-ion cells for HEV and PHEV applications, *SAE Int. J. Passen. Cars – Mech. Syst*, 2008, volume 1, issue 1.
10. Champion CL, Li W, Lucht B. Thermal decomposition of LiPF₆-based electrolytes in lithium-ion batteries. *Journal of the Electrochemical Society* 2005; **152 (12)**: A2327-A2334.
11. Yang H, Shen XD. Dynamic TGA-FTIR studies on the thermal stability of lithium/graphite with electrolyte in lithium-ion cell. *Journal of Power Sources* 2007;**167**: 515-519.
12. Lux SF, Lucas IT, Pollak E, Passerini S, Winter M, KostECKI R. The mechanism of HF formation in LiPF₆ based organic carbonate electrolyte. *Electrochemistry Communications* 2012; **4**: 47-50.
13. Yang, H., Zhuang, G. V. and Ross, P. N. Jr, "Thermal Stability of LiPF₆ salt and Li-ion battery electrolytes containing LiPF₆, *Journal of Power sources* 161 (2006) 573-579.
14. Wang QS, Sun JH, Chu GQ, Yao XL, Chen CH. Effect of LiPF₆ on the thermal behaviors of four organic solvents for lithium ion batteries. *Journal of Thermal Analysis and Calorimetry*, 2007; **89**: **1**: 245-250.
15. Teng XG, Li FQ, Ma PH, Ren QD, Li SY. Study on thermal decomposition of lithium hexafluorophosphate by TG-FT-IR coupling method. *Thermochimica Acta*, 2005; **436**: 30-34.
16. Eshetu, G.G., Grugeon, S., Laruelle, S., Boyanov, S., Lecocq, A., Bertrand, J-P., Marlair, G., In-depth safety-focused analysis of solvents used in electrolytes for large scale lithium ion batteries", *Phys.Chem. Chem. Phys.*, 2013; **15**: 9145
17. Ribière, P., Grugeon, S., Morcrette, M., Boyanov, S., Laruelle, S., Marlair G., *Energy Environ. Sci.*, 5 (2012) 5271-5280.
18. ISO 5660:2002 Reaction-to-fire-tests – Heat release, smoke production and mass loss rate – Part 1: Heat release rate (cone calorimeter method)
19. P. Andersson, P. Blomqvist, A. Lorén, F. Larsson, Investigation of fire emissions from Li-ion batteries, SP Report 2013:5, SP Technical Research Institute of Sweden, Borås, Sweden, ISBN 978-91-87461-00-2, 2013.
20. ISO 19702:2006, Toxicity testing of fire effluents -- Guidance for analysis of gases and vapours in fire effluents using FTIR gas analysis

Paper V

Characteristics of Lithium-ion batteries during fire tests

Fredrik Larsson^{a,b,*}, Petra Andersson^a, Per Blomqvist^a, Anders Lorén^a and Bengt-Erik Mellander^b

^aSP Technical Research Institute of Sweden, Brinellgatan 4, SE-501 15 Borås, Sweden

^bDepartment of Applied Physics, Chalmers University of Technology, SE-412 96 Göteborg, Sweden

*Corresponding author: Tel.: +46 10 5165928; fax: +46 33 125038

E-mail address: fredrik.larsson@sp.se

Abstract

Commercial lithium-ion battery cells are exposed to a controlled propane fire in order to evaluate heat release rate (HRR), emission of toxic gases as well as cell temperature and voltage under this type of abuse. The study includes six abuse tests on cells having lithium-iron phosphate (LFP) cathodes and, as a comparison, one test on conventional laptop battery packs with cobalt based cathode. The influence of different state of charge (SOC) is investigated and a limited study of the effect of water mist application is also performed. The total heat release (THR) per battery energy capacity are determined to be 28-75 kJ/Wh and the maximum HRR values to 110-490 W/Wh. Hydrogen fluoride (HF) is found in the released gases for all tests but no traceable amounts of phosphorous oxyfluoride (POF₃) or phosphorus pentafluoride (PF₅) are detected. An extrapolation of expected HF emissions for a typical automotive 10 kWh battery pack exposed to fire gives a release of 400-1200 g HF. If released in a confined environment such emissions of HF may result in unacceptable exposure levels.

Keywords: Lithium ion, battery, hydrogen fluoride, phosphorous oxyfluoride, heat release rate, fire

1. Introduction

Lithium-ion batteries are widely used since they offer great benefits compared to many other battery technologies. Advantages such as high energy and power density, long life time and the possibility of fast charging make them attractive for consumer products and electrified vehicles. Nevertheless Li-ion batteries contain reactive and flammable materials, therefore safety issues are a concern and a number of incidents involving Li-ion batteries have been reported over the last couple of years [1-4]. Overheating of the batteries may result in exothermal reactions and lead to a thermal runaway with excessive amounts of heat, gas emissions, fire and potentially explosion/rapid dissembling [1,5-6]. Even in case there is no thermal runaway, a heated battery can still vent flammable and toxic gases. Examples of toxic gases that may originate from such events are hydrogen fluoride, HF, and phosphorous oxyfluoride, POF₃. The toxicity of HF is quite well known [7] since it is formed during several chemical decomposition processes and fires but the toxicity of the POF₃ is currently unknown. Actually, the toxicity of POF₃ might act with other poisoning mechanisms than just by formation of three equivalents of HF. Therefore, critical limits of exposure might be lower for POF₃ than for HF as in the chlorine analogue POCl₃/HCl [8]. The origin of the fluorine compounds is primarily the battery electrolyte but emissions can also come from the binder (e.g. PVdF) of the active electrode materials. The electrolyte usually contains flammable organic solvents some of which are volatile at modest temperatures (below 100 °C) and the commonly used Li-salt, lithium hexafluorophosphate, LiPF₆, has a limited thermal stability upon heating. The decomposition of LiPF₆ can be described, according to Yang et al. [9] and Kawamura et al. [10], by:





When LiPF_6 is heated in a dry and inert atmosphere it decomposes to lithium fluoride, LiF , which is a solid compound at temperatures below 845°C and phosphorus pentafluoride, PF_5 , which is a gas and a strong Lewis acid, see eq. (1). In the presence of water/moisture PF_5 produces POF_3 , and HF (eq. (2)). LiPF_6 can also react directly with water/moisture to form LiF , POF_3 and HF according to eq. (3). In fact, LiPF_6 is highly susceptible to hydrolysis by even trace amounts of moisture [11]. Furthermore, Kawamura et al. [10] suggested that POF_3 could react with water and form $\text{POF}_2(\text{OH})$ and HF according to eq. (4).

The decomposition of electrolytes containing LiPF_6 forming HF is complex and has mainly been studied at ambient temperature and during heating (but not in situations where there is a fire) [12-19]. Besides emissions containing fluorine and vaporized solvents, a Li-ion cell can also emit other gases, e.g. H_2 , CO , CO_2 , CH_4 , C_2H_6 and C_2H_4 [20-22]. Gases can actually be emitted from batteries under several types of abuse conditions such as overheating, overcharge [23], short circuit, fires etc. A few studies are published on heat release rate (HRR) and emissions of toxic gases from Li-ion batteries in fire conditions. Ribière et al. [24] used a Tewarson fire calorimeter to study the HRR and toxic gases from commercial 2.9 Wh pouch cells with LiMn_2O_4 (LMO) cathode and graphite anode and found e.g. that the total HF release was higher for lower state of charge (SOC) values. Eshetu et al. [25] studied fire properties and toxicity for commonly used Li-ion battery electrolytes but without Li-salt and thus without the possibility to produce HF .

This paper presents results from fire tests of commercially available Li-ion battery cells. Parameters such as heat release rate, cell voltage and surface temperature are measured as well as HF and POF_3 emissions. The influence of application of water is examined to a limited extent by introducing water mist into the flames.

2. Experimental

The tests were conducted using the measurement and gas collection system of a Single Burning Item (SBI) apparatus, that is normally used for classification of building materials according to the European Classification scheme EN13823 [26]. The experimental setup is shown in Fig 1. The cells/batteries were placed on a wire grating (large gratings about 4 cm x 10 cm) as seen in Fig 2. A propane burner was placed underneath the cells/batteries and was ignited two minutes after the start of the test. The HRR of the burner alone was approximately 15 kW. Abuse tests were performed on 7 Ah EiG LFP pouch cells, 3.2 Ah K2 LFP cylindrical cells, and on 16.8 Ah Lenovo laptop battery packs, see Table 1.

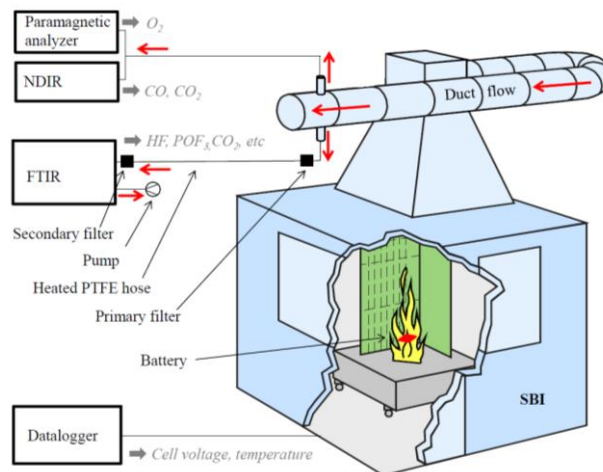


Fig. 1. Schematic illustration over experimental setup.



Fig. 2. The 5-cells pack of EiG cells placed on a wire grating.

Test 1-5 used commercially available pouch cells with lithium-iron phosphate (LFP), LiFePO_4 , cathode and carbon based anode. Each test consisted of five cells that were mechanically fastened together with steel wire (0.8 mm diameter). The terminal tabs of the cells were cut for all cells but the mid one (the third cell), for which the cell voltage was measured. On both sides of the third cell type K thermocouples were centrally attached measuring the cell surface temperature. Temperature values presented in this paper are the average of these thermocouple readings. The temperature and cell voltage was measured with a sample rate of 1 Hz using a data logger, *Pico Technology ADC-24*. In test 3, water mist was manually applied as a spray into the flames above the battery to study any influence from additional water on the composition of the gas emissions. In test 6, nine K2 26650-cells, i.e. cylindrical cells 26 mm in diameter and 65 mm long, were placed standing up next to each other inside a box. The box had side walls made of non-combustible silica board and steel net at the bottom and top. It was used as a safety precaution to avoid possible projectiles. In test 7, two identical laptop battery packs were used and placed inside a steel net and fastened on the wire grating.

Table 1

Test objects.

Test No.	Battery type	No. of cells	Nominal capacity (Ah)	Weight (g)	Test condition
1	EiG ePLB-F007A	5	35	1 227.9	100% SOC
2	EiG ePLB-F007A	5	35	1 229.7	100% SOC
3	EiG ePLB-F007A	5	35	1 229.3	100% SOC + water mist
4	EiG ePLB-F007A	5	35	1 228.6	0% SOC
5	EiG ePLB-F007A	5	35	1 227.6	50% SOC
6	K2 LFP26650EV	9	28.8	734.8	100% SOC
7	Lenovo laptop battery packs	12*	33.6	639.0	100% SOC

* Two laptop battery packs were used at the same time, each with 6 cells.

The cells in test 1-6 were set to the selected SOC-level, according to Table 1, by a charge/discharge procedure using an ordinary laboratory power aggregate and a *Digatron* battery test equipment. The two laptop battery packs in test 7 were fully charged using a laptop computer. All batteries were unused but had different calendar aging. The EiG cells were approximate 2-3 years old, the K2 cells were approximate 1-2 years old and the laptop battery pack was less than 6 months old.

The laptop battery packs in test 7 differ from the other test objects. First, they consist of not only the cells but also electrical connectors, plastic housing and electronic circuits. Secondly, they have cobalt based cell chemistry with a

higher cell voltage, 3.7 V vs 3.2 V for the LFP-cells. Thirdly, in each battery pack, 3 cells are electrically connected in series increasing the voltage to 11.1 V.

All tests were video recorded. The tests were performed during two days and in the beginning of each day a blank test was conducted in order to be able to subtract the burner influence on the HRR values and to make a blank for the gas analysis. The burner was active for a varying duration in the different tests, between 17-32 minutes, i.e. as long as a heat release contribution from the battery was still present. The fire emissions from the test object were collected in a ventilation duct. In test 1-2 a duct flow of 0.6 m³/s was used but in order to increase emission concentrations in the ventilation the duct flow was decreased to 0.4 m³/s in test 3-7.

A *Servomex 4100 Gas purity analyser* was used to measure the oxygen content of the flow by a paramagnetic analyzer and CO and CO₂ were determined by a non-dispersive infrared sensor (NDIR). The HRR was calculated using the method of oxygen consumption and was corrected for CO₂ [26]. A part of the flow in the ventilation duct was extracted for on-line FTIR analysis. This sub-flow was extracted through an 8.5 m sampling PTFE hose, heated to 180 °C, using a pump (3.5 L/min) located after the FTIR measurement cell. The sampled gas is passed through a primary filter (*M&C* ceramic filter, heated to 180 °C) before the heated hose and through a second filter (*M&C* sintered steel filter, heated to 180 °C) before the FTIR. After each test the primary filter was chemically analyzed for fluoride content since it is known that HF may be partly adsorbed by this type of filter [27]. The fluoride adsorbed by the filter was determined by method B.1 (b) of the SS-ISO 19702:2006 Annex B standard, where the filter is leached in water in an ultrasonic bath for at least 10 min. Thereafter the fluoride content in the water is measured by ion chromatography with a conductive detector. The amount of HF is calculated by assuming that all fluoride ions present in the filter derives from HF. The concentration of the emitted gas was measured by Fourier transform infrared spectroscopy (FTIR) using a *Thermo Scientific Antaris IGS analyzer (Nicolet)* with a gas cell. The spectral resolution of the FTIR was 0.5 cm⁻¹. The gas cell was of 0.2 L, had a path length of 2.0 m, a cell pressure of 86.7 kPa was maintained and the cell was heated to 180°C. Each spectrum used 10 scans which gave a new spectrum every 12 seconds. There is a natural time delay between the gas measurement of the SBI and the FTIR in the measurement setup. The HRR and FTIR results presented in this paper were therefore time synchronized by overlaying of CO₂ measurements from the FTIR and the NDIR.

FTIR is a suitable technique to measure the concentrations of HF and POF₃ in the emitted fire gases. The FTIR was calibrated for a number of compounds, e.g. HF, when delivered from the supplier. However, it was found that the HF calibration was not accurate enough so it was recalibrated, see Andersson et al. [28] for a detailed description of the calibration procedure. The FTIR was also calibrated for POF₃. PF₅ could only be qualitatively determined by its spectral signature [28] but no traces of PF₅ could be found in the fire tests probably due to that the PF₅ is highly reactive. The detection limits were 2 ppm for HF and 6 ppm for POF₃. The spectral bands used for Classical Least Square (CLS) type quantification of HF and POF₃ are stated in Table 2.

Table 2

The spectral bands used for HF and POF₃.

Spectral bands (cm ⁻¹)	Type of band
HF	
4203-4202	HF R-branch stretching mode [29]
4175-4172	HF R-branch stretching mode [29]
POF ₃	
1418-1413	P-O stretching mode [9]
874-868	P-F symmetric stretching mode [9]

3. Results and discussion

The HRR results for the EiG battery cells with 0%, 50% and 100% SOC are shown in Fig. 3. High SOC values give high HRR peaks and the temperature and voltage measurements in Fig. 4 confirm that cells with high SOC value give a more reactive response, with rapid temperature increase and earlier voltage breakdown. Studies using other techniques confirm our results that battery cells with higher SOC are more thermally reactive, using e.g.; fire calorimeter [24], accelerating-rate calorimetry (ARC) [5] and VSP2 adiabatic calorimeter [30]. The HRR from the nine K2 cells in test 6 and the two complete laptop battery packs in test 7 can be seen in Fig. 5. The laptop pack includes the plastic box and have Li-ion cells with the more reactive cobalt based cathode, while the K2 cells (as well as the EiG cells) have LFP cathodes which are known to be significantly more stable [5,31-34]. The higher HRR values for the laptop cells are thus expected.

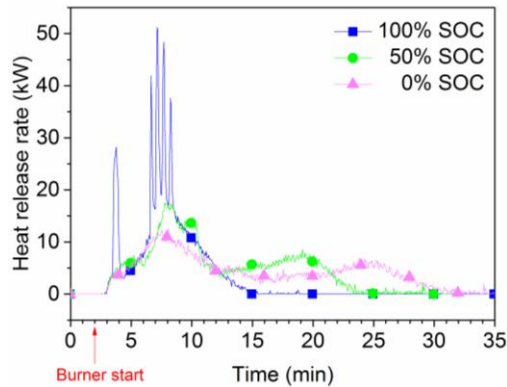


Fig. 3. Heat release rate for EiG cells with 0%, 50% and 100% SOC.

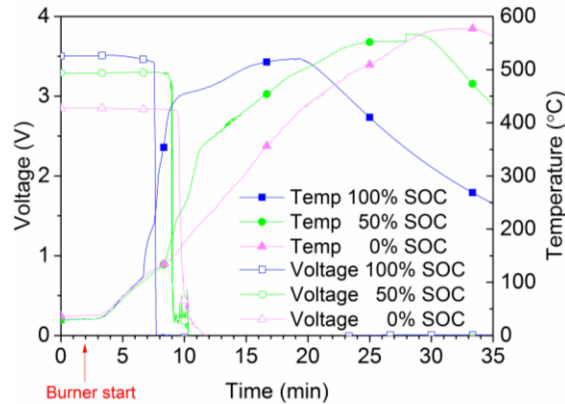


Fig. 4. Mid cell temperature and voltage for EiG with 0%, 50% and 100% SOC.

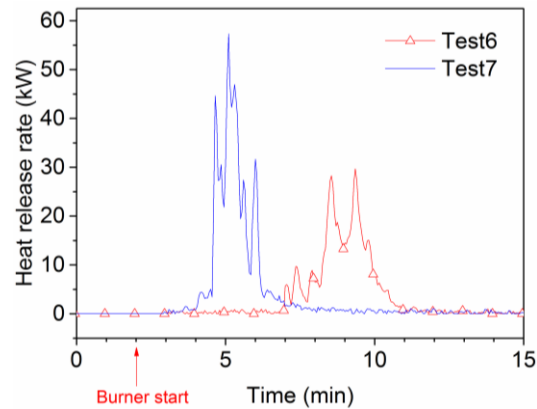


Fig. 5. Heat release rate for K2 cells (test 6) and laptop battery packs (test 7).

Outbursts from fully charged cells (100% SOC) of EiG, K2 and laptop packs were visually observed, see Fig. 6 for a typical example. The outbursts originate from ignition of the rapid gas release from a cell upon opening due to excessive cell pressure and correspond to the sharp spikes in the HRR curves, see Fig. 3 and Fig. 5. In most cases, one HRR-spike could be detected for each individual cell. For EiG cells with 50% and 0% SOC no spikes were observed in the HRR curves, instead two broad maxima were found. The orientation of the cells on the wire grating varied due the different packaging types (pouch, cylindrical, complete battery pack) which might have influenced the results. However, tests 1-5 used the same cell type and setup. The results of tests 6-7 can be seen as examples of possible events for these types of cells.



Fig. 6. Outbursts from EiG 100% SOC (test 1).

The fire test on EiG cells with 100% SOC was repeated two times (tests 1-2) without water mist application and one time (test 3) with water mist applied approximately 6.5 minutes after burner start. Fig. 7 shows HRR, HF emission rate, voltage and temperature for the mid cell, in test 2. Rapidly propagating flames released from the battery cells were visually observed five times during the test and denoted outbursts, marked in Fig. 7, and coincided with the five spikes in the HRR curve. The hydrogen fluoride concentration showed a rapid increase at the end of the HRR peak and the HF maximum plateau was reached just after the HRR spikes. The delay between HF production and HRR is not due to gas transport time since it is compensated by CO₂ synchronisation, the reason is due to delay times in the sampling system. As expected, the temperature of the mid cell showed a steep increase connected to the HRR peaks, the outbursts and the voltage breakdown. The maximum temperature reached in this measurement was 521 °C. Test 1 and test 2 show similar values and behavior, the variation between the tests is due to the nature of the fire characteristics.

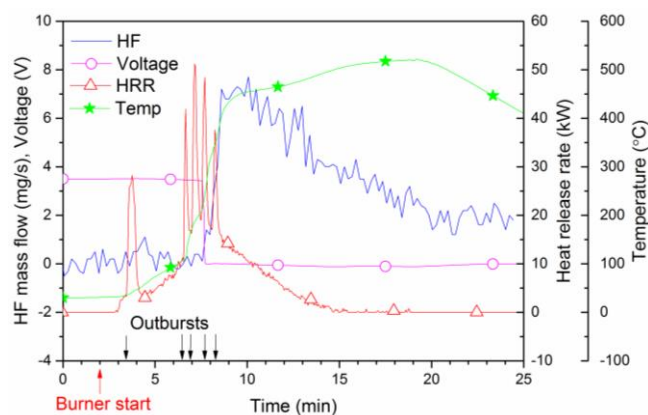
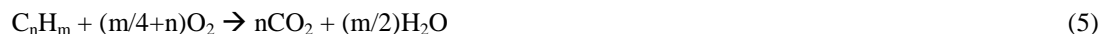


Fig. 7. Results for EiG 100% SOC (test 2).

Fig. 8 shows test 3 where 100% SOC EiG cells were tested with water mist application. Most of the results of the tests with and without water mist are similar, but the maximum HF concentration recorded at the time of applying the water mist into the flames is approximately twice as high as that in tests 1-2. However, the total amount of measured HF from FTIR and absorbed by the primary filter is of the same order for all tests 1-3. The water mist was certainly not the only source of water in this experiment, in addition to water existing in the atmosphere water is produced by the combustion process. In the general case of combustion of hydrocarbons water is produced:



and in the oxidation of ethylene carbonate (EC), $C_3H_4O_3$, a commonly used Li-ion solvent, water is thus produced according to:



When propane, C_3H_8 , is combusted, 1 mol of propane produces 4 mol of water according to eq. (5). In test 1-3 the 15 kW propane burner was active during 17 minutes and given the heat of combustion of propane, 2044 kJ/mol, the amount of water produced from the burner can be calculated to be approximately 550 g.

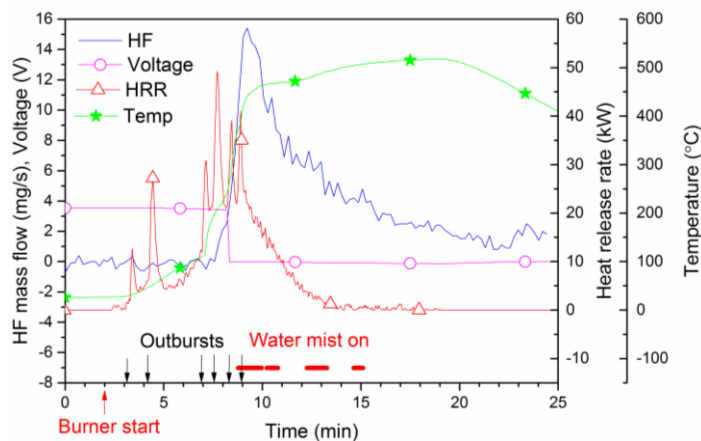


Fig. 8. Results for EiG 100% SOC with water mist (test 3).

The water concentration in the exhaust duct was measured by the FTIR, see Fig. 9 for the results of test 1-3. The water concentration shown for test 3 is scaled (factor 0.4/0.6) due to the lower duct flow in order to allow a comparison with the measured values of test 1-2. The outbursts result in an increased water concentration and the effects on the measured water concentration from the applied water mist is also clearly seen. Calculated from the measured data, the mass of the added water mist was around 400 g while around 350 g water was released due to the combustion of battery materials. The water in the duct flow from ambient air was around 1500 g for test 3 and 2300 g in test 1-2 (due to higher duct flow rate). The time of the water mist application was relatively short and the water mist was applied in the reaction zone, thus the impact from this source of water was potentially high which is also seen in Fig. 9. The amounts of water from ambient air were large but the impact should have been low since only part of the air flow passed the reaction zone above the battery and no effect on the HF concentration was observed due to the higher ambient water content in the duct flow in test 1-2 compared to test 3. Fig. 10 shows the correlation between HF production and water concentration for test 3. No HF production directly associated with the outbursts can be seen but the application of water mist seems to influence the HF production. However, the added water mist only temporarily increased the emission of HF but did not change the total amount of HF produced. Anyhow, only one test with water mist application was performed and the correlation between the water mist application and the increased HF peak production could possibly depend on other factors than the additional water introduced by the water mist.

Fig. 11 shows the measured production rate of HF for all EiG tests. For 0-50% SOC the peaks are broadened compared to the peaks for the 100% SOC cells and the total amount of measured HF is about double that of the 100% SOC cells. Detailed results from all the tests can be found in Table 3. Total yields in mg/g are calculated as total amount of HF divided per weight loss of the batteries. In test 7 the weight loss also included the burning of pack materials, e.g. plastic housing. Total yields in mg/Wh are calculated as total amount HF in mg divided by total energy capacity, Wh, of the batteries for each test. Whichever of these yield values that are used, the EiG cells with 0% or 50% SOC showed the highest HF values. The measured data indicate a relationship between SOC and the total released HF emissions, with increased total amounts of HF emission for lower SOC. Ribière et al. [24] found somewhat similar results by studying single cells with 100%, 50% and 0% SOC, showing an increasing total amount of HF emissions for decreasing SOC value. The reason for this is unknown and an investigation of the relationship would require further studies. The HF concentrations measured were in all cases well above the detection limit but no significant amounts of POF_3 could be detected in any of the tests. FTIR measurements on samples of similar electrolytes with LiPF_6 in a cone calorimeter have shown the production of POF_3 to be in the order of 1/20 of the HF production [28]. The detection limit of POF_3 in the FTIR measurements is 3 times higher than for HF, thus there could have been POF_3 present during the measurements which has not been detectable.

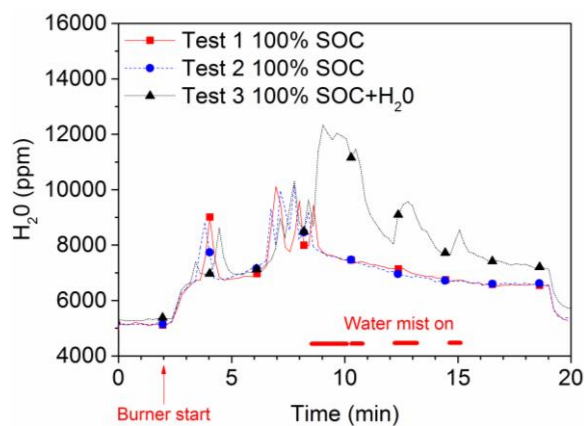


Fig. 9. Water concentrations measured in test 1-3. The increased water level in test 3 due to water mist application is clearly seen.

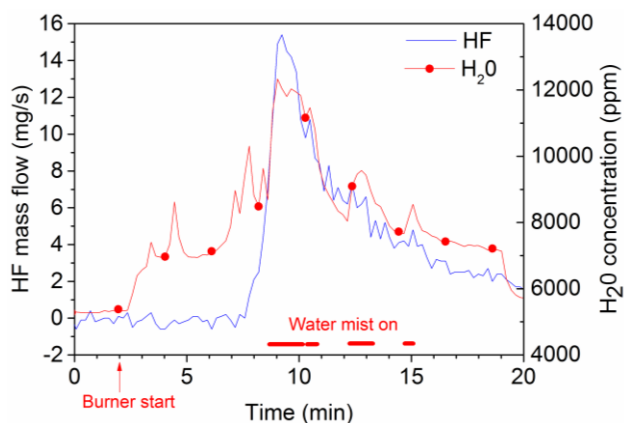


Fig. 10. HF mass flow and water concentration for test 3.

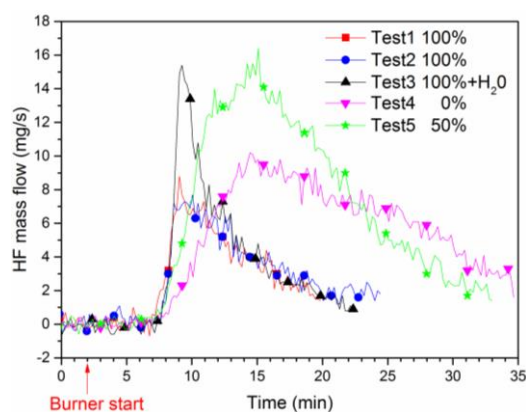


Fig. 11. HF mass flow for EiG cells with different SOC (indicated by % in figure legend) in tests 1-5.

Table 3

Detailed results of heat release rate, energy release, hydrogen fluoride emissions for test 1-7.

Test No.	Weight loss (g)	Max heat release (kW)	Total heat release (kJ)	Hydrogen fluoride					
				Max production rate (g/s)	Total amounts from FTIR (g)	Total amounts from filter (g)	Total amounts (g)	Total yields (mg/g)	Total yields (mg/Wh)
1	346	55	7731	0.0088	3.2	1.7	4.9	14	44
2	342	51	7526	0.0077	3.9	2.4	6.3	18	56
3	341	49	8095	0.0154	4.2	1.5	5.7	17	51
4	353	13	8314	0.0102	9.7	1.6	11.3	32	100
5	354	17	8452	0.0164	12.0	1.9	13.9	39	120
6	145	29	2766	0.0029	1.2	1.0	2.2	15	24
7	258	57	3470	0.0011	Not detected	1.9	1.9	7.3	15

The HRR values presented in this paper are calculated using the oxygen consumption method. This technique is well accepted and used in fire calorimetry measurements. For the case of battery fires, the technique might however have some limitations since it will not account for energy liberated by Joule heating through electrical discharge, e.g. internal short circuits in a cell due to melted separator. Ribière et al. [24] estimates the error to be max 10% and thereby claim the oxygen consumption method to be usable. Besides the issue with Joule heating, the Li-ion battery

can release its own oxygen [5]. The oxygen release varies with different Li-ion cell chemistries, and is typically lowest for LFP. In this test method a large amount of air is passed in the duct flow and the effect of released oxygen is regarded as negligible.

In order to simplify an estimation of the heat and gas emission hazards for this type of lithium-ion batteries the values have been normalized to the energy capacity of the batteries. Table 4 shows such values from our study as well as calculated values using data from Ribière et al. [24]. Again, note that the values for the laptop battery pack also accounts for the plastic housing. The EiG cells have about the double total heat release, 67-75 kJ/Wh, compared to the other batteries in Table 4. Also, the influence of SOC levels is small compared to the differences between the battery types. The maximum HRR per Wh calculated from our experimental data, 110-490 W/Wh, is, however, lower than the values reported by Ribière et al. [24], 300-1900 W/Wh, who used a different test procedure. Normalized values for the total HF release vary in our study between 15-124 mg/Wh, a wider range than that found by Ribière et al. [24].

Table 4

Total heat release, maximum HRR value and total HF release, normalized values for energy capacity.

Battery	Nominal energy capacity (Wh)	Normalized total heat release (kJ/Wh)	Normalized maximum HRR (W/Wh)	Normalized total HF release (mg/Wh)
Five EiG cells	112	67-75	110-490	44-124
Nine K2 cells	92	30	310	24
Two laptop battery packs	124	28	460	15
Single cell, calculated from Ribière et al. [24]	11	28-35	300-1900	37-69

In general, the measured values of the amount of HF produced in fire tests are comparatively high and could pose a serious hazard if released in an enclosed environment. For example, the 7 Ah EiG battery cell can typically be used in a plug-in electric vehicle (PHEV) and a 10 kWh battery pack of a PHEV could consist of 448 such cells (a battery system of 112 cells in series and 4 cells in parallel; cell voltage 3.2 V nominal, pack voltage 358.4 V nominal). If we extrapolate our results for the 5-cell packs by multiplying by a factor of $448/5 = 89.6$, it may represent a scenario of a complete fire of a PHEV battery pack. The extrapolation gives 400-1200 g HF depending on the state of charge for the EiG cells where high SOC gives lower HF. Even though the extrapolation is extensive and therefore can be questionable the result is in the same order of magnitude as that reported by Lecocq et al. [35] who conducted complete vehicle fire tests including HF measurements of two electric vehicles (EV) with fully charged batteries (100% SOC) and on two similar gasoline powered combustion engine passenger cars (none-EV). Lecocq et al. [35] measured significant HF emissions from all four vehicles, both EV and similar none-EV, and suspected that the HF emissions from all vehicles could in part originate from air conditioner system. Using the values in Lecocq et al. [35], and calculating the difference in total HF release between the EV and the similar none-EV an estimate of the contribution to the HF release from the Li-ion battery can be found to be 919 g for a 16.5 kWh Li-ion battery and 657 g for a 23.5 kWh Li-ion battery. Scaling these values for a 10 kWh battery results in 280 to 557 g of released HF.

If we assume that all the emitted HF is released within a closed passenger compartment of 5 m^3 of an electrified vehicle we obtain HF concentrations between 80-240 g/m^3 . NOISH (The National Institute for Occupational Safety and Health) in USA stated the IDLH (Immediately Dangerous To Life or Health) value for HF to 30 ppm corresponding to a concentration of HF in air of 0.025 g/m^3 [7]. Our values which are similar to those of Lecocq et al. [35] exceed the IDLH by about four orders of magnitude. The reported HF values from Ribière et al. [24] also by far exceed the IDLH value. However, the experimental data reported here comes from a limited study and the

calculation assumes a somewhat extreme theoretical situation which differs from real fire situations, i.e. all HF is emitted and trapped in the compartment and that the passenger stays in the compartment. Anyhow, even if the emission occurs in a much larger volume, e.g. in a garage, the HF levels can still be very high. The reported HF values thus indicate that a critical situation might occur in the case of a thermal event in a Li-ion battery pack. Although we could not directly detect the presence of POF_3 , it may also be present in considerable amounts since indications are that HF and POF_3 is produced with a ratio of about 1:20 [28].

4. Conclusions

The tests show that lithium-ion battery cells exposed to fire are significantly more reactive at 100% SOC than at lower SOC values and energetic outbursts were observed. The HRR peak values thus varied in a rather wide range, between 13-57 kW for batteries with approximately 100 Wh energy capacity. The normalized total heat release per energy capacity was 28-75 kJ/Wh and the normalized maximum HRR values were 110-490 W/Wh.

The amount of HF released varied between 15-124 mg/Wh. Lower SOC values gave higher amounts of HF. Extrapolation of data shows that the potential HF release from a 10 kWh PHEV battery is in the range 400-1200 g HF. If this amount of HF would be released inside a passenger compartment of 5 m³ the HF concentration would be 80-240 g/m³, that is magnitudes higher than acceptable short time exposure levels. Besides HF, there may also be significant emissions of POF_3 , a compound which might be more toxic than HF. Although these estimates are based on an extrapolation and can be regarded as a hypothetical case it highlights the risks associated with toxic emissions at battery fires and the need to find replacements for the fluorine content in the Li-salt and binder used in Li-ion battery cells. The influence of additional water in form of water mist seemed to increase the HF emissions momentarily, however the total HF release was the same. Further studies of the relationship between water and HF emissions in fires are needed in order to thoroughly evaluate potential risks related to the use of water as firefighting medium in electric vehicle fires.

Acknowledgements

The authors gratefully acknowledge the Swedish Energy Agency and the FFI-program as well as the Swedish Fire Research Board for financial support. Several persons at SP Fire Technology are acknowledged for their contribution to this work, including Lars Pettersson and Magnus Samuelsson.

References

1. Z. J. Zhang, P. Ramadass, W. Fang, Safety of lithium-ion batteries, in: G. Pistoia (Ed), Lithium-Ion Batteries Advances and Applications, Elsevier, Amsterdam, 2014, pp. 409-435.
2. Q. Wang, P. Ping, X. Zhao, G. Chu, J. Sun, C. Chen, J. of Power Sources, 208 (2012) 210-214.
3. D. Lisbona, T. Snee, , Process safety and environmental protection, 89 (2011) 434-442.
4. <http://edition.cnn.com/2014/01/14/travel/787-dreamliner/>, 2014-05-13
5. D. Doughty, E. P. Roth, The Electrochem. Soc. Interface, summer 2012, 2012 37-44.
6. F. Larsson, P. Andersson, B.-E. Mellander, Are electric vehicles safer than combustion engine vehicles?, in: B. Sandén, P. Wallgren (Eds.), Systems perspectives on Electromobility, Chalmers University of Technology, Goteborg, ISBN 978-91-980973-9-9, 2014, pp. 33-44.
7. Documentation for Immediately Dangerous To Life or Health Concentrations (IDLHs) for Hydrogen fluoride (as F), The National Institute for Occupational Safety and Health (NIOSH), USA, May 1994, <http://www.cdc.gov/niosh/idlh/7664393.html>.
8. Middelmann, Hygiensiska gränsvärden AFS 2011:18, Hygieniska gränsvärden Arbetsmiljöverkets föreskrifter och allmänna råd om hygieniska gränsvärden, ISBN 978-91-7930-559-8, ISSN 1650-3163, Swedish Work Environment Authority, Sweden, 2011.
9. H. Yang, G. V. Zhuang, P. N. Ross Jr, J. of Power Sources 161 (2006) 573-579.

10. T. Kawamura, S. Okada, J.-i. Yamaki, *J. of Power Sources* 156 (2006) 547-554.
11. Q.-S. Wang, J.-H. Sun, G.-Q. Chu, X.-L. Yao, C.H. Chen, *J. of Thermal Analysis and Calorimetry*, 89 (2007) 1, 245-250.
12. C. G. Barlow, *Electrochem. and Solid-State Letters*, 2 (8) (1999) 362-364.
13. S. E. Sloop, J. B. Kerr, K. Kinoshita, *J. of Power Sources*, 119-121 (2003) 330-337.
14. C. L. Campion, W. Li, W. B. Euler, B. L. Lucht, B. Ravdel, J. F. DiCarlo, R. Gitzendanner, K. M. Abraham, *Electrochem. and Solid-State Letters*, 7 (7) (2004) A194-A197.
15. C. L. Campion, W. Li, B. L. Lucht, *J. of the Electrochem. Soc.* 152 (12) (2005) A2327-A2334.
16. S. F. Lux, I. T. Lucas, E. Pollak, S. Passerini, M. Winter, R. Kostecky, *Electrochem. Communications* 14 (2012) 47-50.
17. H. Yang, X.-D. Shen, *J. of Power Sources* 167 (2007) 515-519.
18. M. D. S. Lekgoathi, B. M. Vilakazi, J. B. Wagener, J. P. Le Roux, D. Moolman, *J. of Fluorine Chemistry*, 149 (2013) 53-56.
19. Hammami, N. Raymond, M. Armand, *Nature* 424 (2003) 635-636.
20. T. Ohsaki, T. Kishi, T. Kuboki, N. Takami, N. Shimura, Y. Sato, M. Sekino, A. Satoh, *J. of Power Sources* 146 (2005) 97-100.
21. E. P. Roth, C. J. Orendorff, *The Electrochem. Soc. Interface*, summer 2012. 2012 45-49.
22. D. P. Abraham, E. P. Roth, R. Kostecky, K. McCarthy, S. MacLaren, D. H. Dought, *J. of Power Sources* 161 (2006) 648-657.
23. M. D. Chatelain, T. E. Adams, *Proceedings of the Power Sources Conference*, 42 (2006) 87-89.
24. P. Ribière, S. Grugeon, M. Morcrette, S. Boyanov, S. Laruelle, G. Marlair, *Energy Environ. Sci.*, 5 (2012) 5271-5280.
25. G. G. Eshetu, S. Grugeon, S. Laruelle, S. Boyanov, A. Lecocq, J.-P. Bertrand, G. Marlair, *Phys. Chem. Chem. Phys.* 15 (2013) 9145-9155.
26. EN 13823:2010, Reaction to fire tests for building products – Building products excluding floorings exposed to the thermal attack by a single burning item, European Committee for Standardization, Brussels, 2010.
27. ISO 19702:2006, Toxicity testing of fire effluents -- Guidance for analysis of gases and vapours in fire effluents using FTIR gas analysis, International Organization for Standardization, Geneva, 2006.
28. P. Andersson, P. Blomqvist, A. Lorén, F. Larsson, Investigation of fire emissions from Li-ion batteries, SP Report 2013:5, SP Technical Research Institute of Sweden, Borås, Sweden, ISBN 978-91-87461-00-2, 2013.
29. J. M. Hollas, *Modern Spectroscopy*, 3ed., John Wiley & Sons, Chichester, 1996.
30. C.-Y. Jhu, Y.-W. Wang, C.-M. Shu, J.-C. Chang, H.-C. Wu, *J. of Hazardous Materials*, 192 (2011) 99-107.
31. H. Joachin, T. D. Kaun, K. Zaghbi, J. Prakash, *J. of the Electrochem. Soc.*, 156 (6) (2009), A401-A406
32. G. Chen, T. J. Richardson, *J. of The Electrochem. Soc.*, 156 (9) (2009) A756-A762.
33. G. Chen and T. J. Richardson, *J. of Power Sources*, 195 (201) 1221-1224.
34. K. Zaghbi, J. Dubé, A. Dallaire, K. Galoustov, A. Guerfi, M. Ramanathan, A. Benmayza, J. Prakash, A. Mauger and C. M. Julien, *J. of Power Sources*, 219 (2012) 36-44.
35. Lecocq, M. Bertana, B. Truchot, G. Marlair, Conference proceedings of Fires in vehicles (FIVE) 2012, edited by P. Andersson, B. Sundström, SP Technical Research Institute of Sweden, Borås, Sweden, 2012, pp. 183-193.